The interaction of *Leishmania major* parasites with human myeloid cells and its consequence for adaptive immunity

Dissertation

Zur Erlangung des Grades

Doktor der Naturwissenschaften

Am Fachbereich Biologie

Der Johannes Gutenberg-Universität

Mainz

Peter Crauwels

Geb. am 30.09.1987 in Liège

Mainz, 2014

Dekan:

1. Gutachter:
2. Gutachter:

Tag der mündlichen Prüfung: 15.07.2015

This PhD project, funded by the Carl Zeiss Foundation, was initiated at the University Clinic in Ulm at 15. November 2010. In spring 2011 the research group of Ger van Zandbergen moved to the Paul-Ehrlich Institute, Division of Immunology, in Langen, where this project was continued.

During this time the obtained research data and collaborative studies led to the following publications:

Peter Crauwels, Rebecca Bohn, Meike Thomas, Stefan Gottwalt, Florian Jäckel, Susi Krämer, Elena Bank, Stefan Tenzer, Paul Walther, Max Bastian, Ger van Zandbergen. Apoptotic-like *Leishmania* exploit the host´s autophagy machinery to reduce T-cell mediated parasite elimination. **Autophagy 2015, in press**

Neu C, Sedlag A, Bayer C, Förster S, **Crauwels P**, Niess JH, van Zandbergen G, Frascaroli G, Riedel CU. CD14-dependent monocyte isolation enhances phagocytosis of *listeria monocytogenes* by proinflammatory, GM-CSF-derived macrophages. **PLoS ONE 2013, PMID: 23776701**

Lilija Miller, Sabrina Weißmüller, Eva Ringler, **Peter Crauwels**, Ger van Zandbergen, Rainer Seitz, Zoe Waibler, on behalf of ABIRISK consortium. Danger signal-dependent activation of human dendritic cells by plasma-derived factor VIII products. **Thrombosis and Haemostasis 2014, under revision**

Krämer S, **Crauwels P**, Radzimski C, Szaszák M, Klinger M, Rupp J and van Zandbergen G. AP-1 transcription factor serves as a molecular switch between Chlamydia pneumoniae replication and persistence. **Infection and Immunity 2014, submitted**

Contents

Abbreviations

3-MA	3-methyladenine
ABC	ATP-binding cassette
ANXA5	Annexin V
APC	Antigen presenting cell
ATG	Autophagy related gene
BAFA1	Bafiloymcin A1
CD	Cluster of differentiation
CFSE	Carboxyfluorescein succinimidyl ester
CMV	Cytomegalovirus
CR	Complement receptor
DC	Dendritic cell
FCS	Fetal calf serum
GATA3	GATA binding protein 3
GM-CSF	Granulocyte-macrophage colony-stimulating factor
hMDM	Human monocyte derived macrophages
HSV	Herpes simplex virus
IFN	Interferon
IL	Interleukin
iNOS	Inducible nitric oxide synthase
LAMP	lysosome-associated membrane proteins
LAP	LC3 associated phagocytosis
LC3	Microtubule-associated protein 1A/1B-light chain 3
Lm	*Leishmania*

Log.ph.	Logarithmic growth phase
LPG	Lipophosphoglycan
MACS	Magnetic-activated cell sorting
M-CSF	Macrophage colony-stimulating factor
mDC	Myeloid dendritic cell
MF	Macrophages
MFI	Mean fluorescent intensity
MOI	Multiplicity of infection
MR	Mannose receptor
mTor	Mammalian target of rapamycin
NCCD	Nomenclature on Cell Death
NNN	Novy-MacNeal-Nicolle
NO	Nitric oxide
PAMPS	Pathogen-associated molecular patterns
PBMCs	Peripheral blood mononuclear cell
PHA	Phytohemagglutinin
PI	Propidium iodide
PI3K	Phosphoinositide 3-kinase
PS	Phosphatidylserine
ROS	Reactive oxygen species
SEM	Standard error of the mean
SHARP	Hydrophilic acylated surface protein
SHERP	Small hydrophilic ER-associated protein
SLA	Soluble *Leishmania* antigen
SN	Supernatant fraction
Stat.ph.	Stationary growth phase

TCR	T cell receptor
Th	T-helper
TLR	Toll like receptor
TNF	Tumor necrosis factor
TT	Tetanus toxoid
TUNEL	terminal deoxynucleotidyl transferase (TdT)-mediated dUTP nick end labeling

1. A. Summary

In this study we focused on three biological aspects of *Leishmania* infection. We focused (1) on characterizing the cell death process "apoptosis" in parasites, (2) on defining the suitability of human primary macrophages and dendritic cells as host cells for *Leishmania* parasites and (3) on assessing the consequence of infection for development of an adaptive immune response. Central in this project was the hypothesis that apoptotic *Leishmania* exploit the host´s autophagy machinery to reduce T cell mediated parasite elimination.

Among *Leishmania*, we defined an apoptotic population, which was characterized by a round shaped morphology and phosphatidylserine exposure. In addition, apoptotic parasites contained less DNA as they were in the SubG$_1$ phase and DNA was fragmented, as assessed by a TUNEL assay. During interaction with human macrophages and dendritic cells, we found the anti-inflammatory macrophages to be more susceptible for infection then proinflammatory macrophages and dendritic cells. Interestingly, in the latter cell type, *Leishmania* parasites developed most efficiently in the disease propagating amastigote life stage. As both macrophages and dendritic cells are antigen presenting cells, antigens may be presented to activate T cells of the adaptive immune system. Indeed, during *Leishmania* infection, T cell proliferation was induced. These T cells were characterized as CD3$^+$CD4$^+$ T cells, surprisingly comprising *Leishmania* specific memory CD45RO$^+$ T cells obtained from previously unexposed individuals. Furthermore, dependent on the apoptotic parasite entry in macrophages – but not in dendritic cells – a significant lower T cell proliferation was observed. As a consequence, proliferation restricted intracellular parasites survival the strongest in dendritic cells. Investigating the intracellular fate of apoptotic parasites, we found them to reside in a phagosome decorated with the autophagy marker LC3 in macrophages – but not in dendritic cells. By linking autophagy to T cell proliferation we demonstrated that chemical induction of autophagy, preceding *Leishmania* infection, also strongly reduced T cell proliferation and enhanced parasite survival.

Summary - English

In all, our data suggest apoptosis also to occur in single-celled organisms. During infection, both macrophages and dendritic cells are susceptible, activating the human adaptive immune system. The induced proliferation is reduced in the presence of apoptotic parasites in macrophages, defining macrophages to be more suitable as host cells to dendritic cells. In macrophages, apoptotic *Leishmania* misuse the host cells´ autophagy machinery as an immune evasion mechanism, to reduce T cell proliferation by which the overall population´s survival is guaranteed. These findings explain the benefit of apoptosis in a single-celled parasite and define the host´s autophagy pathway as a potential therapeutic target in treating Leishmaniasis.

1. B. Zusammenfassung

In der vorliegenden Arbeit fokussierten wir uns auf drei verschiedene Aspekte der Leishmanien-Infektion. Wir charakterisierten den Prozess des Zelltods „Apoptose" bei Parasiten (1), untersuchten die Eignung von Makrophagen und dendritischen Zellen als Wirtszelle für die Entwicklung der Parasiten (2) und analysierten die Konsequenzen der Infektion für die Entstehung einer adaptiven Immunantwort im humanen System. Von zentraler Bedeutung für dieses Projekt war die Hypothese, dass apoptotische Leishmanien den Autophagie-Mechanismus ihrer Wirtszellen ausnutzen, um eine T-Zell-vermittelte Abtötung der Parasiten zu vermindern.

Wir definierten eine apoptotische Leishmanien-Population, welche durch eine rundliche Morphologie und die Expression von Phosphatidylserin auf der Parasitenoberfläche charakterisiert war. Die apoptotischen Parasiten befanden sich zudem in der SubG1-Phase und wiesen weniger und fragmentierte DNA auf, welche durch TUNEL-Assay nachgewiesen werden konnte. Bei der Interaktion der Parasiten mit humanen Makrophagen und dendritischen Zellen zeigte sich, dass die anti-inflammatorischen Makrophagen anfälliger für Infektionen waren als die pro-inflammatorischen Makrophagen oder die dendritischen Zellen. Interessanterweise wurde in den dendritischen Zellen jedoch die effektivste Umwandlung zur krankheitsauslösenden, amastigoten Lebensform beobachtet. Da sowohl Makrophagen als auch dendritische Zellen zu den antigenpräsentierenden Zellen gehören, könnte dies zur Aktivierung der T-Zellen des adaptiven Immunsystems führen. Tatsächlich konnte während der Leishmanien-Infektion die Proliferation von T-Zellen beobachtet werden. Dabei stellten wir fest, dass es sich bei den proliferierenden T-Zellen um $CD3^+CD4^+$ T-Zellen handelte, welche sich überraschenderweise als Leishmanien-spezifische $CD45RO^+$ T-Gedächtniszellen herausstellten. Dies war unerwartet, da ein vorheriger Kontakt der Spender mit Leishmanien als unwahrscheinlich gilt. In Gegenwart von apoptotischen Parasiten konnte eine signifikant schwächere T-Zell-Proliferation in Makrophagen, jedoch nicht in dendritischen Zellen beobachtet werden. Da sich die T-Zell-Proliferation negativ auf das Überleben der Parasiten auswirkt, konnten die niedrigsten Überlebensraten in dendritischen Zellen vorgefunden werden. Innerhalb der Zellen befanden sich die Parasiten in

beiden Zelltypen im Phagosom, welches allerdings nur in Makrophagen den Autophagie-Marker LC3 aufwies. Chemische Induktion von Autophagie führte, ebenso wie die Anwesenheit von apoptotischen Parasiten, zu einer stark reduzierten T-Zell-Proliferation und dementsprechend zu einem höheren Überleben der Parasiten.

Zusammenfassend lässt sich aus unseren Daten schließen, dass Apoptose in Einzellern vorkommt. Während der Infektion können sowohl Makrophagen, als auch dendritische Zellen mit Leishmanien infiziert und das adaptive Immunsystem aktivert werden. Die eingeleitete T-Zell-Proliferation nach Infektion von Makrophagen ist in Gegenwart von apoptotischen Parasiten reduziert, weshalb sie im Vergleich zu dendritischen Zellen die geeigneteren Wirtszellen für Leishmanien darstellen. Dafür missbrauchen die Parasiten den Autophagie-Mechanismus der Makrophagen als Fluchtstrategie um das adaptive Immunsystem zu umgehen und somit das Überleben der Gesamtpopulation zu sichern. Diese Ergebnisse erklären den Vorteil von Apoptose in Einzellern und verdeutlichen, dass der Autophagie-Mechanismus als potentielles therapeutisches Ziel für die Behandlung von Leishmaniose dienen kann.

1. C. Samenvatting

In deze studie hebben we ons gericht op drie biologische aspecten van *Leishmania* infectie. We concentreerden ons op (1) het karakteriseren van " apoptose" (sterfte) in parasieten, (2) hoe geschikt menselijke cellen, in het bijzonder macrofagen en dendritische cellen, zijn voor deze parasiet om te overleven, (3) en we onderzochten hoe infectie met deze parasiet, het adaptieve immuun systeem activeerd, meer specifiek de T cellen (witte bloedlichaampjes). Centraal in dit project was de hypothese dat dode parasieten het proces "autophagie" gebruiken om afdoding door T cellen te verhinderen.

We konden celdood in parasieten aantonen, doordat ze meer rond gevormd waren en fosfatidylserine blootstelden. Bovendien bevatten dode parasieten minder DNA (SubG$_1$ fase) en de DNA was gefragmenteerd (TUNNEL assay). Tijdens de interactie met menselijke cellen konden we vaststellen dat ontstekings-remmende macrofagen het meeste parasieten opnamen, gevolgd door ontstekings-bevorderende macrofagen en dendritische cellen. Opvallend was dat in dendritische cellen, de ontwikkeling van de parasiet het meest efficient plaatsvond.

Zowel macrofagen en dendritische cellen kunnen antigenen presenteren, waardoor T cellen geactiveerd worden. Inderdaad, ook in ons model tijdens infectie met de *Leishmania* parasieten konden we delende T cellen detecteren. Deze T cellen werden gekenmerkt door de expressie van CD3 en CD4, maar ook van CD45RO. Deze laatste marker is voorhanden op specifieke geheugen cellen, wat opvallend is, omdat deze cellen afkomstig zijn mensen die nog nooit een *Leishmania* infectie doorgemaakt hebben.

Bovendien, de deling van T cellen was afhankelijk van de celdood in parasieten. Wanneer macrofagen dode parasieten opnamen, was de activatie van T cellen verminderd, wat bij dendritische cellen niet het geval was. Als een gevolg vande T cel deling werden meer parasieten gedood waardoor het overleven van parasieten afnam. Meer in detail konden we aantonen dat de dode parasieten in macrophagen het proces "autophagie" inschakelden. Door dit

mechanisme chemisch in te schakelen konden we aantonen dat het proces autophagie verantwoordelijk was voor een verminderde T cel activatie/deling.

Samengevat konden we aantonen dat celdood (apoptose) ook voorkomt bij eencellige *Leishmania* parsieten. Tijdens infectie zijn zowel menselijke macrofagen en dendritische cellen vatbar, die beide het adaptieve immuun systeem activeerden. De geactiveerde T cellen deelden zich minder sterk in de aanwezigheid van dode parasieten in macrofagen, waardoor macrofagen meer geschikt zijn als gastheercel voor parasieten dan dendritische cellen. Bovendien, in macrofagen gebruiken parasieten het proces autophagie om activatie van het immuun systeem te verhinderen. Hierdoor wordt het overleven van de parasieten populatie versterkt. Deze resultaten verklaren het voordeel van celdood in eencellige parasieten en definiëren het proces autophagie als een potentieel therapeutisch doelwit in de behandeling van leishmaniasis.

2.   Introduction

2.1   Leishmaniasis, an emerging disease

Leishmaniasis is a vector-born disease, caused by protozoan parasites of the genus *Leishmania* (*Lm*). The disease is endemic in 88 countries, tropical regions, where transmission occurs by the phlebotomine sand fly (**Figure 1**) (Bhowmick and Ali, 2008; Ivens et al., 2005). The disease can have three clinical manifestations namely; cutaneous, mucosal and visceral Leishmaniasis. In all three cases, the infection can range from asymptomatic to severe. Cutaneous Leishmaniasis is characterized by skin ulcers, which are mostly self-healing, caused by parasite strains of the Old World (*Lm tropica*, *Lm major*, *Lm aethiopica*, *Lm infantum* and *Lm donovani*) as well as from the New World (*Lm mexicana* and *Lm braziliensis* species complex) (McMahon-Pratt and Alexander, 2004). During mucosal Leishmaniasis the naso-oropharyngeal mucosa is affected. Although this manifestation is poorly understood, studies have shown that once parasites get a viral infection, cutaneous Leishmaniasis progresses, destroying also mucosal tissue (Zangger et al., 2013). The most severe and life threating form is visceral Leishmaniasis. The etiological agents are usually *Lm donovani* and *Lm infantum*, causing weight loss, hepatosplenomegaly and pancytopenia. Globally, 12 million people are affected by Leishmaniasis and 1.3 million new people get infected yearly. Currently, no vaccine is available and an increased drug resistance against the standard pentavalent antimonial drugs is emerging (Croft et al., 2006). As yearly still 20,000 to 30,000 people die, an increasing need for improved therapies or vaccines is required (Dietze et al., 2001; WHO, 2014).

Figure 1: Global distribution of Leishmaniasis, affecting 88 countries (WHO, 2014).

2.2 *Leishmania* life cycle

Leishmania are protozoan parasites belonging to the order of kinetoplastida, an early diverging group of organisms in the eukaryotic lineage. These parasites have a dimorphic, asexual life cycle which starts in the midgut of the sand fly of the Phlebotomus family (Warburg, 2008). In the vector´s alimentary tract, parasites develop into the mammalian-infective metacyclic promastigote form by a process called metacyclogenesis. Essential for a successful development are the stage-specific proteins HASP (hydrophilic acylated surface protein) and SHERP (small hydrophilic ER-associated protein) (Sádlová et al., 2010). In the sand fly´s midgut, due to the increased expansion and development, the parasites cause damage to the sand fly´s stomodeal valve. Subsequently after taking a blood meal, a backflow of ingested blood is created in combination with regurgitation, which allows parasites to enter the skin (Dostálová and Volf, 2012; Rogers et al., 2004). The infectious inoculum reaching the skin comprises a mixture of viable and apoptotic parasites, the latter one required for disease development (van Zandbergen et al., 2006). The first cells these promastigotes encounter are resident dermal macrophages and neutrophils. Neutrophils are the first immune cells to be recruited to the site of infection which phagocytize *Leishmania* promastigotes. *Leishmania* promastigotes delay the programmed cell death of neutrophils and enhance the production of MIP-1B, attracting blood monocyte-derived macrophages to the site of infection (Charmoy et al., 2010; Shio et al., 2012). Upon spontaneously apoptosis of infected neutrophils, engulfment by macrophages occurs. Through this way, parasites can silently enter macrophages (Trojan Horse Strategy) (Laskay et al., 2003; Peters et al., 2008). Once inside macrophages, the parasites´ final host cell, promastigotes reside in the phagolysosomal compartment. Under these temperature and acidic conditions, stage transformation occurs in the disease propagating amastigote form. These amastigotes have a droplet shaped morphology and are non-motile, as the flagellum does not protrude beyond the body´s surface. Concentrating on the genetic background, the ATP-binding cassette (ABC) genes (ABCA3 and ABCG3) are preferentially expressed in the amastigote stage, playing a role in transporting a variety of molecules across the membrane (Leprohon et al., 2006). Once transformed, the amastigotes multiply, after which new macrophages can get infected, leading

to disease dissemination. When a sand fly takes a meal, amastigotes are transferred, and can redifferentiate into promastigotes, completing the *Leishmania* life cycle (**Figure 2**).
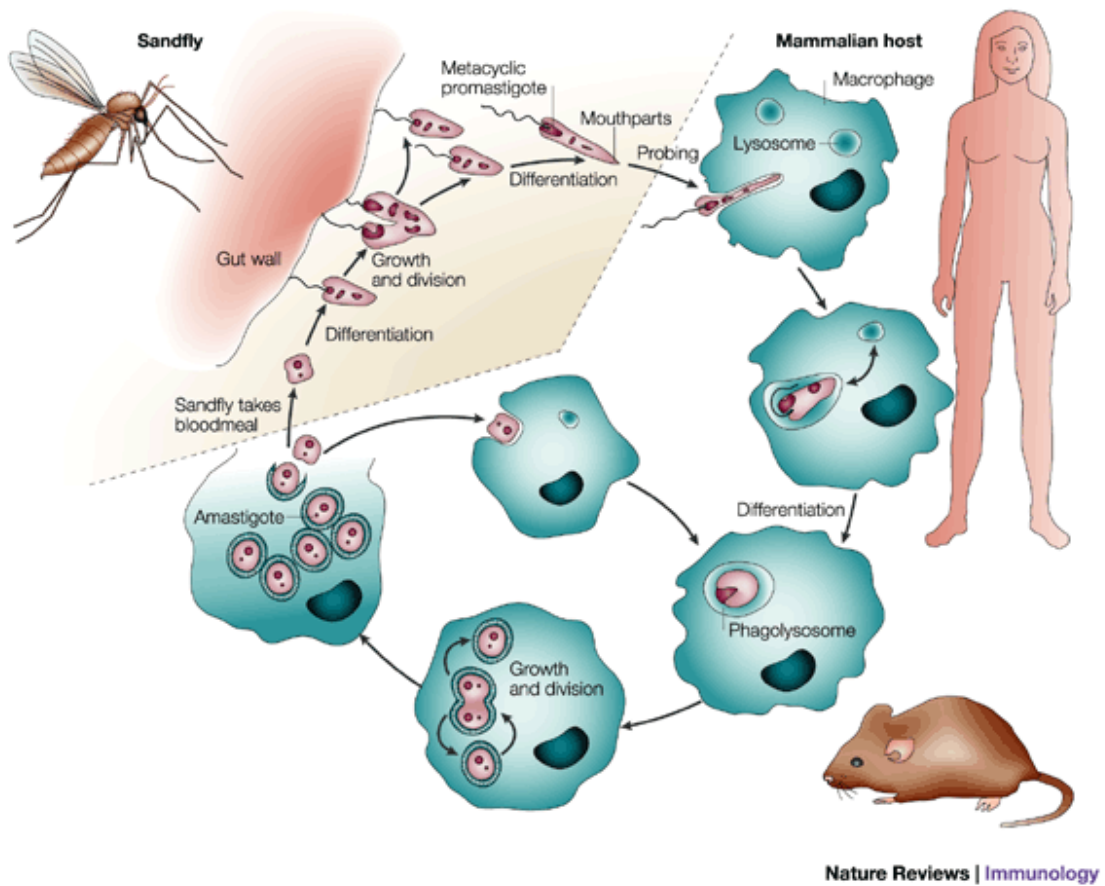
Figure 2: ***Leishmania* life cycle.** *Leishmania* procyclic promastigotes develop in the sand fly to the metacyclic infectious promastigote population. Upon a blood meal, parasites are entering the human host, reaching their final host cell, the human macrophage. Inhere promastigotes develop into the disease propagating amastigote form, re-infecting new cells. Upon a second blood meal, amastigotes are ingested and redifferentation in the sandfly to promastigotes occurs, closing the *Leishmania* life cycle (Sacks and Noben-Trauth, 2002a).

2.3 Innate immunity - macrophages and dendritic cells

During the initial stage of infection, parasites have to breach the defense barriers of the innate immune system. Upon inoculation, the skin barrier is perturbed after which early phase mediators, like chemo-attractants and cytokines, such as MIP1, IL6 and TNFX, cause the first immune cells, neutrophils, to infiltrate. In a second stage, also other leukocytes infiltrate the site of infection, including natural killer cells, dendritic cells and macrophages (Shio et al., 2012). Both macrophages and dendritic cells are phagocytic leukocytes, which can differentiate from monocytes under the right stimulus. Monocytes originally derive from CD34$^+$ myeloid progenitor cells in the bone marrow. During circulation in the bloodstream, monocytes enter peripheral tissues where they mature into resident macrophages. During the steady state, the growth factor M-CFF, present in the plasma, predisposes monocytes to differentiate in an anti-inflammatory macrophage, termed a M2 phenotype (Martinez et al., 2006; Rosenzwajg et al., 1997). In addition, exposure to IL10, glucocorticoids and IL4 also promotes a non-classical form of M2 activation. These type 2 macrophages comprise an IL12^{low} and IL10^{high} phenotype, expressing high levels of scavenger (CD163), mannose (CD206), and galactose-type receptors. They are further characterized for their involvement in homeostatic processes, in clearing apoptotic cells, without releasing inflammatory mediators (Clare and Kharkrang, 2010; Mosser, 2003). On the other hand, during inflammation, increased levels of IFNG, pathogen-associated molecular patterns (PAMPS), TNF and GM-CSF, drive the polarization of monocytes to a classical M1 phenotype of macrophage. Type 1 macrophages are profiled by secretion of proinflammatory mediators IL12, IL23, IL1B, TNFX and IL6, playing a role in host defense against pathogens, anti-tumor responses and autoimmunity (Neu et al., 2013; Xu et al., 2013). A third phenotype, derived from the same progenitor under the influence of GM-CSF and IL4, has been regarded as a distinct cell type, namely the dendritic cells (DCs). DCs comprise a heterogeneous population of plasmacytoid (pDC) and myeloid dendritic cell (mDC). Overall, DCs share a CD1a^{high}, HLA-DR^{high}, CD209^{high} (DC-SIGN) phenotype. Compared to macrophages, DCs are less efficient in phagocytosis and more efficient in stimulating the adaptive immune system (Ferenbach and Hughes, 2008; Grassi et al., 1998; Rosenzwajg et al., 1997) (**Figure 3**).
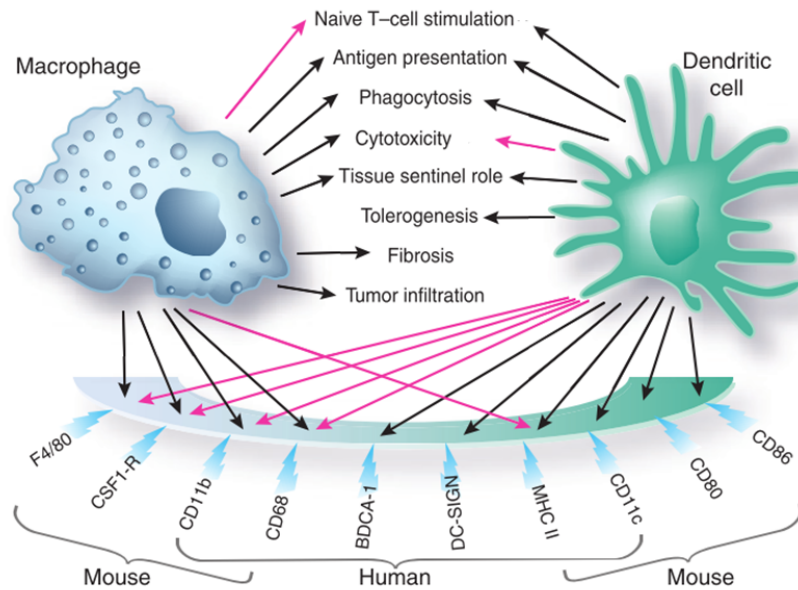
Figure 3: Functional and phenotypical characteristics of macrophage and dendritic cells (Ferenbach and Hughes, 2008).

2.4 Antigen processing and presentation

Upon encountering foreign material, both MFs and DCs, initiate the process of phagocytosis. During internalization, cargo material ends up in a phagosomal compartment. During maturation, the phagosome is trafficked through a cascade of increasingly acidified membrane bound structures. In macrophages, acidification occurs relatively early after phagocytosis, after which cargo is degraded robustly (Vyas et al., 2008). In contrast in DCs, the phagosomal lumen alkalinizes the first few hours after phagocytosis (Russell, 2007). As a consequence, degradation occurs slowly, resulting in the generation of many antigenic peptides. Once the pH is lowered after lysosomal fusion, cysteine proteases and cathepsins, cleave the MHCII-invariant chain (Ii). A small peptide, termed CLIP, remains in the MHCII binding groove. Subsequently, CLIP is exchanged for antigenic peptides, a process favored by the acidic pH and the chaperone molecule HLA-DM. As a result, MHCII molecules, loaded with antigenic fragments, are transported to the cell surface, where antigen presentation to T cells of the adaptive immune system can occur (Mantegazza et al., 2013; Neefjes et al., 2011) (**Figure 4**).
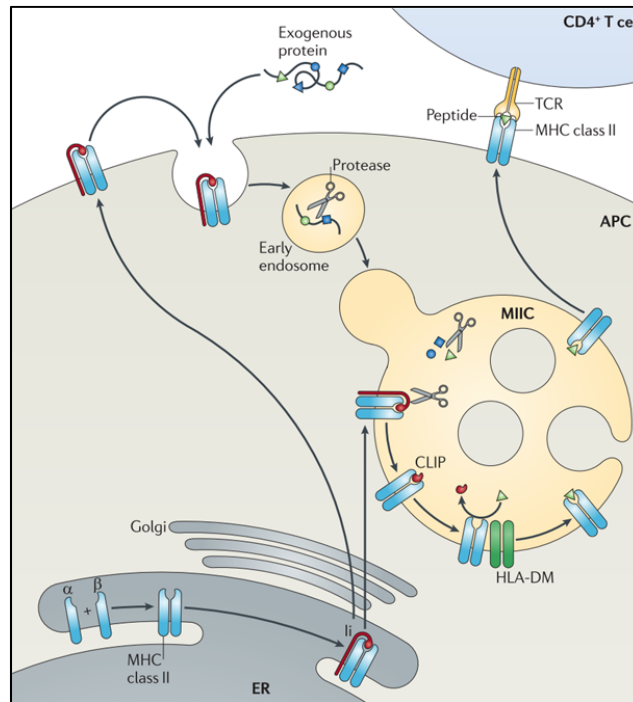
Figure 4: Antigen processing and MHCII loading pathway. MHCII molecules are synthesized after which they get loaded with antigens in a specialized compartment. Under influence of cathepsin activity and chaperone proteins (HLA-DM), the CLIP protein is exchanged by an antigenic peptide. The antigen loaded MHCII reaches the cell surface, activating CD4^{+} T cells (Neefjes et al., 2011).

2.5 Autophagy, an evolutionary ancient system rediscovered

Although the phagolysosomal pathway is a powerful tool to digest foreign material/pathogens, antigen presenting cells harbor a second proteolytic system comprising the autophagy machinery. The process of autophagy is known for its role in times of starvation or stress, by which the cell consumes its own organelles or cytoplasm to regain energy (Ma et al., 2013). The last years however, it has been appreciated that autophagy also plays a role in immune defense and antigen processing (Münz, 2009; Schmid et al., 2007; Yordy and Iwasaki, 2011).

Autophagy covers a complex system in which AuTophaGy related (*ATG*) genes and proteins interact to initiate, elongate and close autophagosomal compartments. Briefly, the initial phase, in which a multi-membrane is acquired, requires the activation of the ULK-Atg13-FIP200

complex, a process which under nutrient replete conditions is inhibited by the mammalian target of rapamycin (mTor). In a next step, Vps34 forms a complex with Beclin-1 and Vps15 to induce membrane elongation. Finally, two ubiquitin-like conjugation systems involving ATG7, promote the lipidation of the autophagy marker microtubule-associated protein 1A/1B-light chain 3 (LC3 or ATG8) leading to elongation and closure of autophagosomes. Upon completion, these multi-membrane compartments further mature and in a final step fuse with lysosomes. Foreign materials, as also scaffold proteins like the p62 protein (SQSTM1-p62), are digested by cathepsins, under the influence of the low pH (Deretic, 2006; Levine and Deretic, 2007).

The last years, an autophagy-related process has been described, in which phagocytosis occurs, after which the autophagy molecule LC3 is recruited to the membrane. A single membrane structure is formed, positive for LC3, a process termed "LC3 associated phagocytosis" (LAP). Martinez et al. highlighted the importance of LAP under homeostatic conditions. During clearance of apoptotic cells by macrophages, the process of LAP suppresses the release of pro-inflammatory mediators, preventing unwanted inflammation (Martinez et al., 2011). Indeed, LAP is indispensable as genetic defects among autophagy related genes result in the development of autoimmune diseases. Mutations in the *ATG5* gene are linked to the pathogenesis of systemic lupus erythematosus, whereas a malfunction in the *ATG16L1* gene influences the pathogenesis during Crohn´s disease (Hampe et al., 2007; Harley et al., 2008; Ma et al., 2013; Parkes et al., 2007).

Not only during homeostasis, but also when encountering pathogens, LAP is crucial. It has been well described that during mycobacterium infection, phagosomal maturation is blocked, promoting bacteria development. However, once infected macrophages recruit LC3 to bacteria containing phagosomes, compartment maturation proceeds following pathogen elimination (Gutierrez et al., 2004; Seto et al., 2013). In the presence of LC3, the intra-compartmental environment is altered. Previous studies have shown autophagy to change the activity of lysosomal proteases, affecting antigen processing (Dengjel et al., 2005; Romao et al., 2013). Taking a closer look at the consequence of autophagy related processes, it can be appreciated that once pathogens or the body´s own cells are degraded, a new pool of antigens is available

(Schmid et al., 2007). Consequently the MHC-peptide loading profile is changed, as also the activation status of the adaptive immune system (**Figure 5**).
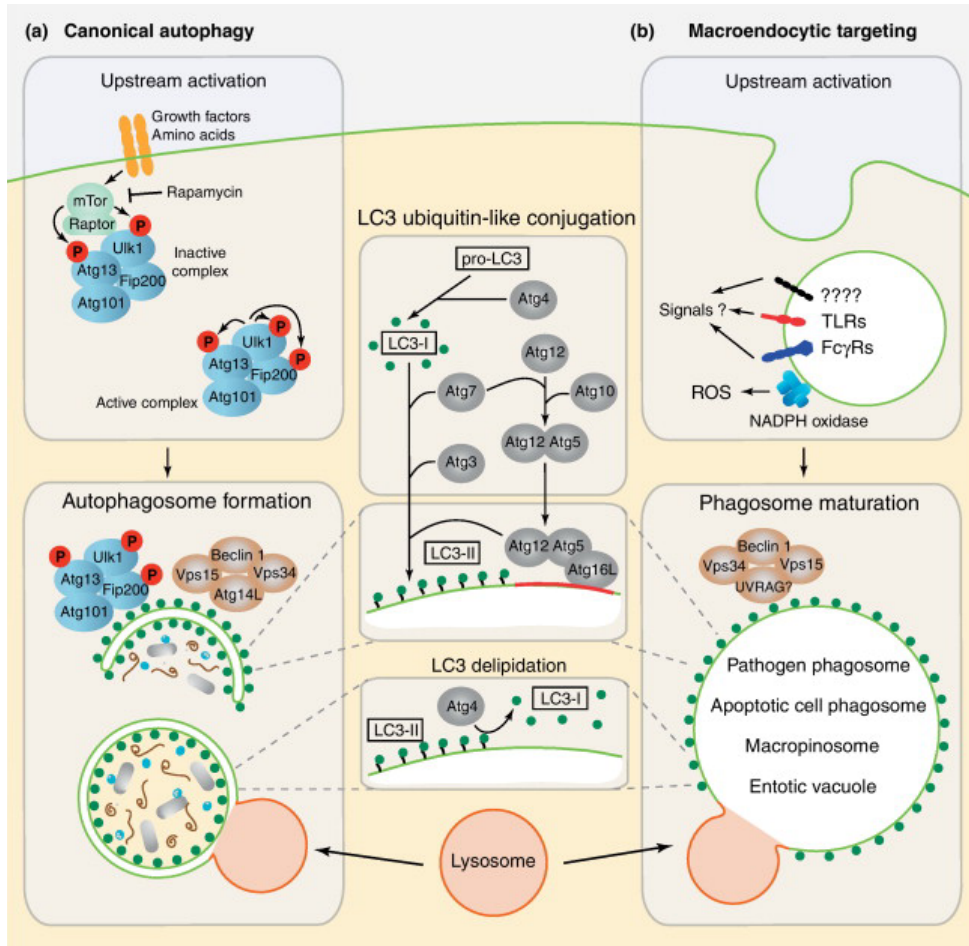
Figure 5: Autophagy and LAP. Conventional autophagy is induced in times of starvation or stress under influence of mTOR. In contrast LC3 associated phagocytosis occurs when TLRs, ROS, etc. induce LC3 to the phagosomal membrane. Although the initial engagement differs, both compartments become LC3 positive and fuse with lysosomes (Florey and Overholtzer, 2012).

2.6 Adaptive immunity – T lymphocytes

T lymphocytes are key players of the adaptive immune system. As guardians, they protect the body against invading pathogens. Although distinct T cell subsets exist, with their unique features, they all have one entity in common, namely the expression of a T cell receptor (TCR). The TCR consists of both constant and variable regions, of which the latter one is determining antigen specificity. The TCR is able to recognize antigens, when loaded in a MHC molecule on the surface of antigen presenting cells. Each T cell however bears a distinct set of different receptors, of which the diversity depends on the recombination of genes encoding the receptors (Davis and Bjorkman, 1988; Jung and Alt, 2004). The cytotoxic CD8$^+$ T cells recognize epitopes presented by MHCI, whereas CD4$^+$ cells recognize antigens displayed on MHCII molecules of antigen presenting cells (APC), such as macrophages and dendritic cells. Upon matching, a first activation signal is provided. The second signal is provided by the APS´s co-stimulatory receptor CD80 or CD86 which crosslinks with the T cell molecule CD28. A third signal is provided by the APC as well, as cytokine production (Lenschow et al., 1996). Upon activation, naïve T cells start to proliferate, undergoing clonal expansion. Depending on the cytokine environment, the terminal lineage commitment and the related cytokine expression profile are determined. In humans, distinct T cell subsets are identified based on the cell surface markers expressed or by the effector molecules produced by the T cell population. Interestingly, T cell can also have a mixed phenotype which can polarize from one distinct phenotype to another. Broadly, T cells can be categorized in: cytotoxic (CD8$^+$), natural killer, regulatory (FoxP3$^+$) and T-helper (CD4$^+$) cells. Of special interest are the T-helper (Th) cells as in humans new subtypes have been identified, changing the current view on the T-helper cell paradigm (Alexander and Brombacher, 2012). Besides the classical Th1 and Th2 subsets, the identification of Th9, Th17 and Th22 T cells shed light on various disease related pathologies (Brand et al., 2006; Soussi-Gounni et al., 2001; Walsh and Mills, 2013).

The well-defined Th1 cells are maintained by a strong IL12 production by antigen presenting cells and are characterized by the transcription factor T-bet. T-bet in turn, increases the expression of IFNG, which contributes in activating macrophages, promoting immunity against intracellular

pathogens, such as *Mycobacterium tuberculosis* and *Leishmania* parasites. In contrast, mainly IL4, besides IL33 and IL25, increase the expression of GATA binding protein 3 (GATA3), maintaining Th2 cell lineage commitment. Th2 responses drive an antibody mediated immune response, to eliminate extracellular pathogens such as metazoan parasites (e.g. *Nippostrongylus brasiliensis*). In addition, a Th2 mediated IL10 production counterbalances the proinflammatory Th1 responses. Also Th9 cells play a role during nematode infections. Although they have been only characterized recently, the critical role of their main cytokine, IL9, in worm expulsion and IgG1/ IgE production was demonstrated years ago. Two other Th subsets, Th17 and Th22, have drawn attention for their role in auto-immune diseases, tissue inflammation and host defense against fungi and bacteria like Candida and Staphylococcus. Both IL17 and IL22 have been shown to play a role during infection, where IL17 promotes inflammation and IL22 exerts a tissue protective role (**Figure 6**).
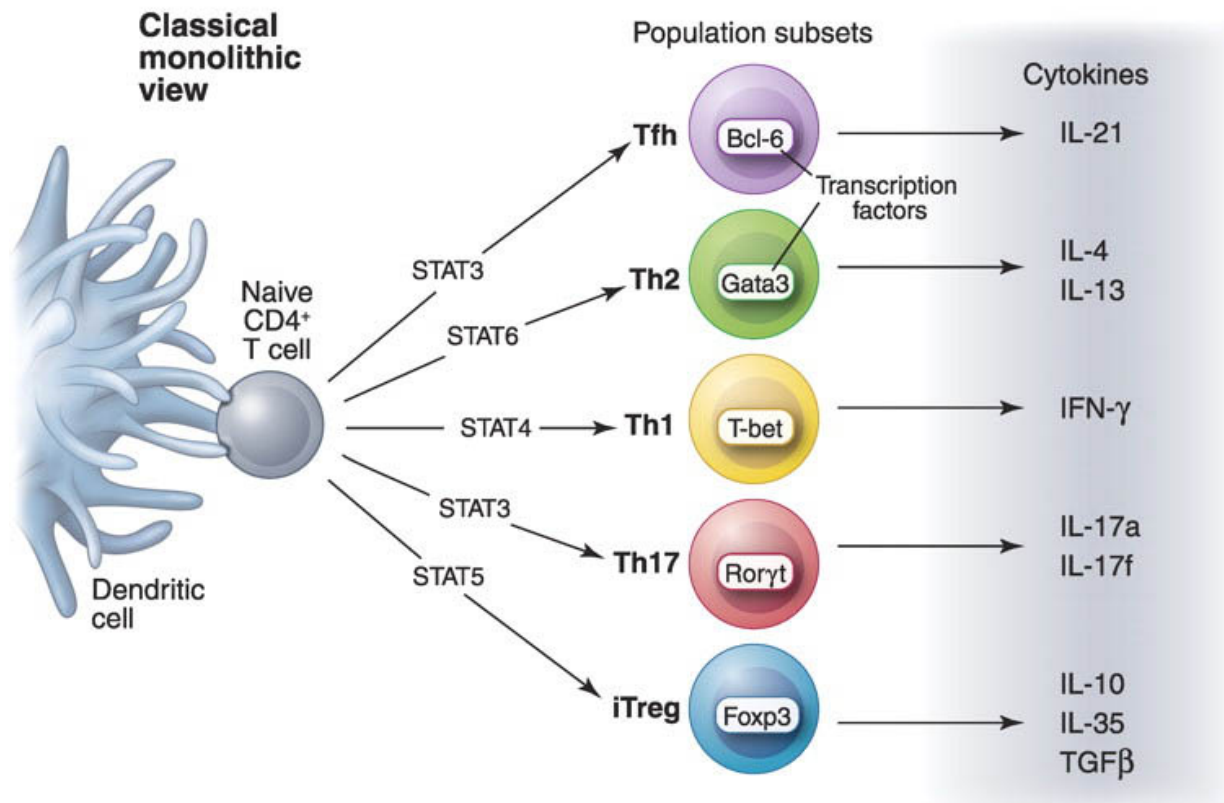
Figure 6: T helper subsets. Once naïve CD4^{+} T cells receive a certain stimulus (antigen + cytokine + costimulation), a differentiation process occurs by which T cell polarize to a specific T-helper phenotype (O'Shea and Paul, 2010).

All T-helper subsets work in hand to clear pathogens, preventing exaggerated inflammation. Once the infection is resolved, the majority of the effector T cells die, known as the contraction period. A minority survives and further develops into a memory T cell phenotype (MacLeod et al., 2010). During a secondary infection, memory T cells offer an early protection. Already upon low levels of antigens, an immune response can be mounted by which disease development is prevented. Based on this immunological concept, vaccines have been developed, in the hope they provide protection against pathogens. In the last years however, the view on vaccine development has been changed (Campion et al., 2014; Su and Davis, 2013). By the development of new techniques, several studies could show that the memory T cell repertoire already contains T cells specific for antigens the body has not encountered before. Already a decade ago, Selin and Welsh stated: "No one is naïve", demonstrating murine and human T cells to possess a high

level of cross reactivity for heterologous viruses like Vaccinia virus (VV), Lymphocytic Choriomeningitis virus (LCMV) and Pichinde virus (PV) (Welsh and Selin, 2002). These data are reinforced by Campion et al. who reveal unexposed donors to contain HIV-1 specific memory CD4^{+} T cells (Campion et al., 2014). More data are confirming these findings, showing individuals, seronegative for HIV, herpes simplex virus (HSV) and cytomegalovirus (CMV) to possess a number of functional virus specific memory CD4^{+} T cells (Su et al., 2013). This memory is absent in cord blood, strengthening the hypothesis that the probability to develop cross memory T cells increases with the number of successive infections. The question is now raised, whether vaccines should aim to develop new memory T cells or to stimulate the cross reactive memory T cells of interest, to expand.

2.7 *Leishmania* infection – a general overview

Much is known about *Leishmania* infection in mice, as *Leishmania* has been used as an infection model to dissect the Th1/Th2 response. In general, C57BL/6 and BALB/c mice are used to examine the influence of Th subset polarizations, as they are genetically predisposed to develop a Th1 and Th2 phenotype, respectively. During *Leishmania* infection, it has been characterized that a predominant Th1 response leads to a healing phenotype in C57BL/6 mice. Healing is characterized by the presence of IFNG and TNFX, leading to activation of infected macrophages, which by increasing oxidative stress are able to eliminate intracellular pathogens. In contrast, an antibody-mediated Th2 response leads to disease development in susceptible BALB/c mice, in which predominantly IL4, IL5 and/or IL13 are shaping the cytokine milieu (Chatelain et al., 1992; Sacks and Noben-Trauth, 2002b; Sypek et al., 1993).

During infection distinct cell types, primarily neutrophils, macrophages and dendritic cells, are infected, of which the latter two are responsible to activate the adaptive immune system. Macrophages, the parasite´s final host cell, are then able to internalize free moving promastigotes and infected (apoptotic) neutrophils. Depending on the activation status of the macrophage, transformation into amastigotes or parasite elimination occurs. Classical

macrophage activation is mediated primarily by IFN, originating from Th1 cells, which promote macrophages to produce oxidative and nitrosative stress. Th1 responses induce the expression of inducible nitric oxide synthase (iNOS), driving the L-arginine metabolism towards nitric oxide (NO) production, leading to parasite elimination. However in the presence of Th2 related cytokines, IL-4 and IL-13, arginase in macrophages is up regulated, catabolizing L-arginine to increase polyamine synthesis, favoring parasite growth and transformation and so, disease dissemination (Kropf et al., 2005; Muleme et al., 2009). Using genetically predisposed mice systems, the role of distinct cell types of interest can be investigated. However, the Th1-Th2 paradigm does completely not hold true in humans. A more complex interplay between various cell populations occurs (Alexander and Brombacher, 2012). Focusing on the naturally occurring intradermal, in contrast to intravenous, route of infection, the parasites also encounter dermal DCs and monocyte derived DC populations. DCs are known to have a lower phagocytosis capacity compared to macrophage, nonetheless DCs are susceptible to *Leishmania* infection (Liu and Uzonna, 2012). Due to their high potential to activate T cells, DCs have a decisive role in shaping adaptive immune responses. Indeed, a strong DC-dependent IL12 production has been reported to drive Th responses towards a protective Th1 phenotype during *Leishmania* infection (León et al., 2007). In addition, DCs are able to sustain parasite survival and growth, reinforcing the hypothesis that DC play a role during persistent infection in maintaining a *Leishmania* specific immune response (Prina et al., 2004).

2.8 *Leishmania* – immune evasion strategies

To establish a successful infection, *Leishmania* parasites have to circumvent host immune defense mechanisms. *Leishmania* promastigotes are equipped with several virulence factors, enabling parasites to survive. The metalloproteinase GP63 is expressed on the outer membrane, making the parasite resistant to complement lysis. In addition, GP63 inactivates lysosomal proteases preventing parasite digestion inside macrophages (Gomez et al., 2009; Shio et al., 2012). A second virulence factor, lipophosphoglycan (LPG), also remains on the surface of

Leishmania promastigotes. Upon promastigote entry, in the macrophage host cell, LPS prevents compartment maturation and acidification. A slower maturation process secures parasite transformation into the amastigote stage (Moradin and Descoteaux, 2012). Moreover, during infection various signaling cascades, such as PKC activity, JAK/STAT and MAPK pathways, are modulated (Privé and Descoteaux, 2000). Subsequently, expression of proinflammatory mediators is suppressed. Besides virulence factors, *Leishmania* secreted antigens possess immunosuppressive properties. These antigen fractions have been reported to enhance IL4 and decrease IFNG production by T cells, shifting adaptive immune responses towards a susceptible Th2 phenotype (Gupta et al., 2013; Tabatabaee et al., 2011). In all, the ability of *Leishmania* parasites to sustain infection depends to a large extent on the parasites´ immune evasion potential.

3. Aims and hypothesis

This project was funded by the Carl Zeiss Foundation, in which 4 collaborative research groups aimed to investigate the effects of different classes of intracellular pathogens (viruses, bacteria and parasites) on the biology of differentially activated human myeloid cells. In particular immune evasion strategies targeting migration, phagolysosomal maturation, antigen presentation and apoptosis will be investigated.

The focus of my PhD project was put on the parasite *Leishmania*, causing still 20,000 to 30,000 people to die yearly. Therefore an increased understanding of host pathogen interactions is required for which have the hypothesis:

"Apoptotic *Leishmania* exploit the host´s autophagy machinery to reduce T cell mediated parasite elimination"

To assess the above hypothesis we aimed to investigate the following aspects:

PARASITOLOGY

(i)   as previous work already showed apoptotic *Leishmania* parasites to be crucial for disease development in mice, we further characterized the *Leishmania* apoptotic population. Following the guidelines of Nomenclature on Cell Death the *Leishmania* parasite population was profiled for distinct morphological characteristics, DNA content / degradation and phosphatidylserine exposure.

INNATE IMMUNITY

(ii)   few is known about the interaction of human myeloid cells with *Leishmania* parasites. We focused the interaction *Leishmania major* parasites with distinct antigen presenting cells, comprising macrophages and dendritic cells. The suitability of proinflammatory, anti-inflammatory macrophages and dendritic cells as host cells for *Leishmania* parasites was investigated.

ADAPTIVE IMMUNITY

(iii)   macrophages can serve as host cell for the parasite and as antigen presenting cell, inducing adaptive immune responses. As T cell responses are crucial during *Leishmania* infection, we aimed to investigate, in a human *in vitro* system, how *Leishmania* parasites modulate proliferative T cell responses.

4. Material and methods

4.1 Materials

4.1.1 Chemicals and compounds

ß-Mercaptoethanol	Sigma-Aldrich, Steinheim (GER)
Acrylamide-Bis 30 %	SERVA Electrophoresis GmbH, Heidelberg (GER)
Agarose, LE	Biozym Scientific GmbH, Hessisch Oldendorf (GER)
Ammonium chloride (0.15 M)	Medienküche PEI, Langen (GER)
Ammonium persulfate (APS)	SERVA Electrophoresis GmbH, Heidelberg (GER)
Aqua distilled	Medienküche PEI, Langen (GER)
AZD-8055	Selleckchem, Houston (USA)
Bafilomycin-A1	Sigma-Aldrich Chemie, Steinheim (GER)
Bovine Serum Albumin	Sigma-Aldrich, Steinheim (GER)
CASYton	Roche Innovatis AG, Reutlingen (GER)
Difco™ Brain Heart Infusion Agar	Becton Dickenson, Sparks (USA)
Diff Quick Fixative, Solution I and II	Medion Diagnostics, Düdingen (CH)
Dimethylsulfoxid	Sigma-Aldrich Chemie, Steinheim (GER)
DNA loading buffer (10x)	New England Biolabs, Ipswich (USA)
dNTP: dATP, dCTP, dGTP, dTTP (100mM)	PeqLab, Erlangen (GER)

Dithiothreitol (DTT)	Sigma-Aldrich Chemie, Steinheim (GER)
ECL Western Blotting Detection Reagents	GE Healthcare, Buckinghamshire (UK)
Ethanol, absolute	VWR, Bruchsal (GER
FACS Clean	Medienküche PEI, Langen (GER)
FACS Flow (Sheath Solution)	Medienküche PEI, Langen (GER)
FACS Rinse	Medienküche PEI, Langen (GER)
FACS Staining buffer	Medienküche PEI, Langen (GER)
Fetal Calf Serum, heat inactivated	Sigma-Aldrich Chemie
Glutamine (L-Glutamine)	Biochrom AG, Berlin (GER)
Glycerol (99 %)	Citifluor, London (UK)
HEPES-Buffer (1 M)	Biochrom AG, Berlin (GER)
Histopaque 1077	PAA, Pasching (AUT)
Human recombinant Granulocyte Macrophage Colony Stimulation Factor (GM-CSF)	Bayer Healthcare Pharmaceutical, Leverkusen (GER)
Human recombinant Macrophage Colony Stimulating Factor (M-CSF)	R&D Systems, Minneapolis (USA)
Human Serum Type AB	Lonza, Walkersville (USA)
Hydrochloric acid (37 %)	VWR International, Fontenay Sous Bois (FR)
Hygromycin B, solution	Invitrogen, San Diego (USA)

Immersion Oil	Carl Zeiss, Jena (GER)
Isopropyl alcohol	Sigma-Aldrich Chemie, Steinheim (GER)
LY294002	Selleckchem, Houston (USA)
Milk powder	EDEKA (GER)
Nuclease free water	Promega Corporation, Madison (USA)
Paraformaldehyde	Sigma-Aldrich Chemie, Deisenhof (GER)
Penicillin/ Streptomycin	Biochrom AG, Berlin (GER)
Phosphate buffered saline (1x PBS) wo/ $Ca^{2+,}\,Mg^{2+}$; pH 7.1	Medienküche PEI, Langen (GER)
PI-103	Selleckchem, Houston (USA)
ProLong® Gold Antifade Reagent	Invitrogen, Darmstadt (GER)
Rabbit Blood, defibrinated	Elocin-Lab GmbH, Gladbeck (GER)
Rapamycin	Cayman Chemical Company, Ann Arbor (USA)
Ringer-Solution	B. Braun Melsungen AG, Melsungen (GER)
RNase AWAY	VWR, Darmstadt (GER)
Roswell Park Memorial Institute (RPMI) 1640 Medium	Sigma-Aldrich Chemie, Steinheim
Saponin from *Quillaja* bark	Sigma-Aldrich Chemie, Steinheim (GER)
Sodium Acetat	Sigma-Aldrich Chemie, Deisenhof (GER)
Sodium Azide	Sigma-Aldrich Chemie, Deisenhof (GER)

Sodium Chloride   Sigma-Aldrich Chemie, Deisenhof (GER)

Sodium dodecyl sulfate (SDS)   Medienküche PEI, Langen (GER)

Sodium Hydroxide 1M   Merck, Darmstadt (GER)

TEMED   Serva, Heidelberg (GER)

Trishydroxylmethylaminomethan (TRIS)   Medienküche PEI, Langen (GER)

Tween 20   Sigma-Aldrich Chemie, Steinheim (GER)

Western Blot Detection Substrate   GE Healthcare, Buckinghamshire (UK)

Wortmannin   Sigma-Aldrich Chemie, Steinheim (GER)

4.1.2 Culture medium and buffers

Novy-Nicolle-McNeal blood agar medium	16.6 %	Rabbit blood defibrinated
	16.6 %	1x PBS
	66.2 %	Brain Heart Infusion Agar
	66.2 U/ml	Penicillin
	66.2 µg/ml	Streptomycin

Leishmania promastigote medium		RPMI 1640 Medium
	5 %	FCS
	2 mM	L-Glutamine
	50 µM	β-Mercaptoethanol
	100 U/ml	Penicillin
	100 µg/ml	Streptomycin

	10 mM	HEPES Buffer
Leishmania amastigote medium		RPMI 1640 Medium
	10 %	FCS
	3 mM	L-Glutamine
	50 µM	β-Mercaptoethanol
	100 U/ml	Penicillin
	100 µg/ml	Streptomycin
		pH 5.5, adjusted with 38 % HCl
		Sterile filtrated
Complete-(macrophages) Medium		RPMI 1640 Medium
	10 %	FCS
	2 mM	L-Glutamine
	50 µM	β-Mercaptoethanol
	100 U/ml	Penicillin
	100 µg/ml	Streptomycin
	10 mM	HEPES Buffer
Macrophage generation - Wash buffer		1x PBS
	5 %	Complete-Medium
MACS-Buffer pH 7.2		1x PBS
	2 mM	EDTA

0.5 %	BSA

4.1.3 Buffers and solutions of immunofluorescence applications

PFA fixation solution		PBS
	4 %	PFA

Buffer 1 (washing)		PBS
	1 %	FCS
	1 %	BSA
	1 %	Human serum

Buffer 2 (permeabilization)		PBS
	1 %	FCS
	1 %	BSA
	1 %	Human serum
	0.5 %	Saponin
		Sterile filtrated

4.1.4 Buffers and solutions for SDS page and western blot

Laemmli buffer		Aqua bidest
	4.125 M	Glycerol
	10 %	SDS
	0.6 M	DTT

	180 µl	Bromphenol blue
Running buffer		Aqua bidest
	0.1 %	SDS
	1.44 %	Glycine
Separation gel buffer		Aqua bidest
	1.5 M	Tris
	0.4 %	SDS
		pH 6.8 with HCl
Stacking gel buffer		Aqua bidest
	500 mM	Tris
	0.4 %	SDS
		pH 8.8 with HCl
TBST solution		Aqua bidest
	0.5 %	Tween
	0.14 M	NaCl
	10 mM	Tris
	1 mM	NaN_3
		pH 8.0
Blotting buffer		Medium kitchen PEI

Blocking solution		TBST solution
	5 %	BSA

Antibody dilution buffer		TBST solution
	5 %	BSA
	0.02 %	NaN$_3$ (primary antibody only)

4.1.5 Human leukocytes

Human peripheral blood mononuclear cells (PBMCs) were obtained from buffy coats of healthy German donors from the DRK-Blutspendedienst in Frankfurt. Subsequently monocytes were isolated and differentiated in macrophages or dendritic cells as described below.

4.1.6 *Leishmania* strains

Leishmania major isolate MHOM/IL/81/FEBNI originally obtained from a skin biopsy of an Israeli patient. Parasites were kindly provided by Dr. Frank Ebert (Bernhard Nocht Institute for Tropical Medicine, Hamburg, GER).

Leishmania major dsRed: MHOM/IL/81/FEBNI isolate genetically transfected with the red fluorescent dsRed gene.

Leishmania aethiopica: isolate MHOM/ET/72/L100 Z14

Leishmania donovani: isolate MHOM/ET/67/HU3 Z18

4.1.7 Ready to use kits

CD14 MicroBeads, human	Miltenyi Biotec,, Bergisch Gladbach (GER)
ImProm-II Reverse Transcription System	Promega, Mannheim (GER)
MESA Blue qPCR MasterMix Plus for SYBR	Eurogentec, Köln (GER)
RNeasy Plus Mini kit	Qiagen, Hilden (GER)
Stemfect™ RNA Transfection kit	Miltenyi Biotec,, Bergisch Gladbach (GER)
Cytokine bead array	BD Pharmingen, Heidelberg (GER)
TUNEL assay	Roche Diagnostics, Mannheim (GER)

4.1.8 Antibodies

Rabbit, α-LC3	Cell Signaling, Danvers (USA)
Goat, α-rabbit-HRP	Santa Cruz, Heidelberg (GER)
Rabbit, α-ATG-7	Cell Signaling, Danvers (USA)
Rabbit, α-beclin-1	Thermo Scientific (Pierce), Bonn (GER)
Mouse, α-human-IgG1κ Isotype (APC)	BD Pharmingen, Heidelberg (GER)
Mouse, α-human-IgG2bκ Isotype (APC)	BD Pharmingen, Heidelberg (GER)
Mouse, α-human-IgG1κ Isotype (PE)	R&D Systems, Minneapolis (USA)
Mouse, α-human- IgG1κ Isotype (FITC)	BD Pharmingen, Heidelberg (GER)
Mouse, α-human-IgG2aκ Isotype (Pacific Blue)	BD Pharmingen, Heidelberg (GER)
Mouse, α-human-IgG1κ Isotype (V450)	BD Pharmingen, Heidelberg (GER)

Mouse, α-human-CD3 (APC)   BD Pharmingen, Heidelberg (GER)

Mouse, α-human-CD45RO (APC)   BD Pharmingen, Heidelberg (GER)

Mouse, α-human-CD4 (APC)   BD Pharmingen, Heidelberg (GER)

Mouse, α-human-CD8 (Pacific Blue)   BD Pharmingen, Heidelberg (GER)

Mouse, α-human-CD14 (Pacific Blue)   BD Pharmingen, Heidelberg (GER)

Mouse, α-human-MHC II (V450)   BD Pharmingen, Heidelberg (GER)

Mouse, α-human-CD206 (PE)   BD Pharmingen, Heidelberg (GER)

Mouse, α-human-CD209 (APC)   BD Pharmingen, Heidelberg (GER)

Mouse, α-human-CD1a (FITC)   BD Pharmingen, Heidelberg (GER)

Mouse, α-human-CD163 (PE)   BD Pharmingen, Heidelberg (GER)

Mouse, α-human-CD80 (V450)   BD Pharmingen, Heidelberg (GER)

Mouse, α-human-CD83 (APC)   BD Pharmingen, Heidelberg (GER)

Mouse, α-human-CD86 (FITC)   BD Pharmingen, Heidelberg (GER)

Mouse, α-human-CR1 (PE)   BD Pharmingen, Heidelberg (GER)

Mouse, α-human-CR3 (PE)   BD Pharmingen, Heidelberg (GER)

Mouse, α-human-GATA3 (Alexa Fluor 647)   BD Pharmingen, Heidelberg (GER)

Mouse, α-human-T-bet (V450)   BD Pharmingen, Heidelberg (GER)

4.1.9 Marker and Dyes

Annexin-V-Alexa Fluor 647   Invitrogen Molecular Probes, Eugene (USA)

Bromphenol blue dye   Serva, Heidelberg (GER)

5(6)-Carboxyfluorescein diacetate N-   Sigma Aldrich Chemie, Steinheim (GER)
succinimidyl ester

DAPI	Molecular Probes Invitrogen (GER)
1 kb DNA Ladder	New England Biolabs, Ipswich (USA)
100 bp DNA Ladder	Promega, Madison (USA)
Ethidium bromide	Merck, Darmstadt (GER)
Full-Range Rainbow Molecular Weight Marker	GE Healthcare, Buckinghamshire (UK)
LysoTracker®	Molecular Probes Invitrogen (GER)
Propidium iodide	Sigma Aldrich Chemie, Steinheim (GER)

4.1.10 Oligonucleotides

Primers	**Eurofins MWG Operon, Ebersberg (GER)**
Beclin1_a Fwd	CCATGCAGGTGAGCTTCGT
Beclin1_a Rew	GAATCTGCGAGAGACACCATC
Beclin1_b Fwd	GGTGTCTCTCGCAGATTCATC
Beclin1_b Rew	TCAGTCTTCGGCTGAGGTTCT
Beclin1_c Fwd	ACCTCAGCCGAAGACTGAAG
Beclin1_c Rew	AACAGCGTTTGTAGTTCTGACA
GAPDH Fwd	GAGTCAACGGATTTGGTCGT
GAPDH Rew	TTGATTTTGGAGGGATCTCG
ATG-7 Fwd	CTGCCAGCTCGCTTAACATTG

ATG-7 Rev	CTTGTTGAGGAGTACAGGGTTTT
All Star Negative control siRNA	Qiagen, Hilden (GER)

4.1.11 Enzymes

Taq Polymerase	New England Biolabs, Ipswich (USA)

4.1.12 Laboratory supplies

Cell culture flasks with filter (25 cm^2, 75 cm^2)	BD labware Europe, Le Pont de Claix (FR)
Cell culture plates (96 well round/V-shaped bottom and 6 well flat bottom)	Sarstedt, Nümbrecht (GER)
Cellfunnel (single; double)	Tharmac GmbH, Waldsolms (GER)
Cellspin filter cards (one/two hole/s)	Tharmac GmbH, Waldsolms (GER)
Centrifuge tubes (15 ml; 50 ml)	BD labware Europe, Le Pont de Claix (FR)
Chamber Slide^{TM} 8 well	Thermo Scientific, Bonn (GER)
Cover Slide (24 x 50 mm)	VWR, Darmstadt (GER)
Cryo tubes (2 ml)	Greiner bio-one, Frickenhausen (GER)
Cytoslides one circle, uncoated	Tharmac GmbH, Waldsolms (GER)
FACS tubes (2 ml)	Micronic, Lelystad (NL)
FACS tubes	BD labware Europe, Le Pont de Claix (FR)

Glass cover (24 x 50 mm)	VWR, Darmstadt (GER)
Hyperfilm^{TM} ECL	GE Healthcare, Buckinghamshire (UK)
Hybond ECL blot membrane	GE Healthcare, Buckinghamshire (UK)
Manufix$^{x^®}$ sensitive (S)	B. Braun Melsungen AG, Melsungen (GER)
Microcentrifuge tubes (1.5 ml; 2.0 ml)	Eppendorf, Hamburg (GER)
Microtest plates, 96-well (V-Bottom)	Sarstedt, Nümbrecht (GER)
Millipore Express® PLUS Membrane Filters, polyethersulfone, 0.22 µm, 13 mm	Merck Millipore, Billerica (US)
Nitril gloves	Ansell Healthcare, Brussels (CH)
Light Cycler 96-well plates with foil, white	Roche Applied Science, Darmstadt (GER)
Pipette tips (1-10 µl; 10-200 µl; 100-1000 µl)	Sarstedt, Nümbrecht (GER)
Pipette filter tips (1-10 µl; 10-200 µl; 100-1000 µl)	Nerbe plus, Winsen/Luhe (GER)
PCR Tube Multiply® Pro (0.2 ml)	Sarstedt, Nümbrecht (GER)
Polypropylene Tubes (PP) – Round Bottom	Greiner Bio-One, Kremsmünster (AT)
Serological pipettes, sterile	Greiner Bio-One, Kremsmünster (AT)
Tissue culture dishes (94 mm x 16 mm)	Greiner Bio-One, Kremsmünster (AT)
Transfer pipette (3.5 ml)	Sarstedt, Nümbrecht (GER)
Whatman paper gel blotting	VWR, Darmstadt (GER)

4.1.13 Instruments

Centrifuges

BIOLiner Buckets (75003670; 75003668)	Thermo Scientific, Dreieich (GER)
Centrifuges 5430 and 5430R	Eppendorf, Hamburg (GER)
Centrifuge "Heraeus Megafuge 40R"	Thermo Scientific, Dreieich (GER)
Cytocentrifuge Cellspin II Universal 320R	Tharmac GmbH, Waldsolms (GER)
Sprout Mini-Centrifuge	Biozym, Hamburg (GER)

Electrophoresis and Blotting

Power Supply "PowerPac™ 200/2.0"	Bio-Rad, München (GER)
Horizontal electrophoresis equipment	Biotec-Fischer, Reiskirchen (GER)
UV-Transilluminator GenoView	VWR International, Darmstadt (GER)
Mini-PROTEAN® Tetra Cell	Bio-Rad, München (GER)
TE 70 Semi-Dry Transfer Unit	GE Healthcare, Buckinghamshire (UK)

Flow Cytometry

Flow Cytometer LSR II	Becton Dickinson, Heidelberg (GER)

Imaging

AxioCam IC	Carl Zeiss, Jena (GER)

Microscope Axiophot   Carl Zeiss, Jena (GER)

Microscope Axio Vert.A1   Carl Zeiss, Jena (GER)

Microscope Primo Star   Carl Zeiss, Jena (GER)

Microscope LSM7 Live   Carl Zeiss, Jena (GER)

Incubators

CO^2-Incubator Forma Series II Water Jacket   Thermo Scientific, Marietta (US)

CO^2 incubator, Heraeus Auto Zero   Thermo Scientific, Dreieich (DE)

PCR Thermo Cycler

LightCycler® 480 System   Roche Applied Science, Mannheim (GER)

Personal Cycler   Biometra, Göttingen (GER)

Others

Analytical balance KB BA 100   Sartorius, Göttingen (DE)

AutoMACS Pro separator   Miltenyi Biotec, Bergisch Gladbach (GER)

CASY Modell TT   Roche Innovatis AG, Reutlingen (GER)

Freezer (-20°C)   Bosch, Stuttgart (DE)

Freezer U725-G (-80°C)   New Brunswick, Eppendorf, Hamburg (DE)

Laminar flow workbench MSC-Advantage   Thermo Scientific, Dreieich (DE)

Magnetic stirrer IKA® C-MAG HS7	IKA®-Werke, Staufen (DE)
Multichannel Pipette (Research® plus)	Eppendorf, Hamburg (DE)
NanoDrop 2000c	PeqLab, Erlangen (GER)
Nalgene™ Mr. Frosty Freezing Container	Thermo Scientific, Dreieich (DE)
Neubauer improved cell counting chamber (depth 0.1 mm, 0.02 mm)	VWR International, Darmstadt (DE)
Nitrogen container "Chronos"	Messer, Bad Soden (DE)
pH Meter PB-11	Sartorius, Göttingen (DE)
Pipette controller (accu-jet® pro)	BRAND, Wertheim (DE)
Pipettes (Research® plus: 0.5-10 µl; 10-100 µl; 20-200 µl; 100-1000 µl)	Eppendorf, Hamburg (DE)
Recirculating cooler	Julabo, Seebach (DE)
Semi-dry transfer unit TE 77 PWR	Amersham Biosciences, Freiburg (GER)
Thermomixer comfort (1.5 ml)	Eppendorf, Hamburg (DE)
Thermomixer 5437 (1.5 ml)	Eppendorf, Hamburg (DE)
UV-Vis Spectrophotometer NanoDrop 2000c	PeqLab, Erlangen (DE)
Vortex mixer VV3	VWR International, Darmstadt (DE)
Water bath	Köttermann VWR International, Darmstadt (DE)

Software

Axiovision 4.7	Carl Zeiss, Jena (DE)
BD Diva software v6.1.3	Becton Dickinson, Heidelberg (DE)
FlowJo vX	Miltenyi Biotec GmbH, Bergisch Gladbach (DE)
ImageJ/Fiji	Open source
GraphPad Prism 6	GraphPad Software, Inc., La Jolla (USA)
LightCycler® software v3.5	Roche Applied Science, Mannheim (GER)
Mendeley Desktop Version 1.8.4	Mendeley Ltd., London (UK)
Microsoft® Office 2010	Microsoft, Redmont (US)
NCBI Primer BLAST®	National Library of Medicine, Bethesda (US)
Inkscape	Open source, drawing program

4.2 Methods

4.2.1 Cell culture

To work under sterile conditions, cell culture work was performed in a laminar air flow workbench under endotoxin free conditions. Both human cells and protozoan parasites were cultivated in humidified incubators.

4.2.2 Methods in parasitology

4.2.2.1 Culturing *Leishmania* promastigotes

Leishmania major promastigotes were stored at liquid nitrogen. Upon thawing, cultivation in biphasic Novy Nicolle McNeal (NNN) blood agar medium occurred at 27°C and 5% CO_2. The first days, parasites reside in the logarithmic growth phase dividing exponentially. After 6-7 days, promastigotes reached the stationary growth phase, after which cultures were passaged up to 10 serial passages before new promastigotes were thawed. For counting and passaging parasites, a hemocytometer was used (Neubauer chamber slide, depth 0.02 mm).

Transgenic dsRed expressing *Leishmania* parasites were cultured using the same cultivation system. In addition, the culture medium was supplemented with the antibiotic Hygromycin (20µg/ml).

4.2.2.2 Generation of soluble *Leishmania* antigen (SLA)

To generate a crude *Leishmania* extract, parasites were collected from a stationary phase culture. After washing with PBS twice, parasites were resuspended in a small volume of PBS after which parasites were lysed by repeatedly freezing (liquid nitrogen) and thawing (water bath, 37°C) (12 cycles).

4.2.2.3   Generation of axenic *Leishmania* amastigotes *in vitro*

For the generation of the amastigote life stage, promastigotes (3-4 wells) were harvested during the logarithmic growth phase. After 3 days in culturing in liquid medium supplemented with FCS, parasites were washed (1400 g, 20°C). The pellet was resuspended in AAM (acidified medium) and washed to remove excessive liquid medium. Next, parasites were incubated in 25 cm^2 culture flasks (20 x 10^6 *Lm*/ml) for 10-14 days at 33°C, 5% CO_2. During this time, parasite transform in the droplet shaped amastigote form (without a visible flagellum).

4.2.3 Assessing apoptosis

4.2.3.1   TUNEL assay

To assess apoptosis, parasites were treated with 25 µM staurosporine or 25 µM miltefosine for 48 h. DNA fragmentation was analyzed by an in situ cell death detection kit, based on terminal deoxynucleotidyl transferase dUTP nick end labeling (TUNEL), as described by the manufacturer. Briefly, *Leishmania* parasites were centrifuged on cytospins slides. Slides were air-dried and fixed following incubation with the TUNEL reaction mixture that contains TdT and fluorescein-dUTP. During this incubation period, TdT catalyzes the addition of fluorescein-dUTP at free 3'-OH groups in single- and double-stranded DNA. After washing, the label incorporated at the damaged sites of the DNA is visualized by flow cytometry and/or fluorescence microscopy.

4.2.3.2   Phosphatidylserine exposure

To assess phosphatidylserine exposure, *Leishmania* parasites were analyzed for Annexin V binding or labeled using a PS specific antibody. 2-5 x 10^6 promastigotes were put in duplicates in a V-shaped 96-well plate. The *Leishmania* were washed in ringer solution to remove the remaining medium (300 g, 4 min, 4°C). Staining for ANXA5$^+$ was performed in ringer as ANXA5

binds PS in a calcium depending manner. Samples were incubated 20-30 min in the dark at 4°C. To wash away unbound annexin-V, the plate was centrifuged (300 g, 4 min, 4°C) and the supernatant was discarded. All pellets were resuspended in 100 µl Ringer-Solution and transferred into FACS tubes. Staining using the PS antibody was performed similarly; instead of ringer, FACS buffer was used.

4.2.3.3   Cell cycle analysis

For cell cycle analysis 10×10^6 *Leishmania* were washed in cold PBMS (2400 g, 5 min) after which samples are resuspended in cold 70% (v/v) ethanol. After 24 h of incubation at -20°C, samples were washed using PBS (+ 50 mM EDTA) (2000 g, 6 min). Samples were treated with a RNA digestive control solution (50 µg RNase, DNase free / ml in washing solution) after which samples were stained using propidium iodide (1 µg PI + 50 µg RNase, DNase free / ml in washing solution) for 37°C, 30 min. Subsequently flow cytometry analysis was performed.

4.2.4 Methods regarding human immune cells

4.2.4.1   Isolation of Peripheral Blood Mononuclear Cells

The peripheral blood mononuclear cells (PBMCs) were isolated from buffy coats obtained from the DRK blood donation center in Frankfurt. The 50 ml of blood was diluted 1:1 using prewarmed PBS. Subsequently 25 ml of diluted blood was layered on 15 ml of prewarmed gradient medium (leukocyte separation medium 1077). After centrifugation at 545 g, 30 min, 20°C, acceleration and deceleration at minimum level, the interphase containing the PBMCs was collected. Subsequently, PBMCs were washed using wash buffer (PBS + 5% complete medium) using different centrifugation speeds (1024 g, 545 g, 135 g, 8 min, 20°C)to remove remaining granulocytes or erythrocytes. To remove excessive erythrocytes, PBMCs were incubated with cold ammonium chloride for 10-15 min. The cells were again washed after which the cell number was determined by counting manually (hemocytometer; Neubauer chamber slide, depth 0.1

mm) or automatically (CASY Cell Counter). Isolation of monocytes (CD14$^+$ cells) was achieved by plastic adherence or CD14$^+$ selection.

4.2.4.2   Isolation of monocytes by plastic adherence

For the isolation of monocytes by plastic adherence, PBMCs were seeded at 8 x 10^6 PBMCs/ml in 25 cm^2 flasks (5ml) in the presence of 1% human serum. Cells were incubated for 1 h at 37°C, 5% CO_2 giving the monocytes time to adhere to the plastic. Next flasks were washed using wash buffer to remove the non-adherent cells.

4.2.4.3   Isolation of monocytes by CD14$^+$ selection

The obtained PBMCs were washed (135 g, 8 min, 20°C) in MACS-buffer after which the pellet was resuspended in 95 µl MACS-buffer/ 1 x 10^7 cells and 5 µl/ 1 x 10^7 cells CD14 beads were added. PBMCs and beads were incubated for 15 min at 6°C. Afterwards, cells were washed in MACS-buffer (545 g, 8 min, 20°C) and resuspended in 3 ml MACS-buffer. The solution was given on a LS column which was place into a magnetic field of the MidiMACS Separator (on ice). The column was washed and the flow-through (CD14- cells) was frozen for further experiments. After removal of the column, the CD14+ cells were collected and used for the generation of macrophages or dendritic cells as described below.

4.2.4.4   Generation of macrophages and dendritic cells

To generate macrophages, monocytes were cultured in complete medium, supplemented with the growth factors GM-CSF (10 ng/ml) or M-CSF (30 ng/ml) to differentiate monocytes to anti-inflammatory macrophages (hMDM1) or proinflammatory macrophages (hMDM2) respectively. The differentiation process occurred at 37°C, 5% CO_2 for 5-7 days.

For the generation of DCs, monocytes were plated in 6-well plates at 1.5 x 10^6 cells/well, supplemented with GM-CSF (5 ng/ml) and IL4 (10 ng/ml). After 3 days of incubation at 37°C and 5% CO_2, medium and growth factors were added for an additional 2-3 days.

4.2.4.5   Freezing monocyte depleted PBMCs

The non-adherent fraction of PBMCs (plastic adherence isolation) or CD14$^-$ PBMCs (MACS isolation) were resuspended in complete medium supplemented with 40% fetal calf serum and 10% DMSO. After transfer in cryo-tubes, cells were gradually (1°C/min) frozen in -80°C.

4.2.4.6   Thawing PBMCs

The frozen cryo-tube containing PBMCs were thawed by 37°C (water bath). Subsequently PBMCs were transferred in 7 ml of prewarmed complete medium. By washing in complete medium, the DMSO was removed. Subsequently cells were counted using a hemocytometer (Neubauer chamber slide, depth 0.1 mm)

4.2.5 Establishing proliferation assay

4.2.5.1   Carboxyfluorescein succinimidyl ester

The CFSE was dissolved in DMSO at a final concentration of 10 mM. For labeling 10 x 10^6 cells were put in 2 ml of complete medium. Another 500 µl of complete medium was added containing 1 µl of CFSE, to have a final concentration of 4µM. Cells were resuspended very good after which cells were incubated at 37°C for 10 min. Subsequently 2 washing steps occurred with complete medium (135 g, 8 min) to remove excessive CFSE. Next cells were resuspended in the desired volume to perform a proliferation assay.

4.2.5.2   PKH26 Red Fluorescent Cell Linker Kit

Cells were labeled using the membrane labeling dye PKH26 according to the manufacturer guidelines. Cells, 4×10^6, were washed in PBS (135 g, 8 min) and subsequently resuspended in 100 µl Diluent C. Another 100 µl Diluent C containing 2 µl of the PKH26 staining dye was added to the samples. After incubation of 5 min the volume was increased with complete medium till 10 ml. Cells were washed twice in complete medium (135 g, 8 min) to remove excessive PKH26. The cells were put in the desired volume to perform proliferation assays.

4.2.5.3   Proliferation assay

For the proliferation assay, cells were cultured in distinct media to test the optimal settings. Medium 1 was defined as the normal macrophage culture medium; medium 2 comprises X-vivo medium; medium 3 was macrophages culture medium in which the FCS was replaced by 1% human AB serum. To assess proliferation, hMDMs and DCs were generated as describe, using distinct media. After differentiation, cells were put on ice to allow cells to detach. Using a cell scraper, cells were removed mechanically from the plastic flasks/wells. After counting the cells, labeling with PKH26 or CFSE occurred. Cells were seeded in microcentrifuge tubes at 0.4×10^6/ml after cells were left untreated (control) or were stimulated with tetanus toxoid or were infected with Leishmania parasites (MOI=10). After 24 h of incubation at 37°C, 5% CO_2 the excessive parasites/stimulus was removed by washing microcentrifuge tubes using complete medium (135 g, 8 min). Subsequently, 20,000 cells were seeded (50 µl) in round bottom 96 well plates, after which autologous, thawed and CFSE/PKH26 labeled PBMCs were added at a ratio of 1:5 (100,000 PBMCs in 100 µl). Cells were further incubated for an additional 6 days at 37°C, 5% CO_2 after which proliferation is assessed microscopically by cluster formation or by flow cytometry.

4.2.6 Fluorescence Activated Cell Sorting (FACS)

To assess several aspects, such as surface and transcription factor expression on human cells, proliferation of PBMCs, phenotypical characterization of cells, lysosomal acidification, etc. flow cytometry analysis was performed. For FACS experiments a BD^{TM} LSR II flow cytometer was used and data analysis was carried out with FACSDiva^{TM} and FlowJo^{TM} software.

4.2.6.1   Assessing proliferation

PKH26 and CFSE were used to label PBMCs. After proliferation of PBMCs, FACS analysis was applied, gating on the lymphocyte population based on forward and sideward scatter and/or CD3 staining. When a cell divides, each daughter cell contains half the amount of CFSE/PKH26 as the parent cell, which can be assessed by flow cytometry as a PKH26^{low}/ CFSE^{low} population.

4.2.6.2   Characterization of human APCs

Macrophages and dendritic cells were generated as described above. After differentiation, cells were put on ice to allow cells to detach. Using a cell scraper, cells were removed mechanically from the plastic flasks/wells. After counting the cells, cells were seeded in a V-shaped 96 well plate (3-5 x 10^6/well) and washed with FACS buffer (300 g, 4 min, 4°C). Next, cells were resuspended in FACS blocking buffer and incubated for 15 min on ice. Subsequently cells were washed again and incubated with the desired antibody/isotype for 30 min, on ice, in the dark. After incubation, cells were washed with FACS buffer. After resuspending the cells in 100 µl FACS buffer, cells were transferred in FACS tubes to assess surface marker expression by flow cytometry.

4.2.6.3　　Characterization of proliferating PBMCs

After proliferation of PBMCs, the proliferating subset was characterized for surface markers and intracellular transcription factors. Therefor cells, obtained from the proliferation assay, were washed in FACS buffer (300 g, 4 min, 4°C). Next, cells were resuspended in FACS blocking buffer and incubated for 15 min on ice. Subsequently cells were washed again and incubated with the desired antibody/isotype for 30 min, on ice, in the dark. For intracellular transcription factor staining, cells were first permeabilized using FACS buffer containing 0.5 % saponin. The latter buffer was also used for antibody staining, which also occurred for 30 min, on ice, in the dark. After incubation, cells were washed with FACS buffer. After resuspending the cells in 100 µl FACS buffer, cells were transferred in FACS tubes to assess surface marker or transcription factor by flow cytometry.

4.2.6.4　　Lysosomal acidification

Lysotracker® Red DND-99 was applied to assess acidic organelles in hMDM, namely the lysosomes. First hMDM were pretreated with several concentrations of Bafilomycin-A1 (BAFA1) for 1 h at 37°C, which is known to inhibit lysosomal acidification. Subsequently cells were incubated with Lysotracker (50 nM) for 10 at 37°C. Following incubation cells were washed with PBS and fluorescence was immediately assessed by flow cytometry.

4.2.6.5　　Detection of cytokines by FACS analysis

To profile cytokine production, hMDM were infected with *Lm* (MOI=10) for 24 h after which the supernatant fraction was collected. Infected hMDM were additionally co-cultured with autologous PBMCs for 6 days, after which supernatant was collected. Both samples were tested for the presence of IL6, IL10, TNF, IFNG and IL1B using the BD CBA Flex Set System, according to the manufacturer's instruction.

4.2.7 Autophagy modulation

4.2.7.1 Induction and inhibition of autophagy

For the modulation of autophagy we applied several autophagy inducing chemicals. Both hMDM and DCs were stimulated with PI-103 (10 µM), AZD8055 (10 µM) and rapamycin (1 µM) for the desired time points at 37°C, 5% CO_2. For proliferation assays and western blot samples, cells were seeded in 1.5 ml microcentrifuge tubes (0.4×10^6 /ml). After stimulation cells were washed with prewarmed complete medium and further used for the desired experiment. Inhibition of autophagy was by incubation of hMDM with 3-Methyladenine (2 mM), LY294002 (20 µM) and Wortmannin (100 nM) for 1 h at 37°C.

4.2.7.2 Assessing autophagy

By immunofluorescence the recruitment of LC3 was assessed. Therefor hMDM were seeded in chamber slides at 1×10^6 cell/ml. After infection or autophagy modulation, cells were fixed using paraformaldehyde (10 min, on ice). Subsequently, cells were washed with PBS and permeabilized using saponin buffer (FACS buffer + 0.05% saponin). Cells were stained using a polyclonal rabbit LC3 primary antibody, an anti-*Lm* polyclonal Ab obtained from *Lm* infected Balb/c mice, and counterstained with DAPI (30 min, on ice, in the dark). Excessive antibody was removed by washing, followed by incubation with a secondary antibody, conjugated with a fluorochrome (30 min, on ice, in the dark). Chamber slides were washed and treated with gold antifade reagent to suppress photobleaching and preserve the signals of the fluorescently labelled target molecules.

4.2.8 Molecular biology methods

4.2.8.1 siRNA knockdown approach in human primary cells

For the siRNA approach, monocytes were isolated by CD14$^+$ selection using MACS. The obtained monocytes were seeded in 6 well plates (3-4 x 10^6/well). After the differentiation period of 5 days, medium was removed. Cells were washed with PBS to remove the remaining complete medium (containing FCS), and were transfected as followed. For each well 40 µl of 20µM siRNA was mixed with 20µM of Stemfect Buffer and 4.6 µl of Stemfect Reagent was mixed with 20µl Stemfect Buffer. In a timeframe of 5 min, both solutions were mixed and added to the hMDM for 7 h at 37°C, 5% CO$_2$. Next, the medium was replaced by fresh prewarmed complete medium for an additional 2 days. During these 2 days the knockdown was established after which cells were harvested for further experiments comprising RNA isolation, proliferation assays, western blot analysis and infection experiments.

4.1.1.1 RNA isolation

Cells obtained from siRNA knockdown experiments were harvested. RNA was isolated using the RNeasy Plus Mini Kit according to the manufacturer's instructions. A minimum of 0.5 x 10^6 hMDM was used for isolation. First cells were pelleted and washed with cold PBS (1024 g, 8 min, 20°C). The pellet was lysed in 350 µl RLT-Plus-Buffer after which the lysate was transferred to a gDNA Eliminator spin column. By centrifuging (15300 g, 30 sec, 20°C), genomic DNA was removed as it only RNA passes the column. The flow-through was mixed with 70% ethanol (ratio 1:1) after which the mixture was transferred to a RNeasy spin column. Columns were spinned by 15300 g, 30 sec, 20°C. Next the flow-through was discarded and the column was washed twice with 500 µl RPE-buffer (15300 g, 30 sec and 2 min, 20°C). Subsequently the column was placed in a fresh 1.5 ml microcentrifuge tube. To elute the RNA from the column, 30 µl RNase-free water was added following centrifugation (15300 g, 1 min, 20°C). The samples were put on ice for further use or frozen at -80°C for a later use. For measuring RNA concentrations (duplicates), a NanoDrop2000c was used. RNA was verified to be DNA-free by a test-PCR.

4.1.1.2   cDNA synthesis

For synthesizing cDNA the ImProm-II Reverse Transcription System Kit^{TM} was used according the manufacturer's instructions. For one reaction:

Volume (µl)	Reagent
1	ImPromII^{TM} Random Primer Mix
100ng	Template RNA
…	Nuclease-free H_2O
ad 5 µl	

The primer/template RNA mix was incubated (5 min, 70°C) for thermally denaturation and subsequently chilled on ice. A reverse transcription reaction mix was assembled on ice and added to the samples. For one reaction:

Volume (µl)	Reagent
6.5	Nuclease-free H_2O
4	ImPromII^{TM} 5x Reaction Buffer
2	$MgCl_2$
1	dNTP Mix
0.5	Recombinant RNasin® Ribonuclease Inhibitor
1	ImPromII^{TM} Reverse Transcriptase

After addition of the Master Mix, the tubes were shortly centrifuged and put into the PCR cycler performing the following program:

	Temp. (°C)	Time (s)
Annealing	25	5
cDNA synthesis	42	60

| Inactivation | 70 | 15 |
| Cooling | 4 | ∞ |

All cDNA samples were stored at -20°C.

4.1.1.3   Quantitative real-time PCR

To assess the amount of cDNA, we applied a MESA Blue qPCR MasterMix Plus for SYBR Assay No Rox Kit, according to the manufacturer's instructions. The fluorescent dye SYBR Green intercalate into double-strand DNA, which is present after amplification. Based on the fluorescence intensity, which is proportional to the DNA amount, the amplification of the target genes can be measured, using specific primers as listed above.

4.2.9 Western Blot analysis

4.2.9.1   Sample preparation

For the generation of western blot probes, standard 0.5×10^6 hMDMs or DCs or 5×10^6 *Lm* parasites were harvested and washed using PBS (300 g, 8 min, 20°C and 2400 g, 8 min, 20°C respectively). The pellets were lysed in 20 µl Laemmli-Buffer (1x) by heating at 95°C for 10 min. Samples were stored at -20°C before performing SDS-PAGE.

4.2.9.2   SDS-PAGE and Western Blot

In a next step protein lysates were separated according to the molecular weight using SDS-PAGE. The SDS binds non-specifically to hydrophobic sequences of the proteins, leading to negative charges. Due to these negative charges the proteins migrate in an electric field towards the anode and are separated according to their molecular weight as smaller proteins migrate faster through the mesh of the polyacrylamide than larger proteins. For each test, 20 µl of sample was loaded onto the gel. The electrophoresis was performed at constant 80 Volt for protein passage

through the stacking gel and with constant 100 Volt through the separation gel. The separated proteins were blotted in a semi-dry blotting apparatus onto a Transfer membrane (Nitrocellulose) (constant 1.5 mA/cm^2 for 1 h).

Chemicals	Separation Gel (15 %)	Stacking Gel (3.3 %)
Aqua bidest	4.5 ml	4 ml
Separation-Gel-Buffer	4.5 ml	-
Stacking-Gel-Buffer	-	3.2 ml
Acrylamide stock 30%	9 ml	0.8 ml
TEMED	30 µl	20 µl
APS 10%	150 µl	80 µl

4.2.9.3   Band detection

After blotting, membranes were blocked in TBST + 5 % skimmed milk for 1 h at room temperature or overnight at 4°C by gentle agitation on a shake table. In a next step membranes were washed with TBST to remove excessive milk. The primary antibody (polyclonal rabbit α-LC3, 1:1000 in TBST + 5 % w/v BSA; monoclonal mouse α-SQSTM1/p62, 1:1000 in TBST + 5 % w/v BSA) was added overnight at 4°C by gentle agitation on a shake table. Equal loading and blotting efficiency were verified mouse monoclonal α-ß-actin (1:1000 in TBST + 5 % w/v BSA) Subsequently the membrane was washed 3 times (10 min) with TBST and incubated with HRP-coupled secondary antibody (goat α-rabbit, 1:1000 (Pierce) or 1:4000 (Santa Cruz) in TBST + 5 % w/v BSA) for 1 h at room temperature on a shake table. After an additional 3 washing steps, protein bands were detected using ECL substrate. High performance ECL films were exposed to the membrane in the dark for 30 min followed by development in a processor.

4.2.10 Microscopy

4.2.10.1 Generation of cytospins slides

For the generation of cytospins, 2 x 10^6 *Lm* parasites or 1 x 10^6 human cells were centrifuged on cytospins using a Cytocentrifuge (500 g, 10 min and 75 g, 5 min, respectively). Slides were air-dried for DiffQuick® staining.

4.2.10.2 DiffQuick® staining

Air-dried cytospin slides were incubated for 2 min in Fixation Solution of a DiffQuick® kit. Subsequently, they were incubated in Staining Solution 1 (eosinophilic to stain the cytoplasm) for 2 min followed by 2 min in Staining Solution 2 (basophilic to stain nucleic acids). The slides were rinsed in tap water and air-dried for further microscopical analysis. Cytospin slides were analysed with an AxioPhot microscope.

4.2.10.3 Live cell imaging

To investigate dynamic cellular processes, a new live cell imaging platform was established. Using a LSM7 Live (Zeiss) we were able to visualize how parasites were internalized. Therefor hMDM were seeded in chamber slides as described above. Subsequently, cells were labelled after which transgenic *Lm* parasites were added. Immediately, the acquisition of movies, in 3D (Z-stacks) was started, which were analysed by ZEN black/blue software.

4.2.11 Statistical analysis

All data are presented as mean ± SEM (standard error of the mean). The data concerning proliferation were tested for normality and distribution. All data were distributed normally and

therefore statistical analyses were performed using a student t test (two tailed distribution, paired). Data were analysed using Microsoft Excel 2010 and Graph pad prism software. Values of $p < 0.05$ (*), $p < 0.01$ (**) and $p < 0.001$ (***) were considered as significant.

5. Results

5.1 *Leishmania* parasites

5.1.1 The infective *Leishmania* parasite inoculum contains apoptotic parasites

To cultivate *Leishmania* promastigotes *in vitro*, a NNN blood agar culture system is used. The first few days after promastigote culturing, parasites reside in a logarithmic growth phase (log.ph. *Lm*), in which parasites divide exponentially (**Figure 7A**). After day 6 to 8, parasites enter a plateau phase of growth, after which parasites are termed stationary phase *Lm* (stat.ph. *Lm*). The *Leishmania* population comprises both elongated, viable and round shaped, apoptotic parasites, defined as the infectious inoculum (**Figure 7B**). As a tool to investigate the importance of each subpopulation, a magnetic separation technique (MACS) was applied (**Figure 7C**). Using magnetically labeled Annexin V (ANXA5) beads, which bind phosphatidylserine, apoptotic parasites can be isolated from viable ones, as depicted (**Figure 7D and E**).
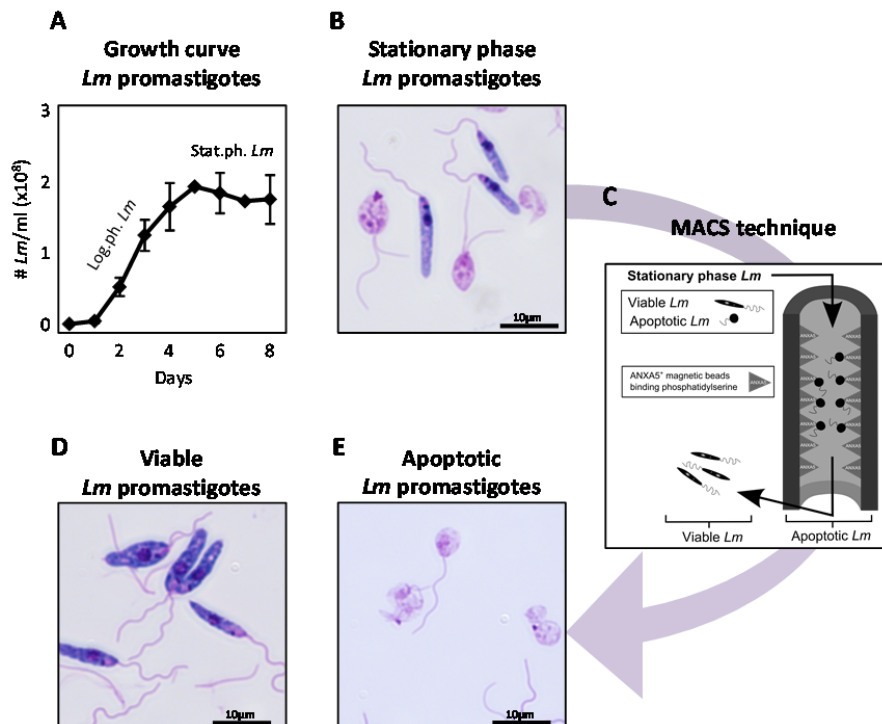
Figure 7: The *Leishmania* infectious inoculum consists of viable and apoptotic parasites. *Leishmania* promastigotes were cultured on NNN blood agar over a period of 8 days. (**A**) The *in vitro* expansion of *Leishmania* parasites was determined by counting parasite numbers daily, depicted as a growth curve. (**B**) Stat.ph. *Lm* were stained using DiffQuick staining. (**C**) Magnetic Cell Separation (MACS) was applied to purify apoptotic parasites using ANXA5 labeled magnetic beads. The MACS purified viable (**D**) and apoptotic (**E**) parasites were stained using DiffQuick©. Graphs present mean ± SEM and DiffQuick pictures are presentative for at least 3 independent experiments.

Previous work already showed the importance of a dying parasite population with apoptotic characteristics for disease development in a susceptible BALB/c infection model (van Zandbergen et al., 2006). As apoptosis among protozoan parasites is still debated extensively, we characterized the dying population in more detail (El-Hani et al., 2012). We applied the guidelines of the Nomenclature on Cell Death (NCCD) to define apoptotic cell dead. The NCCD defines apoptosis as a process by which a cell is considered dead when (1) the cell has lost the integrity of the plasma membrane, as defined by vital dyes in vitro; or (2) the cell including its nucleus has undergone complete fragmentation into discrete and/or (3) its corpse (or its fragments) have been engulfed by an adjacent cell *in vivo* (Kroemer et al., 2005). In a first step, we characterized log.ph. *Lm* and stat.ph. *Lm* by cell cycle analysis, using propidium iodide (PI) staining. PI binds to DNA by intercalating between bases randomly making it an efficient tool to assess DNA amounts. When not in preparation for division, cells remain in the G_1 phase. However once division occurs, cells, residing in the G_2 phase, contain double the amount of DNA, required for the daughter cells. In case of cell death, DNA degradation precedes a loss of DNA, in which the cell is constricted to the $SubG_1$ phase. Assessing the cell cycle profile among *Lm*, we could demonstrate that only a minority (20.8% ± 1.1) of the stat.ph. *Lm* is in the G_1 phase (**Figure 8A**), whereas the majority (78.7% ± 3.5) of log.ph. *Lm* is in the G_1 phase (**Figure** 8**B**). The cellular DNA content histograms showed the greater part (74.8% ± 1.2) of stat.ph. *Lm* to remain in the $SubG_1$ phase, a marker for dying and apoptotic cells (**Figure 7A**). Upon separation of stat.ph. *Lm*, the purified non ANXA5-binding *Lm* had only low levels of $SubG_1$ phase (36.3% ± 7.7), similar as found for the log.ph. *Lm* and both these populations comprise a G_2 phase, indicating multiplying promastigotes.
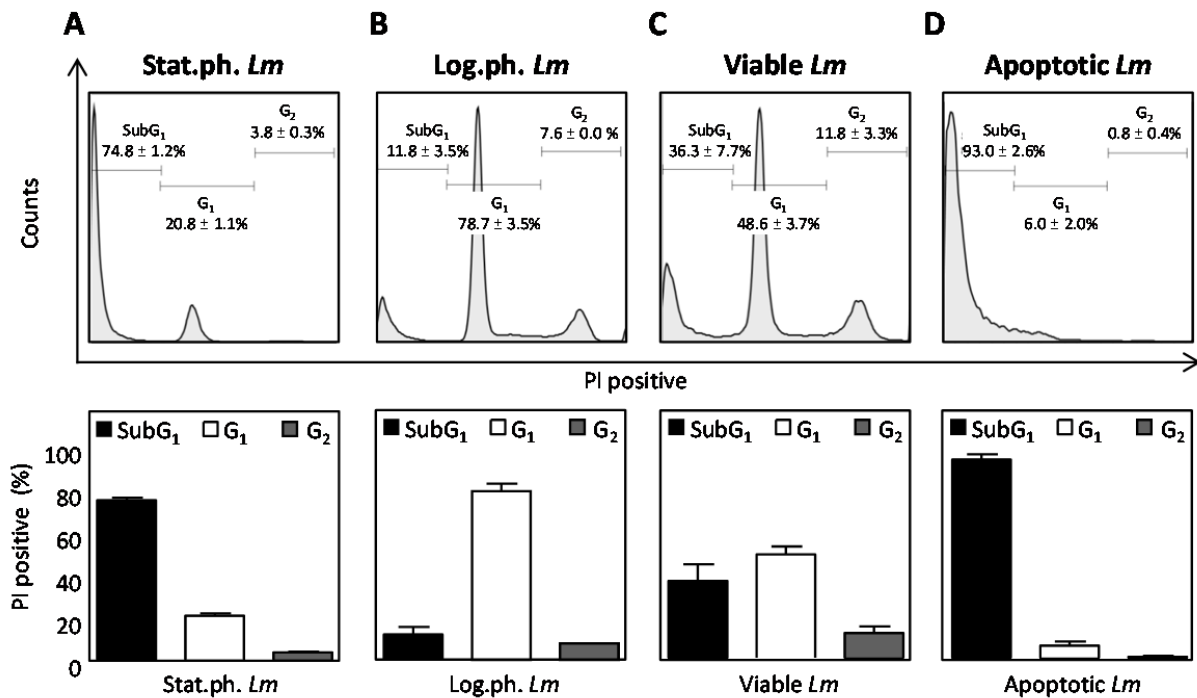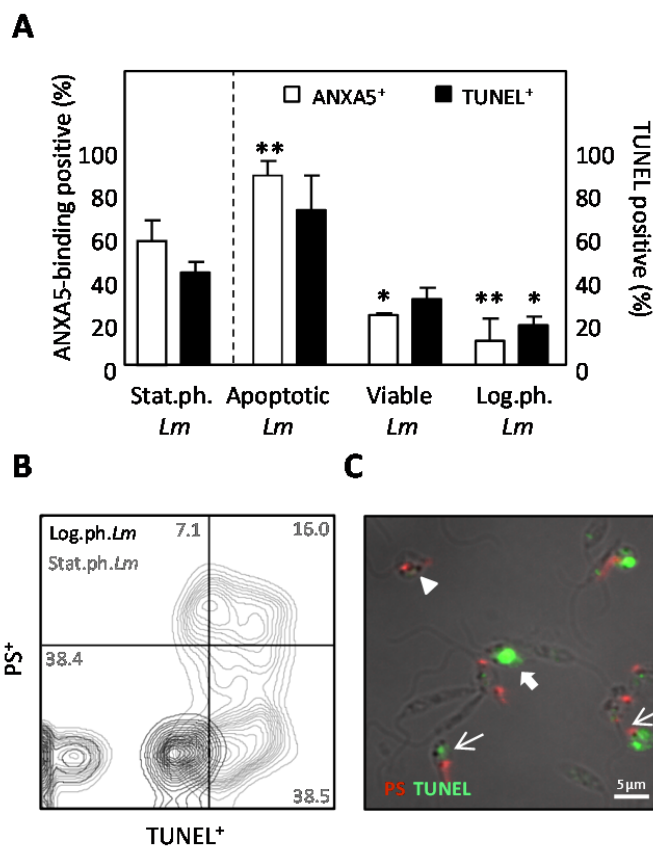
Figure 8: The *Leishmania* infectious inoculum contains SubG$_1$ positive parasites. Log.ph. *Lm*, stat.ph. *Lm* and MACS separated ANXA5$^+$ apoptotic and viable *Lm* were used to perform cell cycle analysis using propidiumiodide (PI) staining. Analyzed by flow cytometry, DNA content histograms show the cell cycle profile (SubG$_1$, G$_1$, G$_2$) of stat.ph. *Lm* (**A**), log.ph. *Lm* (**B**), viable *Lm* (**C**) and apoptotic *Lm* (**D**) in the upper row, which were marked to quantify the proportion of SubG$_1$ (black bars), G$_1$ (white bars) and G$_2$ (gray bars), as depicted in the lower row. The flow cytometry histograms and data, presented as mean ± SEM, are representative of at least three independent experiments.

Besides DNA quantification, we analyzed DNA fragmentation by means of a terminal deoxynucleotidyl transferase (TdT)-mediated dUTP nick end labeling (TUNEL) assay. In addition we assessed ANXA5-binding. We could show stat.ph. *Lm* to contain a proportion of cells being TUNEL$^+$ (42.4% ± 1.5) and ANXA5-binding$^+$ (57.3% ± 5.6). In contrast, among log.ph. *Lm* significant less parasites were TUNEL$^+$ (18.3% ± 2.3) and ANXA5-binding$^+$ (11.1% ± 5.9) (**Figure 9A**). Upon separation of viable from apoptotic parasites, we found the latter to be TUNEL$^+$ (71.6% ± 9.2) as well as ANXA5-binding$^+$ (87.6% ± 3.9). The purified viable *Lm* had only low levels of TUNEL$^+$ (30.4% ± 3.1) and ANXA5-binding$^+$ (23.2% ± 0.5) parasites (**Figure 9A**). Using a specific PS-binding monoclonal antibody in combination with a TUNEL staining, we could distinguish between parasites being solely PS$^+$, (10.5% ± 3.3), or PS$^+$TUNEL$^+$ (16.4% ± 0.4), or only TUNEL$^+$ (37.8% ±

0.8%) (**Figure 9B**). Similar like ANXA5-binding promastigotes, PS$^+$TUNEL$^+$ *Lm* have a round-shaped body morphology and lack flagellular movement (**Figure 9C**).

In all, stationary phase *Lm* comprise a mixture of viable and apoptotic, the latter characterized by a loss of DNA (SubG$_1^+$), being TUNEL positive and ANXA5-binding positive. Among log.ph. *Lm* a minor amount (11.8% ± 3.5) of apoptotic parasites is present, therefor we used log.ph. *Lm* parasites as a model for ANXA5-depleted viable promastigotes and stat.ph. *Lm* as a model for the virulent inoculum, in which apoptotic *Lm* are present.

Figure 9: The *Leishmania* infectious inoculum contains ANXA5$^+$-binding and TUNEL$^+$ parasites. Log.ph. *Lm*, stat.ph. *Lm* and MACS separated ANXA5$^+$ apoptotic and viable *Lm* were used to assess DNA fragmentation (**A**) DNA fragmentation and PS exposure was assessed using TUNEL assay (black bars) and ANXA5-binding (white bars) by flow cytometry. (**B-C**) Stat.ph. *Lm* (gray) and log.ph. *Lm* (black) were double stained by a TUNEL and PS antibody staining. Samples were analyzed by flow cytometry (**B**) and immunofluorescence microscopy (**C**) as depicted (arrow head – PS positive *Lm*, thick arrow – TUNEL positive *Lm*, thin arrow – double positive *Lm*). Data are presented as mean ± SEM of at least three independent experiments. The IF and flow cytometry micrographs are representative of at least 3 independent experiments.

We could demonstrate the *Leishmania* infectious population to contain a mixture of viable parasites and parasites that spontaneously underwent an apoptosis like process. To further define the presence of an apoptotic mechanism, we induced apoptosis chemically in promastigotes, using either miltefosine or staurosporine. Both compounds are well described to induce apoptosis among *Leishmania* and other protozoans (Jiménez-Ruiz et al., 2010; Lüder et al., 2010). Upon treatment of both log.ph. (**Figure 10A-B**) or stat.ph. *Lm* (**Figure 10C-D**), with either miltefosine or staurosporine, the majority of log.ph. (91.6% ± 3.3; 67.4% ± 12.0) and stat.ph. promastigotes (87.8% ± 2.4; 94.6% ± 0.5) were found to be in SubG$_1^+$ phase. The fraction of dividing parasites (G$_2$) was minimal upon treating stat.ph. *Lm* (0.9% ± 0.1; 0.7% ± 0.1) and log.ph. *Lm* (1.3% ± 0.6; 7.2% ± 4.0) with both compounds. In addition, only a small population resided in the G$_1$ phase upon treatment of log.ph. *Lm* (6.9% ± 2.6; 23.9% ± 7.3) and stat.ph. *Lm* (11.3% ± 2.3; 4.7% ± 0.5) with miltefosine and staurosporine, respectively (**Figure 10**).
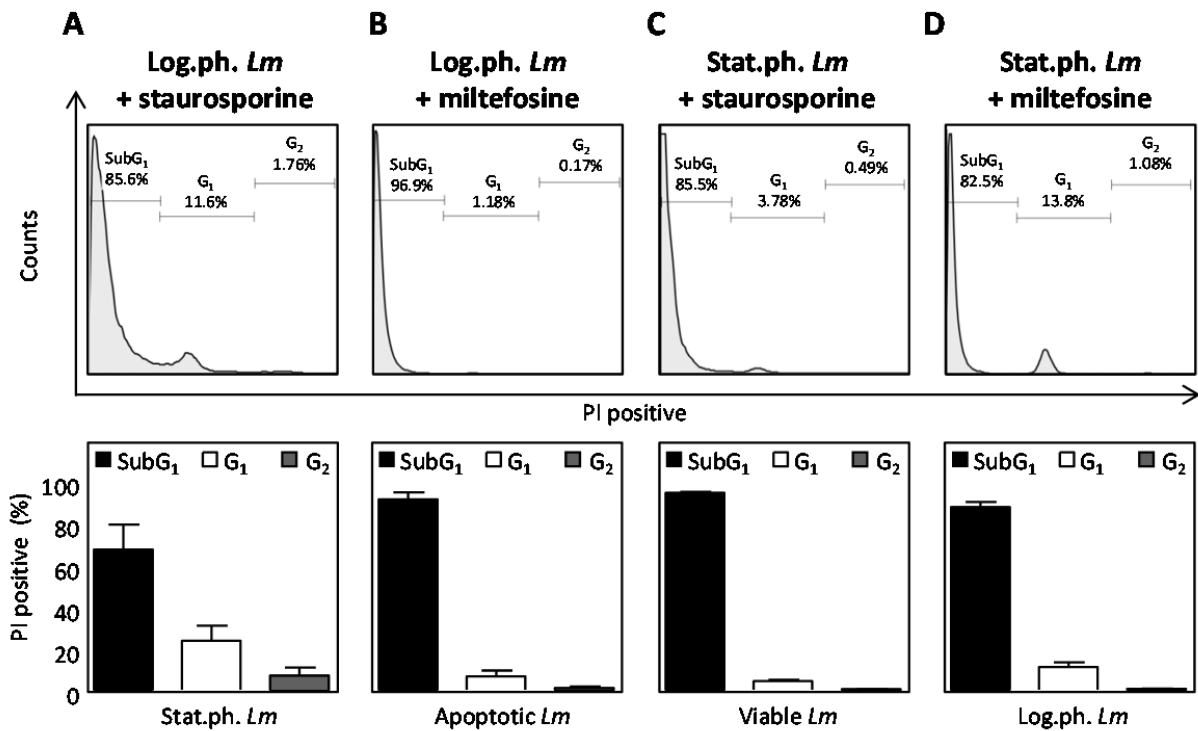
Figure 10: Chemical induction of apoptosis in *Leishmania* results in SubG$_1$ phase positive promastigotes. *Leishmania* promastigotes were cultured on NNN blood agar, from which log.ph. and stat.ph. *Lm* were harvested (**A-D**) Log.ph. *Lm* or stat.ph. *Lm* promastigotes were treated with apoptosis inducing drugs, 25 µM staurosporine (**A and C**) or 25 µM miltefosine (**B and D**). After 48 h, promastigotes were washed and cell cycle analysis using PI staining was performed. By flow cytometry (histograms) cells were marked to quantify the proportion of SubG$_1$ (black bars), G$_1$ (white bars) and G$_2$ (gray bars), as depicted in bar graphs underneath. Flow cytometry histograms and data, presented as mean ± SEM, are representative of at least three independent experiments.

Next ANXA5-binding[+] and TUNEL[+] were analyzed. Upon treatment, with either miltefosine or staurosporine, a significant increase of ANXA5-binding[+] parasites among stat.ph. *Lm* (77.0% ± 1.9; 74.0% ± 3.7) and log.ph. *Lm* (72.8% ± 6.0; 55.8% ± 9.7) (**Figure 11A and B, upper lanes**) was observed. In addition, also a significant increase in TUNEL[+] staining was observed among stat.ph. *Lm* (53.8% ± 11.6; 83.6% ± 2.1) and log.ph. *Lm* (59.3% ± 9.7; 83.1% ± 1.7) (**Figure 11A and B, lower lanes**). From these data we can conclude that parasites undergo an apoptotic process. This process is characterized by an early phase, where parasites bind ANXA5, suggestive for PS exposure and a late phase, where DNA fragmentation and degradation occurs (TUNEL/SubG$_1$ positivity).

A

Stat.ph. *Lm*

B

Log.ph. *Lm*

untreated *Lm*	+	-	-
Lm + miltefosine	-	+	-
Lm + staurosporine	-	-	+
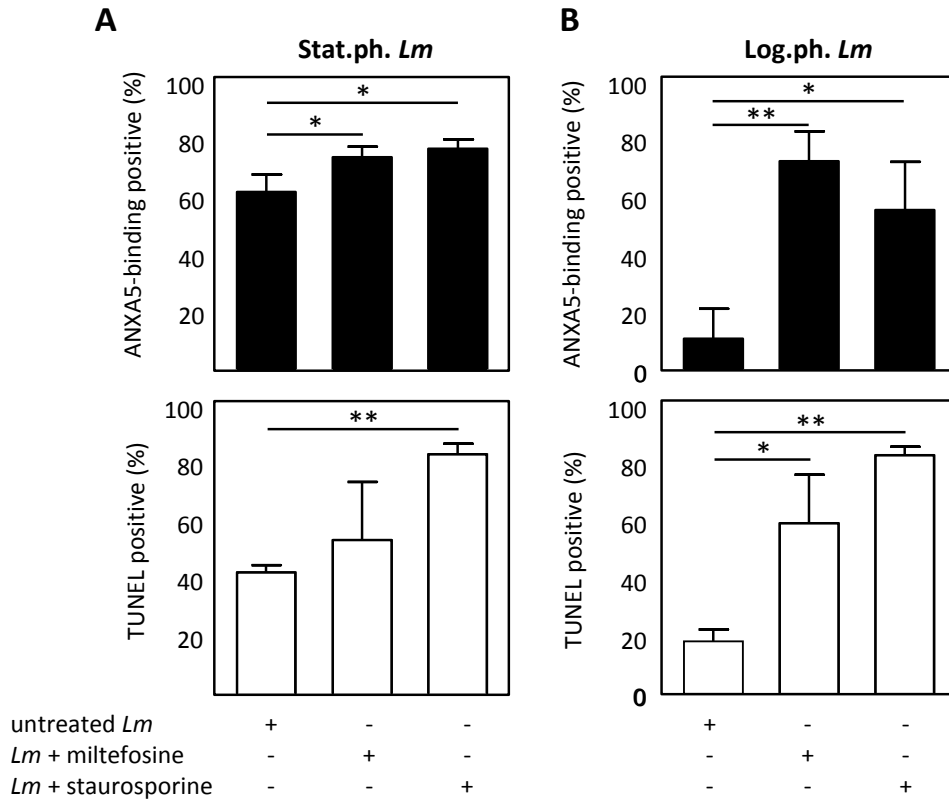
Figure 11: Chemical induction of apoptosis in *Leishmania* results in ANXA5^{+}-binding and TUNEL[+] promastigotes. *Leishmania* promastigotes were cultured on NNN blood agar, from which log.ph. and stat.ph. *Lm* were harvested. (**A-B**) Log.ph. *Lm* or stat.ph. *Lm* promastigotes were treated with apoptosis inducing drugs, 25 µM staurosporin or 25 µM miltefosine. After 48 h, ANXA5-binding and DNA fragmentation were assessed of stat.ph. *Lm* (**A**) and log.ph. *Lm* (**B**) using flow cytometry (black bars) and TUNEL assay (white bars). Data are presented as mean ± SEM of at least three independent experiments (*: $p < 0.05$; ** $p < 0.01$).

Of note, upon TUNEL staining of viable *Leishmania* promastigotes, an interesting observation was made. By flow cytometry, an increased auto-fluorescence was detected compared to unstained parasites (data not shown). Using microscopy, we could confirm this finding. Using a TUNEL assay, not the nuclei, but the mitochondria of viable parasites, termed the kinetoplast, stained positively, as depicted (**Figure 12a, thin arrows**).
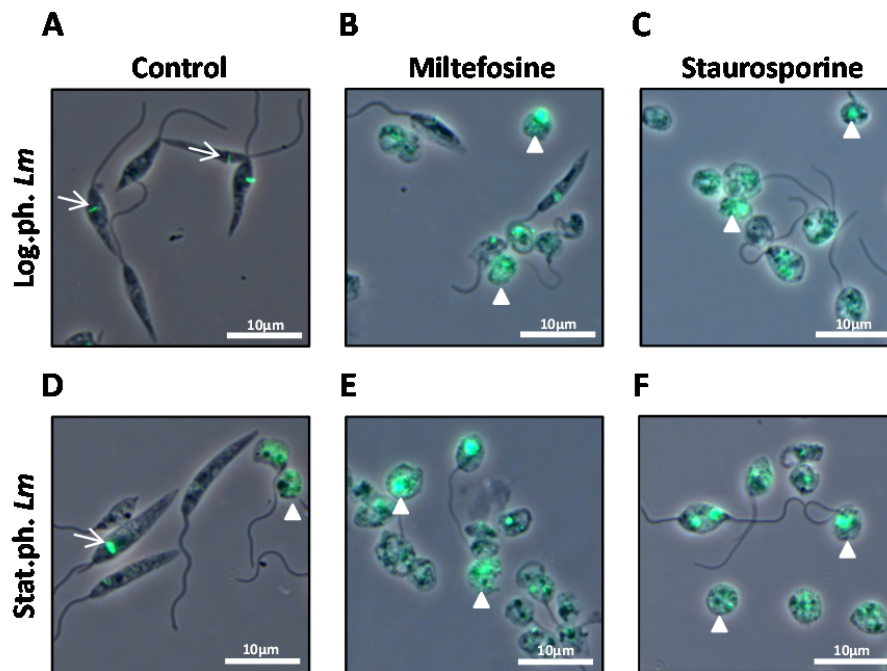
Figure 12: Chemical induction of apoptosis in *Leishmania* results in TUNEL[+] promastigotes. *Leishmania* promastigotes were cultured on NNN blood agar, from which log.ph. and stat.ph. *Lm* were collected. Log.ph. *Lm* (**A-C**) or stat.ph. *Lm* (**D-F**) promastigotes were treated with apoptosis inducing drugs, 25 µM staurosporine or 25 µM miltefosine. After 48 h, DNA fragmentation was analyzed using a TUNEL assay, following microscopic analysis. Data are presented as mean ± SEM of at least three independent experiments (arrow head, TUNEL[+] nuclei; thin arrow, TUNEL[+] kinetoplast).

5.2 Innate immune cells: human macrophages and dendritic cells

5.2.1 Generation and phenotypical characterization

Human macrophages (hMDMs) as well as dendritic cells (DCs) can internalize *Leishmania* parasites and serve as antigen presenting cells playing a key role in T cell activation. In a first step we generated proinflammatory hMDM1, anti-inflammatory hMDM2 and DCs from CD14$^+$ monocytes. By flow cytometry, expression of cell specific surface markers was assessed, as the mean fluorescence intensity (MFI). After differentiation, CD14 was expressed only in low levels on DCs (MFI=73 ± 11). The hMDM1 (MFI=335 ± 39) expressed a higher amount of CD14, which was even expressed 3.6 fold higher on hMDM2 (MFI=1219 ± 150). The hMDM1 could be specifically characterized by the high expression of CD206 (MFI=2577 ± 530), which was in lower amounts present on hMDM2 (MFI=790 ± 49) and DCs (MFI=814 ± 101). A feature of hMDM2 is the presence of CD163. Indeed the expression hMDM2 (MFI=3721 ± 1106) was strongly enhanced compared to its presence on hMDM1 (MFI=274 ± 99) and DCs (147 ± 51). DCs on the other hand are characterized by the expression of CD1a (MFI= 9202 ± 2998) and CD209 (MFI=978 ± 59), of which the latter one was expressed higher on DCs compared to hMDM1 and hMDM2. A lower level of CD1a (MFI=432 ± 50; 554 ± 250) and CD209 (MFI=283 ± 94; 268 ± 97) was detected on hMDM1 and hMDM2, respectively. Of note, in all cell types, in hMDM1 (MFI=1561 ± 338), hMDM2 (MFI=2421 ± 1521) and DCs (MFI=2217 ± 152), a similar level of MHCII surface expression was detectable (**Figure** 13). In conclusion, we can profile hMDM1 as CD14$^+$, CD206^{++}, CD209$^+$, CD163$^-$ and MHCII$^+$, hMDM2 to be CD14^{++}, CD206$^+$, CD209$^+$, CD163^{++} and MHCII$^+$ and the DCs to have a CD14$^-$, CD1a$^+$, CD206$^+$, CD209^{++}, CD163$^-$, MHCII$^+$ phenotype.
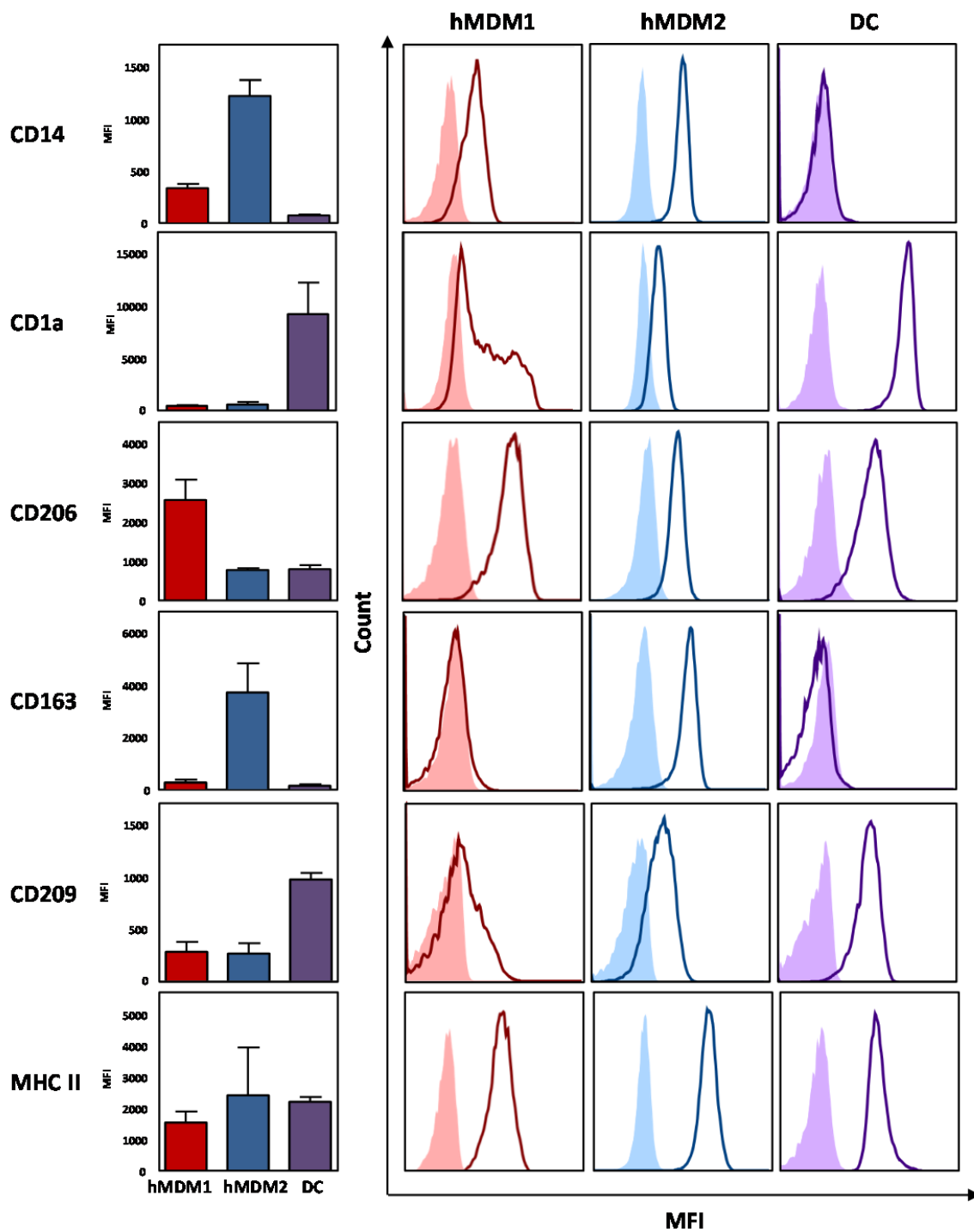
Figure 13: Phenotypical characterization of hMDMs and DCs. From CD14^{+} monocytes, hMDM1, hMDM2 and DCs were generated by addition of the growth factor GM-CSF, M-CSF and GM-CSF + IL-4, respectively. After 5-6 days of cell culture, surface expression of CD14, CD1a, CD206, CD163, CD209 and MHCII was assessed by flow cytometry. Data, as mean ± SEM, and histograms are representative of 3 independent experiments. (MFI= Mean Fluorescence Intensity)

5.2.2 Infection of human primary APCs

As few is known about human myeloid cells in the context of *Leishmania major* infection, we compared infection of human DCs with proinflammatory macrophages hMDM1 and anti-inflammatory macrophages hMDM2. Upon infection with (transgenic) *Leishmania major* promastigotes we could demonstrate all 3 cell types to be prone to *Leishmania* infection. After 24 hours, hMDM2 (45.5 % ± 5.9) were found to be the most susceptible to *Lm* infection, followed by hMDM1 (32.5 % ± 2.5) and DCs (12.4% ± 1.8) (**Figure 14A**). In addition to infection rates also parasite load, analyzed as MFI, was the highest in hMDM2 (MFI=1907.5 ± 476.9), followed by hMDM1 (MFI=1558 ± 347.1) and DCs (MFI=1370.7 ± 265.2) (**Figure 14B**). Remarkably, over a period of 7 days parasites developed the strongest in DCs. Development can be assessed by the intensity of the dsRed protein; during promastigote to amastigote transformation, an increased translation of the dsRed protein occurs, making amastigote to light brighter, which can be assessed by the MFI by flow cytometry. After 7 days in DCs, the infection rate was the highest (77.2% ± 5.0) followed by hMDM2 (58.4% ± 5.2) and hMDM1 (49.5% ± 4.2) (**Figure 14A**). In addition, also the parasite load was significantly increased; DCs (MFI=15706.0 ± 2404.6), hMDM2 (MFI=7882.7 ± 1547.5) and hMDM1 (MFI=5247.6 ± 578.7) (**Figure 14B**).   Illustrative to the quantitative data, it can be visualized that 24 h after infection, both hMDM and DCs are susceptible for promastigote (arrow heads) infection (**Figure 14C, upper row**). Over time, internalized promastigotes transform into the multiplying amastigote (arrow heads) form, which results in an increased intracellular parasite load (**Figure 14C, lower row**).
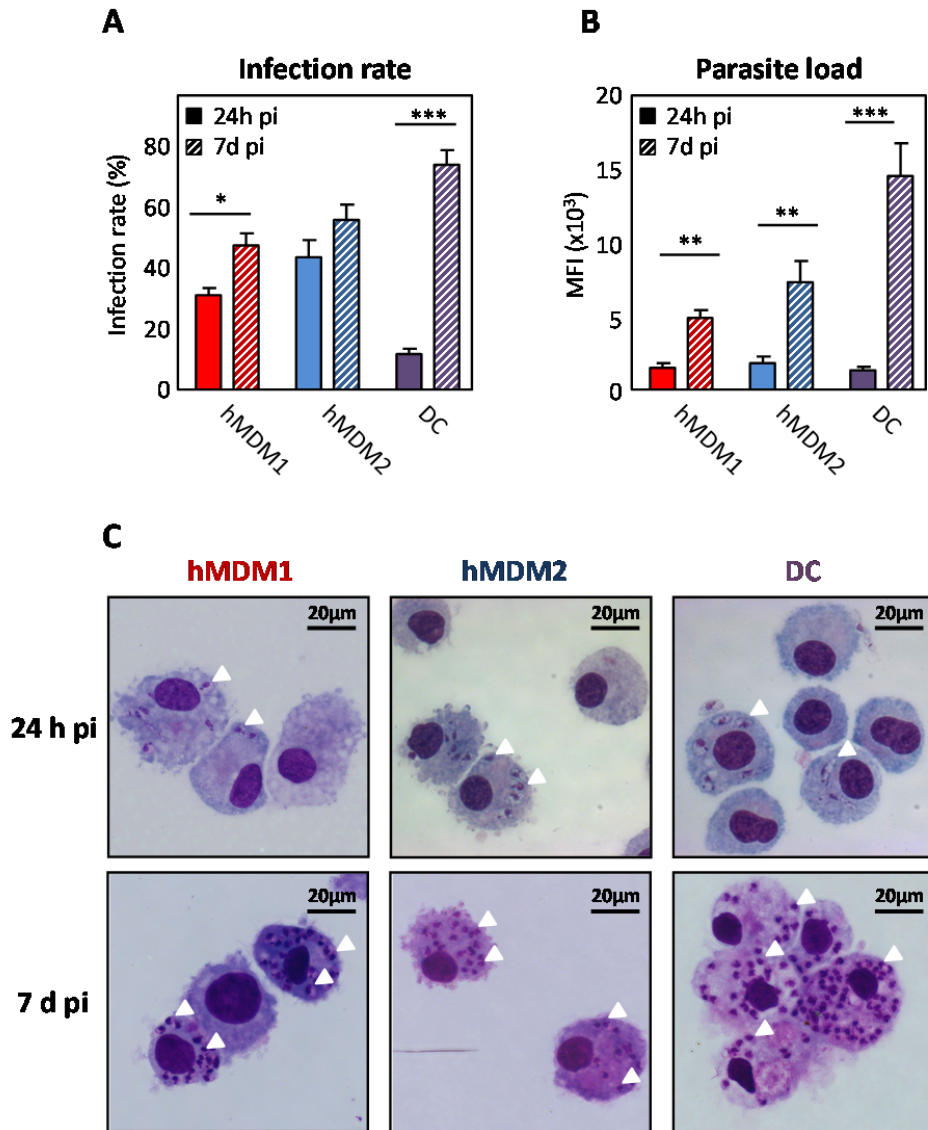
Figure 14: Parasite development in hMDMs and DCs. hMDMs and DCs were infected with transgenic dsRed stat.ph. *Lm* (MOI=10). After 24 h (filled bars) and 7 d (stripped bars) infection rate (**A**) and parasite load (**B**) were assessed by flow cytometry and visualized by microscopic analysis using DiffQuick© staining (arrow heads indicate *Lm* parasites) (**C**). Graphs, presented as mean ± SEM, and micrographs are representative for at least 3 independent experiments (*: p < 0.05; ** p < 0.01; *** p < 0.001).

5.2.3 Cytokine profile of hMDM upon *Leishmania* infection

In a next step we examined the cytokine profile of both phenotypes of hMDM in response to infection with stat.ph. *Lm* for 24 hours. We could observe anti-inflammatory hMDM2 to respond with a strong IL10 production in response to *Leishmania* infection. In addition, also IFNG and TNF were produced, however a great variability between donors was observed. Proinflammatory hMDM1 did not produce the anti-inflammatory IL10, only a strong proinflammatory response comprising IFNG and TNF was detected (**Figure 15A-C**).
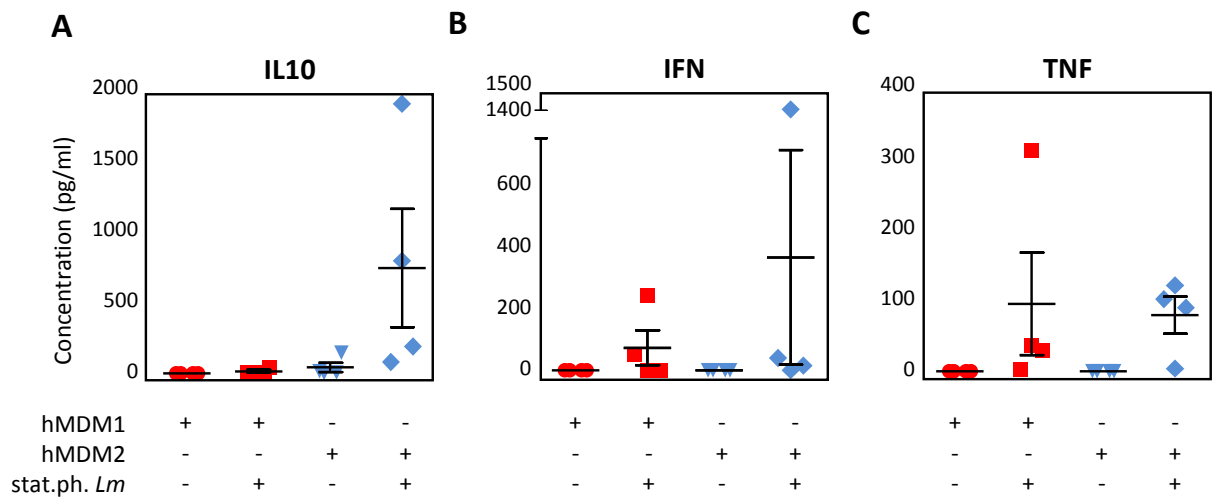
Figure 15: Cytokine profile of hMDM in response to *Leishmania* infection. hMDM1 and hMDM2 were infected for 24 h with stat.ph. *Lm* (MOI=10). After 24 h the supernatant fraction was collected from uninfected and infected hMDM1 (red) and hMDM2 (blue). Subsequently the presence of IL10 (**A**), IFN (**B**) and TNF (**C**) was assessed by ELISA. Data are presented as SEM ± SEM and are representative of at least 2 independent experiments, comprising 4 donors.

Subsequently, we assessed the cytokine profile of hMDM2 in response to log.ph. or stat.ph. *Lm* infection and after 6 days during PBMC cocultivation. Upon infection of hMDM2 with log.ph. *Lm* an increased production of the proinflammatory cytokines IL1B, IFNG, IL6 and TNF, was observed, of which the latter two were significantly lower in the presence of apoptotic-like parasites (stat.ph. *Lm*) (**Figure 16A-C**). The anti-inflammatory IL10 was produced in significantly greater amounts upon infection of hMDM with log.ph. *Lm* (**Figure 16E**). After PBMC cocultivation

we could again demonstrate a strong proinflammatory response, primarily by the production of IFNG upon of infection with log.ph. *Lm*. In the presence of apoptotic parasites, the production of IFNG was significantly reduced (**Figure 16D**).
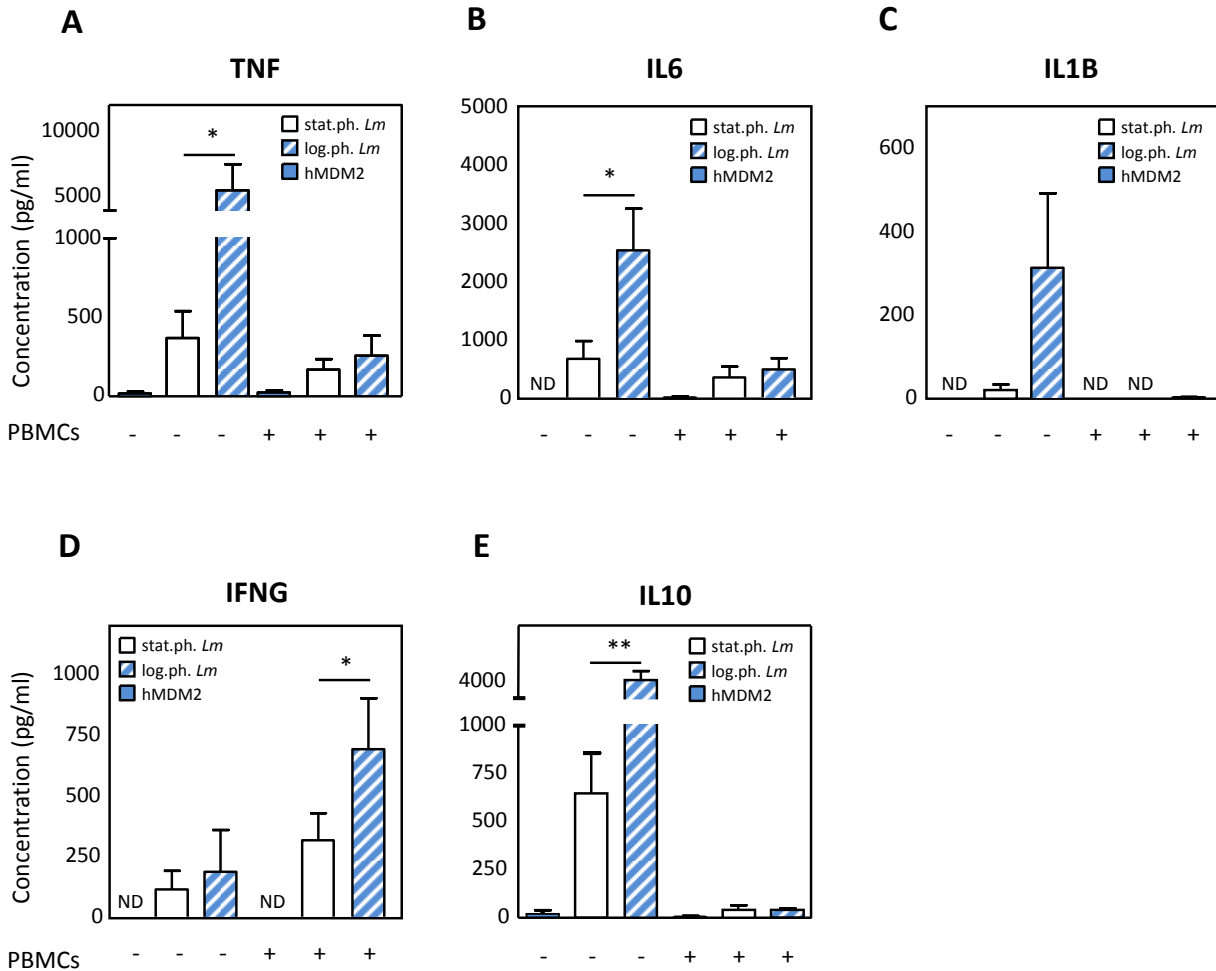
Figure 16: Cytokine profile of hMDM2 in response to *Leishmania* infection with and without PBMC coculturing. The hMDM2 were infected for 24 h with stat.ph. *Lm* (MOI10). Next, extracellular parasites were removed and hMDM2 were further cultured in medium or autologous CFSE labeled PBMCs were cocultured. After an additional 6 days, supernatant fraction was collected. Subsequently the presence of TNF (**A**), IL6 (**B**), IL1B (**C**), IFNG (**D**) and IL10 (**E**) was assessed by ELISA. Data are presented as mean ± SEM and are representative of at least 3 independent experiments (*: p < 0.05; **: p < 0.01; ND: not detectable).

5.2.4 Parasite transformation in human APCs

By DiffQuick staining (i) the more elongated shaped promastigotes (thin arrows) were shown to transform into a more round-droplet shaped morphology (arrow heads) and (ii) the distance between the nuclei and kinetoplast decreased, compared to the distance seen in promastigotes (**Figure 17A**). These two features indicate that promastigote to amastigote transformation occurred. To analyze transformation in more detail, the leishmanial gene expression profile was investigated of hMDMs and DCs infected with (a) promastigotes for 3 h (promastigote), (b) with axenic amastigotes for 3 h (axenic amastigote) or (c) promastigotes for 7 d (promastigote → amastigote), which were able to transform into amastigotes in their host cell.

From all samples RNA was isolated after which the expression of 3 genes was analyzed: the ATP-binding cassette (ABC), the *Leishmania* surface protease GP63 and the Small Hydrophilic Endoplasmic Reticulum-associated Protein (SHERP). Gene profiling showed promastigotes to be ABC$^+$, GP63$^-$ and SHERP$^+$. Regarding amastigotes, we found axenic amastigotes to be ABC^{++}, GP63$^+$ and SHERP$^-$. Amastigotes which transformed in macrophages or DCs were also GP63$^+$ and SHERP$^-$, but ABC$^-$ (**Figure 17B**).
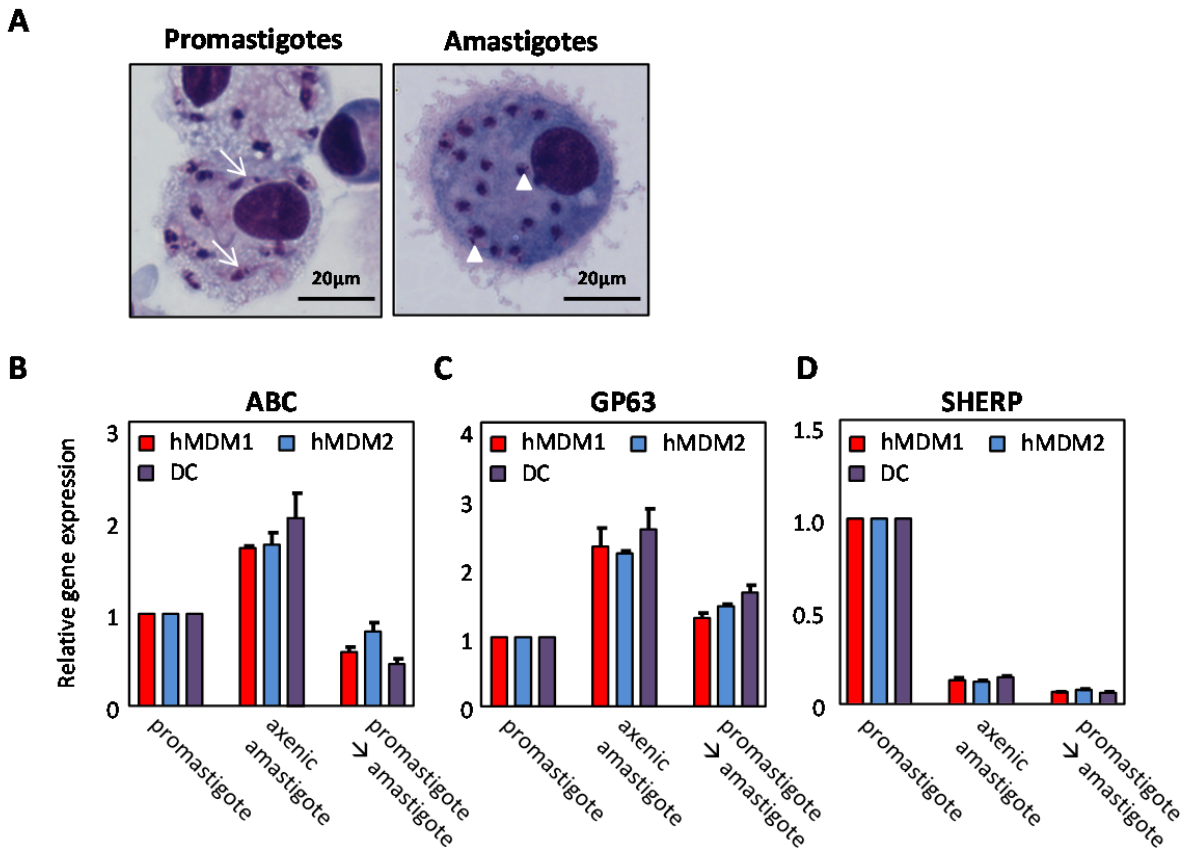
Figure 17: Promastigotes transform in ABC^low GP63^high SHERP^low amastigotes in both hMDMs and DCs. hMDMs and DCs were infected with promastigotes (thin arrows) and amastigotes (arrow heads) (MOI=10) and stained using DiffQuick staining, as depicted (**A**). After 3 h and 7 d, cells were collected for RNA extraction and cDNA synthesis. Using stage specific primers, the expression of ABC (**B**), GP63 (**C**) and SHERP (**D**) was analyzed by qRT-PCR. Micrographs and bar graphs, presented as mean ± SEM, are representative for at least 3 independent experiments.

5.3 Adaptive immune system

5.3.1 Establishment of a proliferation assay

To investigate how *Leishmania* infection, either in DCs or hMDMs, influences the adaptive immune response, a lymphocyte proliferation assay was established. We aimed to assess T cell proliferation by flow cytometry and first compared the suitability of two labeling compounds, PKH26 and CFSE, to investigate proliferation. In addition, different compositions of culture medium were used.

Therefore CFSE or PKH26 labeled PBMCs, cultured in distinct media, were stimulated with the recall antigen tetanus toxoid (TT) or phytohemagglutinin (PHA). After 6 days, proliferation was analyzed, first, by microscopic analysis (cluster formation) prior to flow cytometry. In the control group, no cluster formation of cells was observed; neither the culture medium nor the labeling induced spontaneously proliferation (**Figure 18A**). Upon stimulation with TT, cluster formation was observed in most conditions (**Figure 18B**). As a positive control, PHA was used to stimulate proliferation, as depicted (**Figure 18C**).
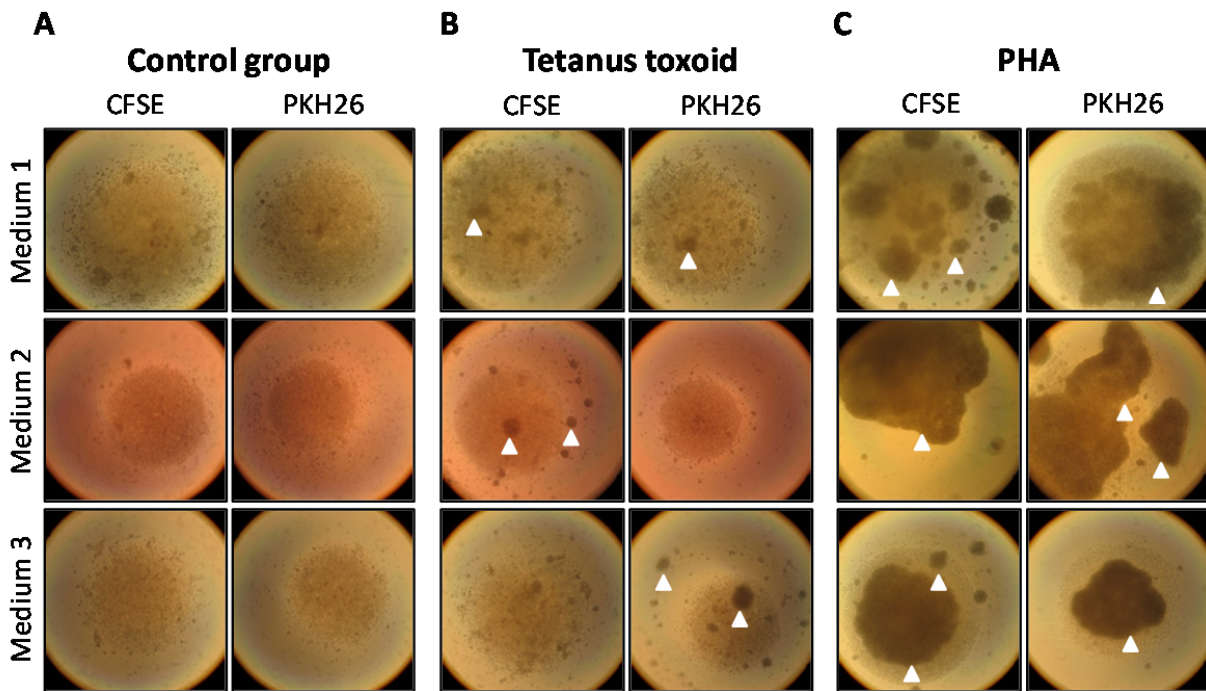
Figure 18: Assessing proliferation by microscopic observation of cluster formation. (**A-C**) PBMCs were cultured using 3 different medium compositions, as described in material and methods. Subsequently, CFSE or PKH26 labeled PBMCs, alone (**A**) or stimulated with tetanus toxoid (TT, 10ng/ml) (**B**) or phytohemagglutinin (PHA; 500ng/ml) (**C**) were cultured for 6 d, after which proliferation was assessed by the formation of clusters (arrow heads). Micrographs are representative of at least 2 independent experiments.

By flow cytometry a more quantitative profile of proliferation was acquired. Upon division of a cell, its progeny are endowed with an equal number of labeled molecules. Each division is assessed by measuring the decrease in fluorescent intensity. Based on the Forward (FSC) and Sideward Scatter (SSC) the lymphocyte proliferation was gated, after which fluorescent intensities were analyzed, depicted as dot plots (**Figure 19**).
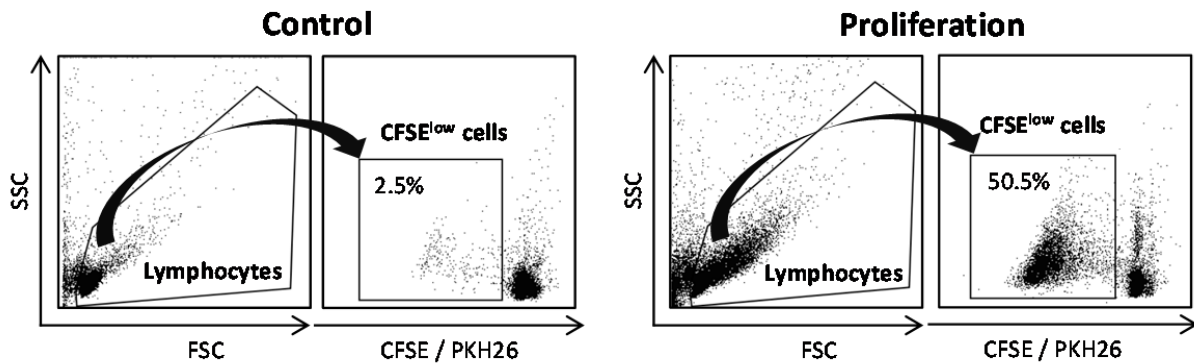
Figure 19: Gating strategy to assess proliferation by flow cytometry. PBMCs were labeled using CFSE or PKH26 and cultured in different media. Subsequently, PBMCs remained untreated (**A**) or were stimulated with phytohemagglutinin (PHA; 500ng/ml) (**B**) for 6 days after which proliferation was assessed by flow cytometry. First a gate was put on the lymphocyte population using the Forwards Scatter (FSC) and Sideward Scatter (SSC), after which a gate was placed on the proliferating lymphocytes, characterized by reduced fluorescence intensity for CFSE of PKH26. Flow cytometry histograms are representative for at least 3 independent experiments.

It was observed that the labeling procedure or the composition of the medium did not change the proliferation status of the PBMCs, as no reduced fluorescent intensity was observed (**Figure 20A**). In contrast, upon stimulation using PHA, in each condition a strong proliferation was demonstrated (**Figure 20C**). Interestingly, stimulation with TT revealed different proliferation profiles, indicating that culture medium or the labeling procedures do influence the process of proliferation. It was observed that upon TT stimulation, proliferation could be measured using CFSE in combination with medium 1 (macrophage culture medium) and 2 (X-vivo medium). In contrast, using PKH26 labeling, proliferation could only be demonstrated using medium 3 (macrophage culture medium, in which FCS is replaced by 1% human AB serum) (**Figure 20B**). Since for APC generation medium 1 is used, we selected this medium to be the most suitable and convenient in combination with CFSE to assess lymphocyte proliferation.
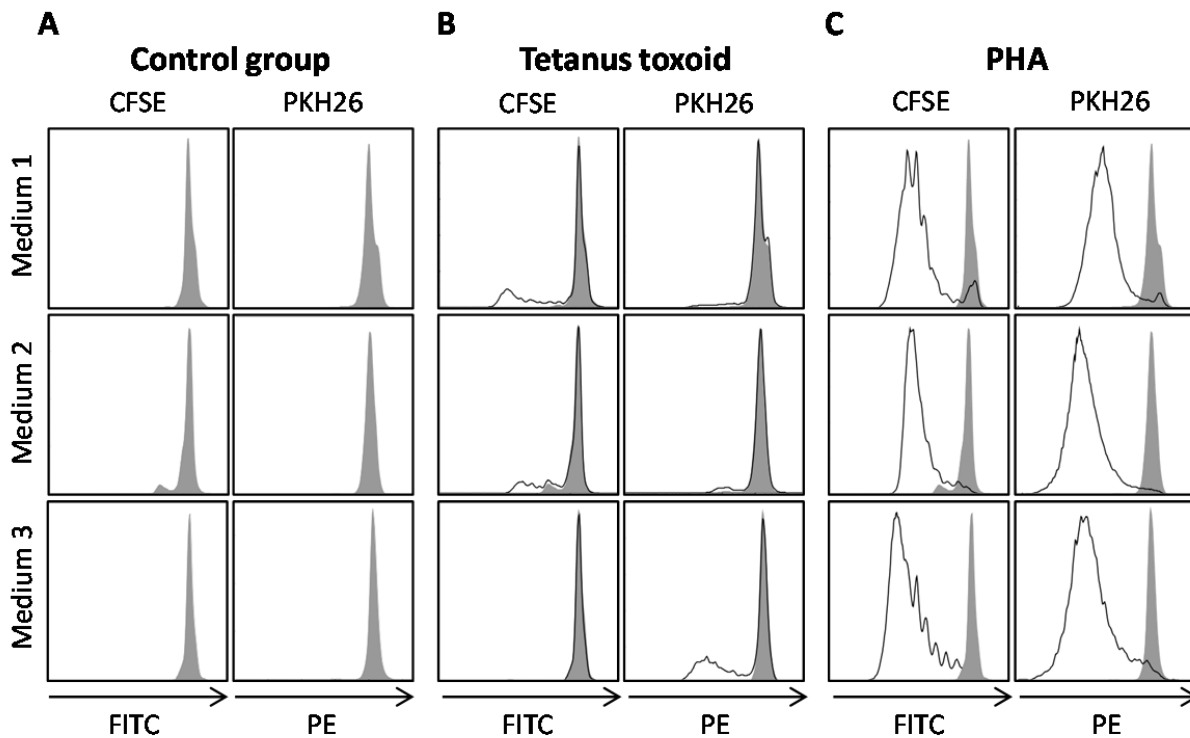
Figure 20: Assessing proliferation by flow cytometry. (**A-C**) PBMCs were cultured using 3 different medium compositions, as described in material and methods. Subsequently, CFSE or PKH26 labeled PBMCs, alone (**A**) or stimulated with tetanus toxoid (TT, 10ng/ml) (**B**) or phytohemagglutinin (PHA; 500ng/ml) (**C**) were cultured for 6 d, after which proliferation was assessed by the amount of CFSE^{low}/PKH26^{low} PBMCs by flow cytometry, using the FITC and PE channel respectively. Histograms are representative of at least 2 independent experiments.

5.3.2 In the presence of apoptotic *Lm* parasites proliferation is reduced

T lymphocyte effector functions are of great importance to clear intracellular infections. In a next step we aimed to investigate the role of T cells in our *Leishmania* model, first focusing on hMDM2. Upon TT treatment of hMDM2 for 24 h following co-incubation of autologous CFSE labeled PBMCs for an additional 6 days, a proliferating, CFSE^{low} subset (19.1% ± 1.7) was detected (**Figure 21A**). To analyze whether *Leishmania* modulate TT-induced proliferation, hMDM2 were treated with TT in combination with log.ph. *Lm*. Remarkably, after cocultivation of autologous CFSE labeled PBMCs, an even higher proliferating response (47.2% ± 3.0) was observed to proliferation induced by TT alone. When analyzing proliferation upon treating hMDM2 with TT in combination with apoptotic *Lm* (stat.ph. *Lm*), a significant reduction of proliferation could be

demonstrated (33.9% ± 2.5). Interestingly, this significant reduction could also be observed in the absence of TT. The hMDM2 infected with log.ph. *Lm* only, induced a strong proliferation (31.1% ± 2.1) which was significantly reduced in the presence of apoptotic parasites (19.3% ± 1.8) (**Figure 21A**). A similar observation was made with regard to hMDM1. In response to *Leishmania*, also a significant lower proliferation could be demonstrated when apoptotic parasites (stat.ph. *Lm*) where present (22.3% ± 1.3), compared to log.ph. *Lm* (35.3% ± 1.4), comprising viable parasites (**Figure 21 B**). Interestingly, upon infection of DCs with either stat.ph. *Lm* (44.4% ± 2.9) or log.ph. *Lm* (49.0% ± 2.3), a strong proliferating response was induced which did not differ significantly. In all, the presence of apoptotic parasites leads to a reduced proliferative response, when infecting macrophages and not dendritic cells.
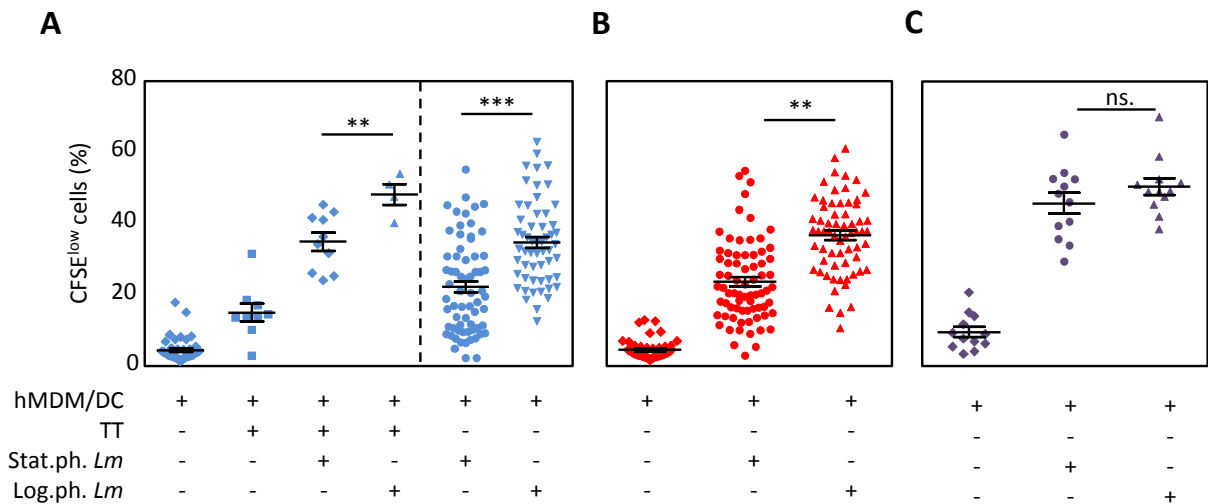
Figure 21: The presence of apoptotic parasites reduces T-cell proliferation upon *Lm* infection of hMDM, but not DCs. hMDM2 (**A**) were coincubated with tetanus toxoid (TT; 10 ng/ml) alone or with stat.ph. *Lm* or log.ph. *Lm* (MOI=10). hMDM1 (**B**) and DCs (**C**) were incubated alone or infected with stat.ph. *Lm* or log.ph. *Lm* (MOI=10). After 24 h cells were washed and co-cultured with autologous CFSE labeled PBMCs (ratio 1:5). After 6 days the CFSE^{low}, proliferating cells were quantified by flow cytometry (n=4-73). Data are presented as mean ± SEM and are representative for at least 3 independent experiments (**: p < 0.01; ***: p < 0.001).

To better compare (a) the magnitude of proliferation in our model to (b) the frequencies described in literature for MHC tetramer stainings (to detect antigen specific T cells) we applied an algorithm to calculate the precursor frequency. In response to TT and *Leishmania*, in the

context of hMDM2, a similar precursor frequency was observed. A precursor frequency of 0.01% (± 0.002) for TT and 0.02% (± 0.005) for *Leishmania* was calculated (**Figure 22**).
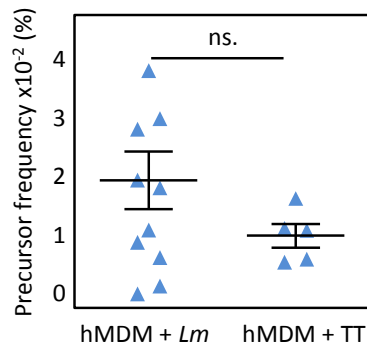
Figure 22: In response to *Leishmania* and the recall antigen tetanus toxoid a similar precursor frequency of proliferating cells was observed. hMDM2 were coincubated with Tetanus Toxoid (TT; 10 ng/ml) or infected with stat.ph. *Lm* (MOI=10). After 24 h hMDM2 were washed and cocultured with autologous CFSE labeled PBMCs (ratio 1:5). After 6 days the CFSE^low, proliferating cells were quantified by flow cytometry. The precursor frequency of proliferating cells in response to *Leishmania* or TT was calculated, as described in material and methods. Data are presented as mean ± SEM and are representative of at least 3 independent experiments.

To strengthen the finding, that the reduced proliferation is due to apoptotic parasites, we separated the stat.ph. *Lm* into viable and ANXA5-binding apoptotic parasites only, using magnetic separation. As shown for hMDM2, upon coculturing hMDM2 with apoptotic parasites, a lower proliferating subset (16.5% ± 4.8) was detected, compared to proliferation induced by viable parasites only (37.2% ± 6.3) or by the mixture of apoptotic and viable parasites (31.8% ± 5.2) (**Figure 23A**). Furthermore, upon infection of hMDM2 with either stat.ph. or log.ph. *Lm* treated with apoptosis inducing compounds, a significant reduction of proliferation was observed. Treatment of stat.ph. *Lm* with miltefosine and staurosporine reduced proliferation from 18.9% (± 1.7) to 6.4% (± 1.8) and 3.8% (± 1.0) respectively. Similarly, treatment of log.ph. *Lm* with miltefosine or staurosporine reduced proliferation from 28.8% (± 1.9) to 4.4% (± 1.1) and 4.9% (± 3.1) respectively (**Figure 23B**).

A

B
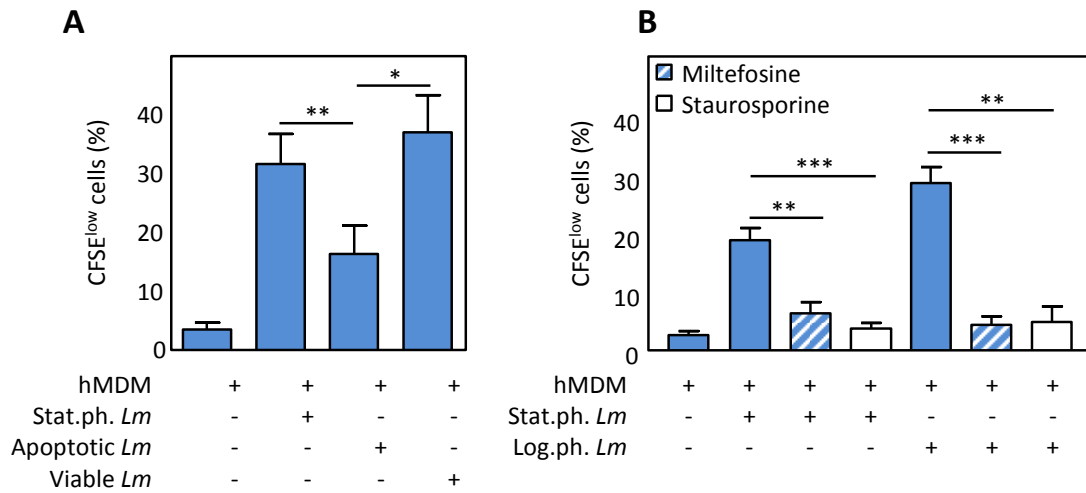
Figure 23: The presence of apoptotic parasites reduces T cell proliferation upon *Lm* infection of hMDM2. (**A**) hMDM2 were cocultured with stat.ph. *Lm*, MACS purified ANXA5⁻ viable or ANXA5⁺ apoptotic *Lm* (MOI=10). After 24 h hMDM2 were washed and cocultured with autologous CFSE labeled PBMCs (ratio 1:5). After 6 days the CFSE^low, proliferating cells were quantified by flow cytometry. (**B**) hMDM1 were infected with log.ph and stat.ph. *Lm* (MOI=10) which were pretreated with apoptosis inducing drugs, 25 µM miltefosine (stripped bars) or 25 µM staurosporine (empty bars), for 48 h prior to infection. After 24 h hMDM2 were washed and co-cultured with autologous CFSE labeled PBMCs (ratio 1:5). After 6 days the CFSE^low, proliferating cells were quantified by flow cytometry (n=6). Data are presented as mean ± SEM and are representative for at least 3 independent experiments (*: $p < 0.05$; **: $p < 0.01$; ***: $p < 0.001$).

We further wanted to shed light on the difference in proliferation, observed in the presence of apoptotic parasites. Therefore from proliferating PBMCs, in response to log.ph. and stat.ph. *Lm*, precursor frequencies were calculated. Upon infection of hMDM1 and hMDM2 – but not DCs – with log.ph. *Lm*, a significant higher precursor frequency was observed, when compared to precursor frequencies calculated upon infection with stat.ph. *Lm* (hMDM1: 0.04% ± 0.005 to 0.02% ± 0.007; hMDM2: 0.03% ± 0.004 to 0.02% ± 0.003; DC: 0.05% ± 0.006 to 0.03% ± 0.006) (**Figure 24A**). Of note, not only precursor frequencies were increased, also the proliferating indexes, reflecting the biology of the responding system, were significantly enhanced when apoptotic parasites were absent (hMDM1: 3.6 ± 0.1 to 3.3 ± 0.1; hMDM2: 3.6 ± 0.1 to 3.4 ± 0.1; DC: 3.7 ± 0.1 to 3.5 ± 0.1) (**Figure 24B**).
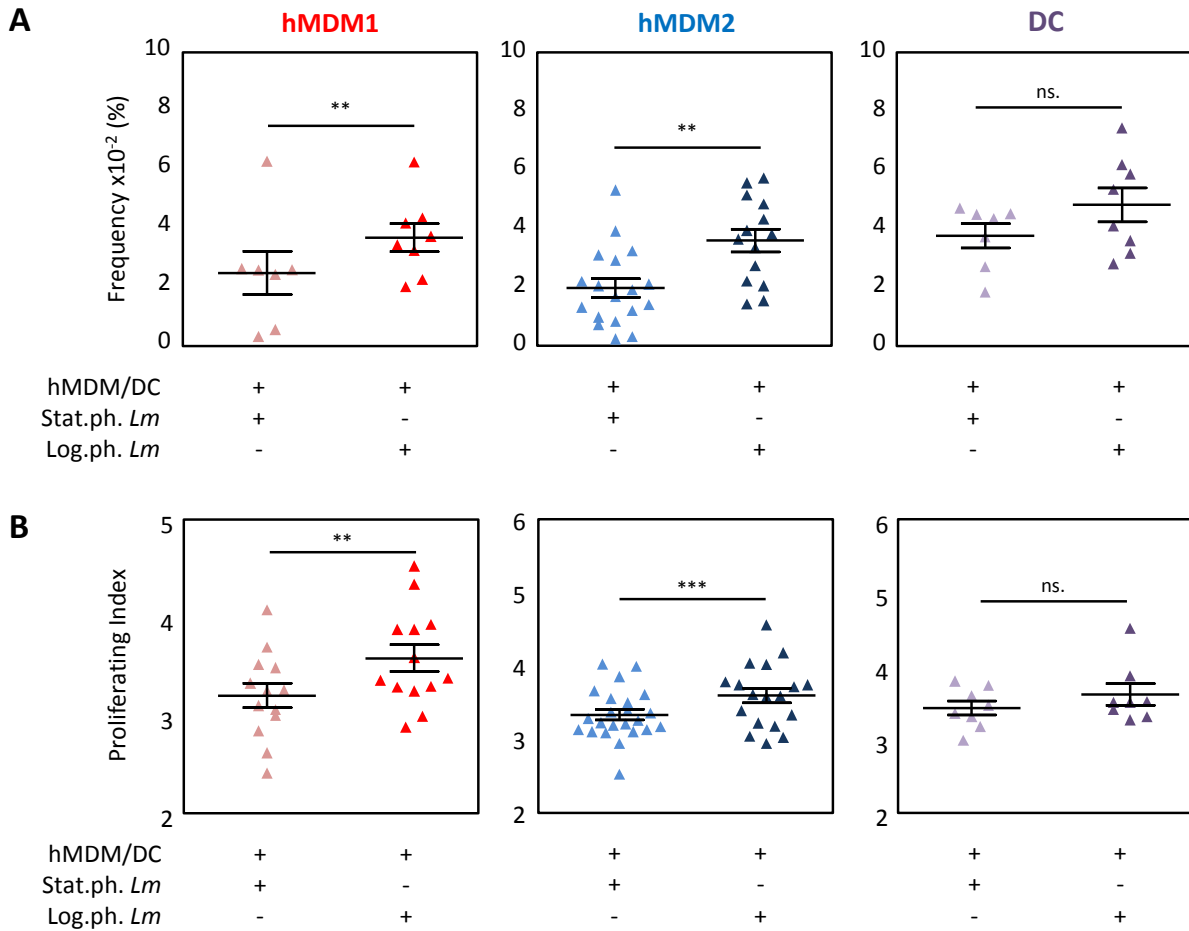
Figure 24: Precursor frequency and proliferation index are elevated in the absence of apoptotic parasites in hMDM and DCs. (**A-B**) Precursor frequency (**A**) and proliferating index (**B**) of proliferating cells in response to hMDMs or DCs, infected with stat.ph. or log.ph. *Lm* were calculated, as described in material and methods (n= 6-11). Graphs present mean ± SEM are representative for at least 3 independent experiments (**: p < 0.01; ***: p < 0.001; ns.: not significant).

5.3.3 Phenotypical characterization of the CFSE^{low} PBMCs upon *Lm* infection

Leishmania has been used extensively as a model to investigate T cell responses in mice, where a predominant Th1 response (C57BL/6 mice) leads to a healing phenotype. In BALB/c mice, characterized by a Th2 phenotype, susceptibility to disease occurs. As in humans, new T-helper subsets are discovered and the paradigm of Th1/Th2 does not always hold true, we characterized the proliferating subset in our human *Leishmania* model. Upon phenotyping the proliferation

subset, either upon infection with stat.ph. or log.ph. *Lm* we gated using the FSC/SSC on the lymphocyte proliferation. Subsequently the proliferating CFSE^{low} PBMCs were found to be CD3$^+$ (hMDM1: 85.0% ± 2.7; hMDM2: 88.4% ± 2.3; DC: 91.8% ± 2.2). The majority of these T cells were demonstrated to be CD4$^+$ (hMDM1: 81.3% ± 2.8; hMDM2: 86.0% ± 2.1; DC: 87.1% ± 1.6) and not CD8$^+$ (hMDM1: 9.0% ± 2.4; hMDM2: 5.7% ± 1.5; DC: 6.9% ± 1.8) (**Figure 25**). Interestingly, we found these T cells to be decorated with the surface marker CD45RO (hMDM1: 80.3% ± 2.8; hMDM2: 83.1% ± 2.8; DC: 88.1% ± 1.5), normally present on memory T cells, a finding in agreement with previous reports (Su and Davis, 2013).
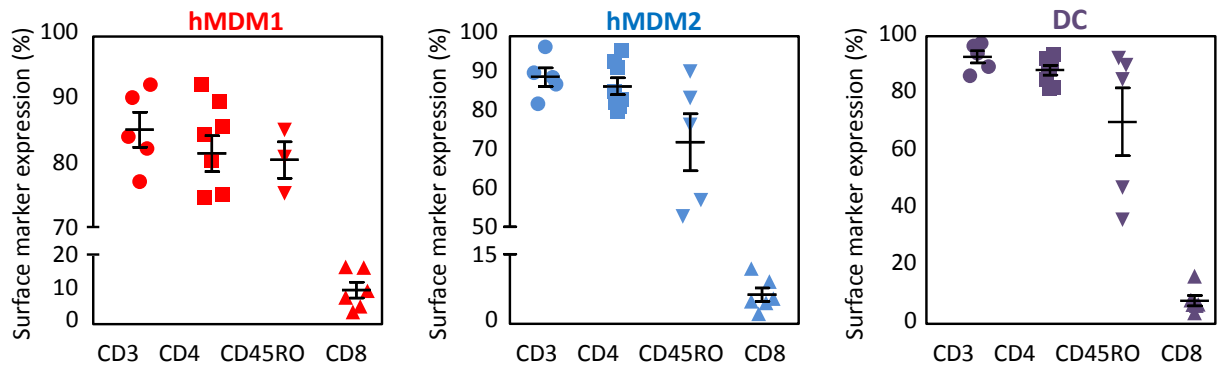
Figure 25: Upon *Lm* infection, proliferating cells comprise a CD3$^+$CD4$^+$CD45RO$^+$ phenotype. hMDMs and DCs were infected with *Lm* (MOI=10). After 24 h cells were washed after which autologous CFSE labeled PBMCs were cocultured (ratio 1:5). After 6 days the CFSE^{low}, proliferating cells were phenotyped for CD3, CD4, CD45RO and CD8 by flow cytometry. Data present the mean ± SEM and are representative for at least 3 independent experiments.

Memory T cells are crucial in boosting an early immune response hereby preventing disease development. We further characterized the memory T cells by assessing the presence of L-selectin. Preliminary data suggested L-selectin, also termed CD62L, to be present on 93.4% (± 0.5) of the proliferating T cells, indicative for a central memory T cell phenotype (**Figure 26C**). In addition to surface marker profiling, the presence of transcription factors was analyzed. It could be demonstrated that upon proliferation, the proportion GATA3$^+$ T cells was significantly higher than T-bet$^+$ T cells, in response to either log.ph. or stat.ph. *Lm*, stained positive for the

transcription factor GATA3, 94.3% (± 5.4) to 5.7% (± 5.4) and 93.6% (± 4.8) to 6.5% (± 4.8) respectively (**Figure 26A and B**).
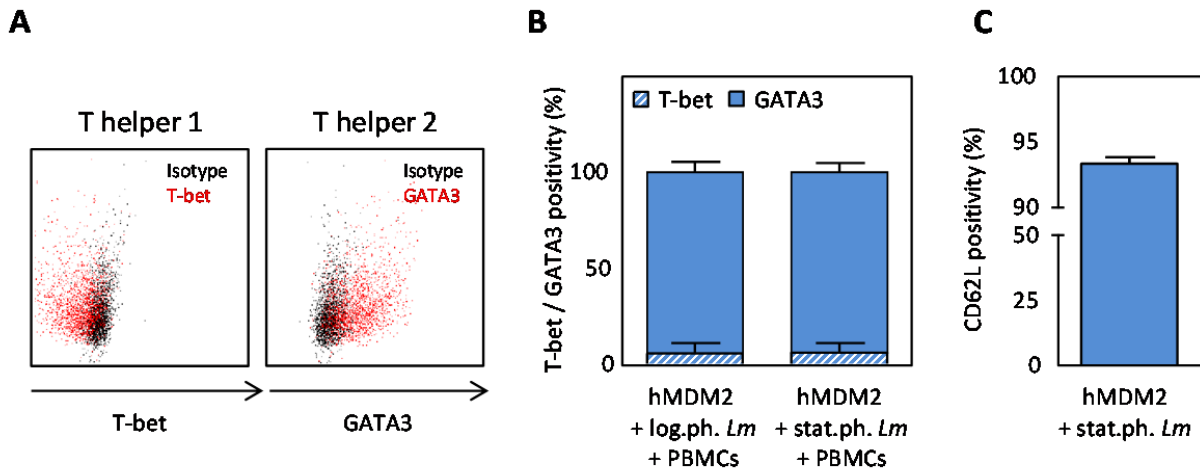
Figure 26: Proliferating subset comprises effector memory T cells. hMDM2 were infected with either log.ph. or stat.ph. *Lm* for 24 h (MOI=10). Autologous CFSE labeled PBMCs were cocultured for 6 days after which proliferating CFSE^{low} cells were phenotyped for the transcription factors T-bet and GATA3 by intracellular staining (**A,B**) or for the surface marker CD62L (**C**), assessed by flow cytometry. Data, as mean ± SEM and dot plots are representative for 2 independent experiments.

Activation of CD4$^+$ T cells requires antigen presentation by MHCII molecules. To test the MHC restriction in our human *in vitro* system we treated *Lm* infected hMDM2 with blocking antibodies specific for human MHCI or MHCII. After 6 days of co-cultivation with autologous PBMCs, T cell proliferation was analyzed by flow cytometry. No effect of increasing amounts of MHCI specific antibodies was detectable (**Figure 27A**). By contrast, when exposing hMDM2 to increasing amounts of MHCII specific antibodies, a dose dependent reduction of CFSE^{low} PBMCs was observed. Proliferation was significantly reduced (0.3 ± 0.01 fold change) compared to the control, when treating hMDM2 with anti-MHCII antibodies at the highest tested dose (**Figure 27A**). In addition, the role of antigen processing in hMDM2 was investigated. Lysosomal acidification was inhibited by Bafilomycin A1 (BAFA1) dose dependently, assessed by a reduced Lysotracker positivity (**Figure 27B and C**). By preventing MHCII antigen processing, proliferation could be demonstrated to be significantly reduced during infection of hMDM2 with log.ph. *Lm* (42.1% ± 2.9 to 6.7% ± 1.2) and stat.ph. *Lm* (32.6% ± 4.1 to 8.0% ± 1.3) (**Figure 27D**).
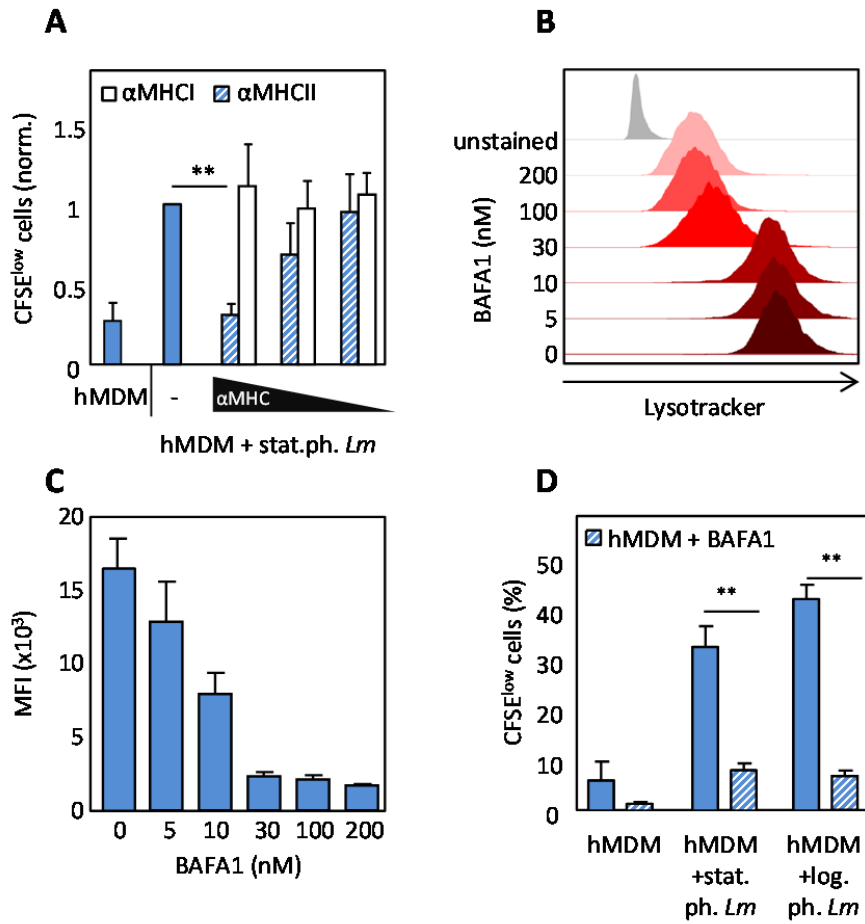
Figure 27: *Lm* **induced proliferation is MHCII and antigen processing depending.** (**A**) hMDM2 were treated with α-MHCI (white bars) and α-MHCII (stripped bars) antibodies at various dilutions prior to infection with stat.ph. *Lm* (MOI=10). After 24 h hMDM2 were cocultured with autologous CFSE labeled PBMCs (ratio 1:5). After 6 days the CFSE[low], proliferating cells were quantified by flow cytometry. (**B-C**) hMDM2 were treated with increasing amounts of Bafilomycin (BAFA1) to inhibit lysosomal acidification, assessed by lysotracker staining using flow cytometry. (**D**) hMDM2 were treated with 30nM BAFA1 prior to infection with stat.ph. and log.ph. *Lm* (MOI=10). After 24 h, hMDM2 were cocultured with autologous CFSE labeled PBMCs (ratio 1:5). After 6 d, CFSE^{low} proliferating cells were assessed by flow cytometry. Histograms and data, presented as mean ± SEM, are representative for at least 3 independent experiments (**: p < 0.01).

5.3.4 A MHCII restricted and antigen processing dependent proliferation

Different hypotheses about the reduced proliferation by the apoptotic parasites can be raised. Underneath, several potential factors are investigated which may influence proliferation, hereby focusing on hMDM2. A first parameter influencing proliferation may be antigen availability. During the process of apoptosis various proteins are targeted for degradation. To exclude the possibility that the reduced protein amount in apoptotic parasites could be responsible for the significant lower proliferation, parasite protein levels were normalized. By applying the micro-Kjeldahl method the protein concentration of the parasites in both growth stages was determined (Röder et al., 2013). Next, hMDM2 were infected with log.ph. (MOI=10) and stat.ph. *Lm* parasites (MOI=17), normalized for protein content. However, hMDM2 infected with stat.ph. *Lm* parasites (MOI=17) still induced a significant lower proliferation (18.9% ± 3.6), compared to proliferation induced by hMDM2 harboring viable parasites (27.2% ± 2.8) (**Figure 28A**). Second, the importance of parasite integrity was assessed. Stimulating hMDM2 with Soluble *Leishmania* Antigen (SLA) led to a significant reduction of proliferation, compared to proliferation induced upon infection with intact parasites (**Figure 28A**). Third, parasites like Trypanosomes are able to secrete antigens themselves which might be able to induce proliferation early after exposure to immune cells (Berrizbeitia et al., 2006; Santarém et al., 2007). To determine whether the observed *Leishmania* induced T cell response is elicited by such antigens and thus dependent on the viability of the parasites, hMDM2 were incubated with supernatant fraction (SN), collected from stat.ph. *Lm* parasite cultures and subsequently cocultivated with autologous PBMCs. After 6 days, no significant higher proliferation could be observed compared to proliferation induced by the non-treated hMDM2 (**Figure 28B**). Moreover, analyzing proliferation over time showed proliferation to start at day 3-4 after PBMC coculturing (**Figure 28C**). A fourth explanation lies in the fact that parasites are able to directly interact with PBMCs as described for natural killer cells (Lieke et al., 2008). To address this question, we directly cocultured parasites with PBMCs (from which monocytes were depleted by plastic adherence), containing T cells, as well as dendritic cells and a small fraction of remaining monocytes. An increasing amount of *Leishmania* promastigotes did however only induce a minor proliferation of CD4$^+$ cells (6.2% ± 1.7), which

was lower compared to proliferation induced by infected APCs (**Figure 28D**). In all, these data demonstrate that human primary macrophages, upon *Leishmania* infection, induce an antigen specific, MHCII dependent T cell response, which is dampened in the presence of apoptotic parasites.
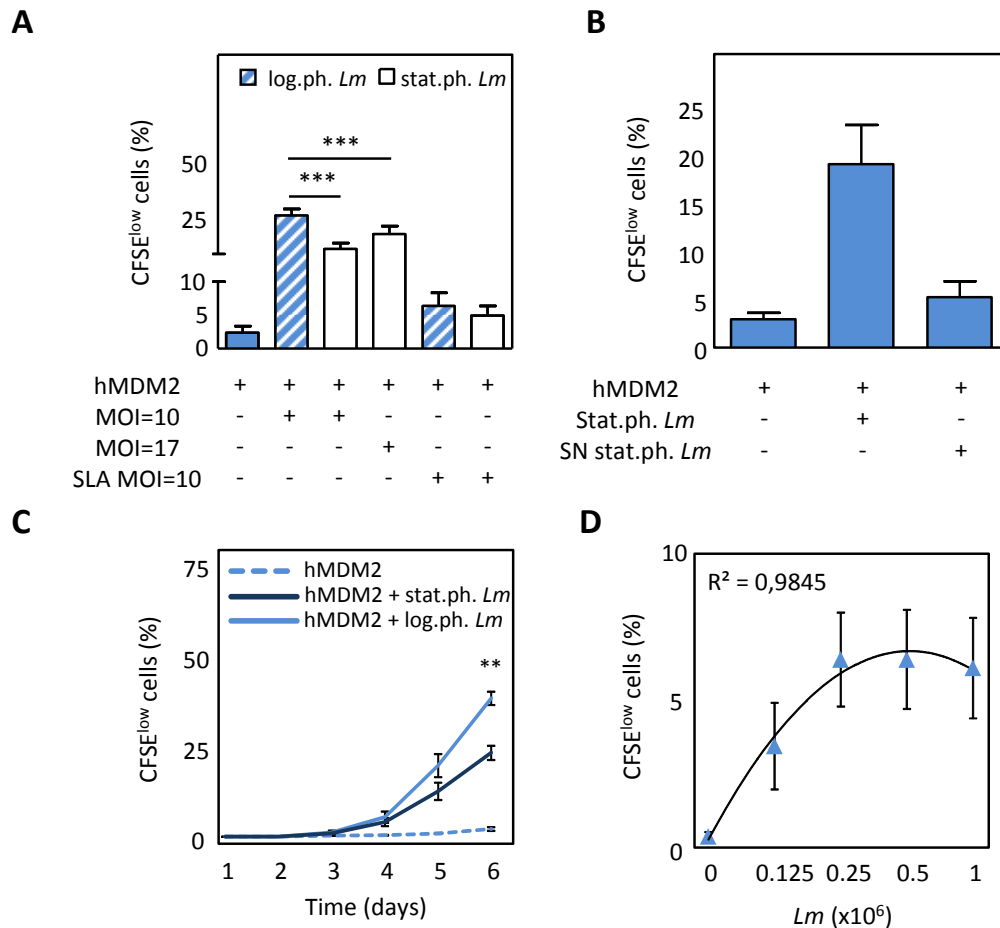

Figure 28: Characteristics of *Lm* induced proliferation. (**A**) hMDM2 were treated with Soluble *Leishmania* Antigen (SLA) or infected with log.ph. or stat.ph. *Lm*. Intact parasites were normalized for the absolute parasite number of parasites or protein concentration, as determined by the micro-Kjeldahl method (MOI=10 and MOI=17 respectively). After 24 h hMDM2 were washed following coculturing with autologous CFSE labeled PBMCs (ratio 1:5). After 6 days the CFSE^low, proliferating cells were quantified by flow cytometry (n=7). (**B**) hMDM2 were co-cultured with the supernatant fraction (SN) of infected hMDM2. After 24h, autologous CFSE labeled PBMCs were cocultured (ratio 1:5). After 6 d CFSE^low, proliferating cells were quantified by flow cytometry. (**C**) hMDM2 were infected with stat.ph. or log.ph. *Lm* (MOI=10). After 24 h hMDM2 were washed following coculturing with autologous CFSE labeled PBMCs (ratio 1:5) after which daily CFSE^low, proliferating cells were quantified by flow cytometry. (**D**) CFSE labeled PBMCs were cocultured with various dilutions of stat.ph. *Lm* for 6 d after which CFSE^low, proliferating cells were quantified by flow cytometry. Data are presented as mean ± SEM of at least 3 independent experiments (**: $p < 0.01$; ***: $p < 0.001$).

5.3.5 Proliferation contributes to a reduced *Lm* infection

To investigate the consequences of proliferation on parasite infection rate and parasite load we used transgenic *Lm* parasites, of which the viable parasites express the dsRed protein. This offered us the ability to use flow cytometry to analyze parasite survival by means of infection rate (dsRed$^+$ cells) and parasite load (Mean Fluorescent Intensity, MFI). Next, the hMDMs or DCs were infected with the infectious stat.ph. transgenic *Lm* parasites for 24 hours, following coculturing with or without PBMCs for an additional 5-6 days.

Interestingly, the presence of proliferating T cells significantly reduced both the infection rate and parasite load in hMDMs and DC. As already shown, the highest infection rate was observed in DCs in the absence of PBMC coculturing. However, upon coculturing with autologous PBMCs, the strongest reduction of infection rate was observed among infected DCs (65.0% ± 7.2), followed by hMDM2 (49.8% ± 6.8) and hMDM1 (32.2% ± 8.3) (**Figure 29A**). In line, also parasite load was reduced in DCs (69.0% ± 4.8), hMDM1 (31.9% ± 3.0) and hMDM2 (28.0% ± 6.7) (**Figure 29B**). Illustrative to the quantitative data, it can be visualized that after 7 days of infection with dsRed transgenic stat.ph. *Lm*, parasites are able to transform into the amastigote form, confirming previous data of wild-type parasites (**Figure 14**). Upon coculturing PBMCs for 6 days, a strongly reduced intracellular parasite load (thin arrows) is visualized (**Figure 29C**).
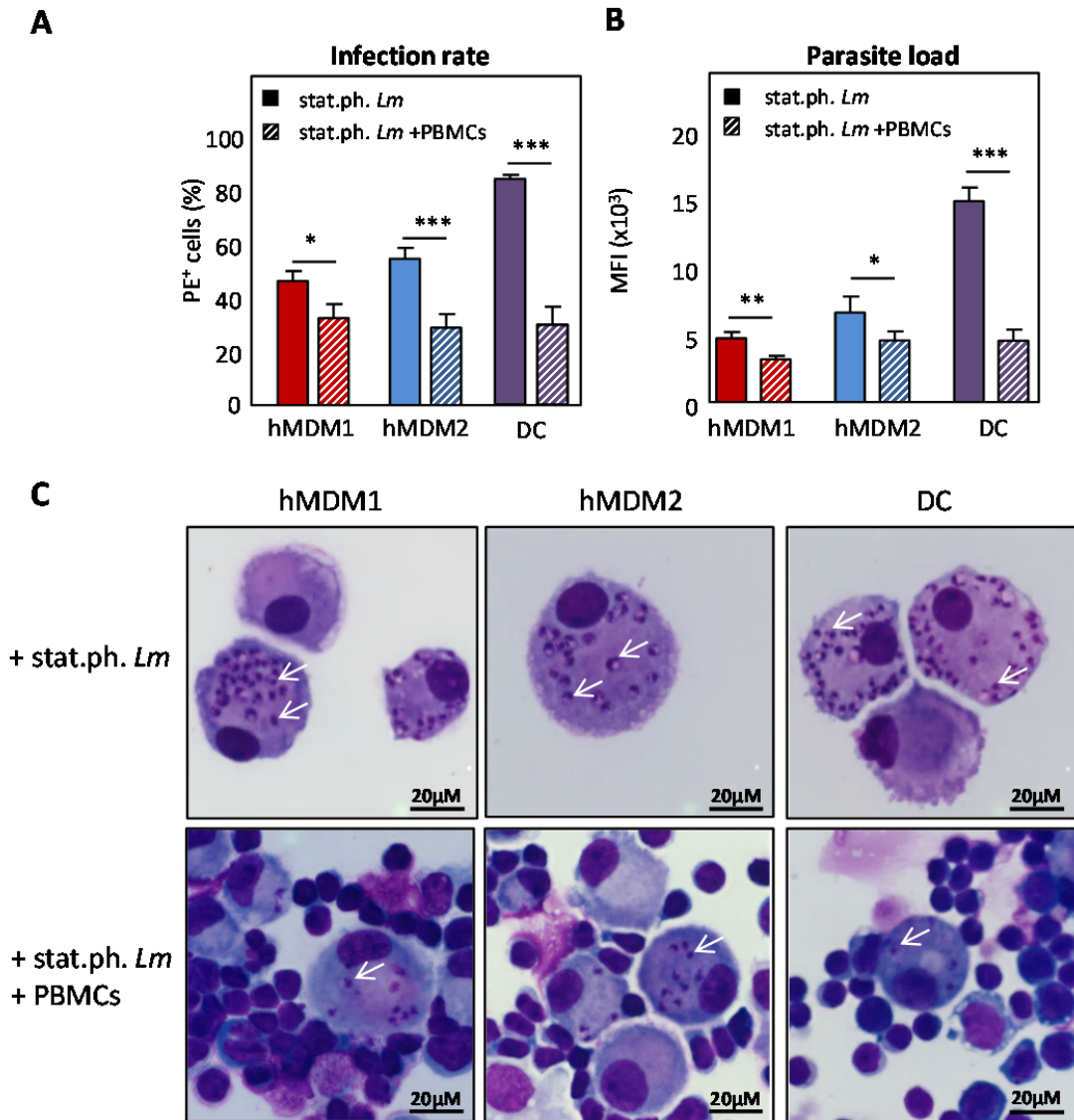
Figure 29: Proliferation leads to a reduced parasite survival. (**A-B**) hMDMs and DCs were infected with stat.ph. transgenic dsRed expressing *Lm* (MOI=10). After 24 h cells were washed following co-culturing with (stripped bars) or without (filled bars) autologous CFSE labeled PBMCS (ratio 1:5). After 6 days, infection rates of hMDMs and DCs were analyzed by flow cytometry, as dsRed (PE^{+}) positive cells (**A**). The mean fluorescence intensity (MFI) of *Lm* dsRed infected (PE^{+}) cells was analyzed to determine the parasite load (**B**). Data were normalized. (**C**) Representative DiffQuick pictures of hMDMs and DCs infected with stat.ph. *Lm* in the presence or absence of autologous PBMCs, are depicted (thins arrows indicate *Lm* parasites). Data, presented as mean ± SEM, are of at least independent experiments (*: $p < 0.05$; **: $p < 0.01$; ***: $p < 0.001$; ns.: not significant).

In the context of hMDM2, the impact of apoptotic parasites on parasite survival during PBMC cocultivation was further pursued. It could be demonstrated that the presence of apoptotic parasites reduced parasite elimination; infection with stat.ph. *Lm* during PBMCs coculturing led

to a 1.7 (± 0.1) fold reduction in infection rate, whereas infection with log.ph. *Lm* led to a 2.5 (± 0.3) fold reduction (**Figure 30A**). Parasite load was reduced in a similar extent, a 1.41 (± 0.19) fold and a 1.45 (± 0.08) fold reduction, respectively (**Figure 30C**). Of notice, when comparing infection of stat.ph. and log.ph. *Lm* parasites, it was observed that although initial infection with log.ph. *Lm* occurred with a greater proportion of viable parasites, they survive less good (**Figure 30A**). Indeed, in the presence of apoptotic parasites (stat.ph. *Lm*, thin arrows), a significant higher overall parasite survival was achieved compared to infection with log.ph. *Lm* (arrow heads), which manifests itself in an increased infection rate and parasite load, as depicted (**Figure 30B**). In conclusion, these data demonstrate the importance of the apoptotic parasites, as part of the *Leishmania* infectious inoculum, to secure survival of the overall population in hMDM.
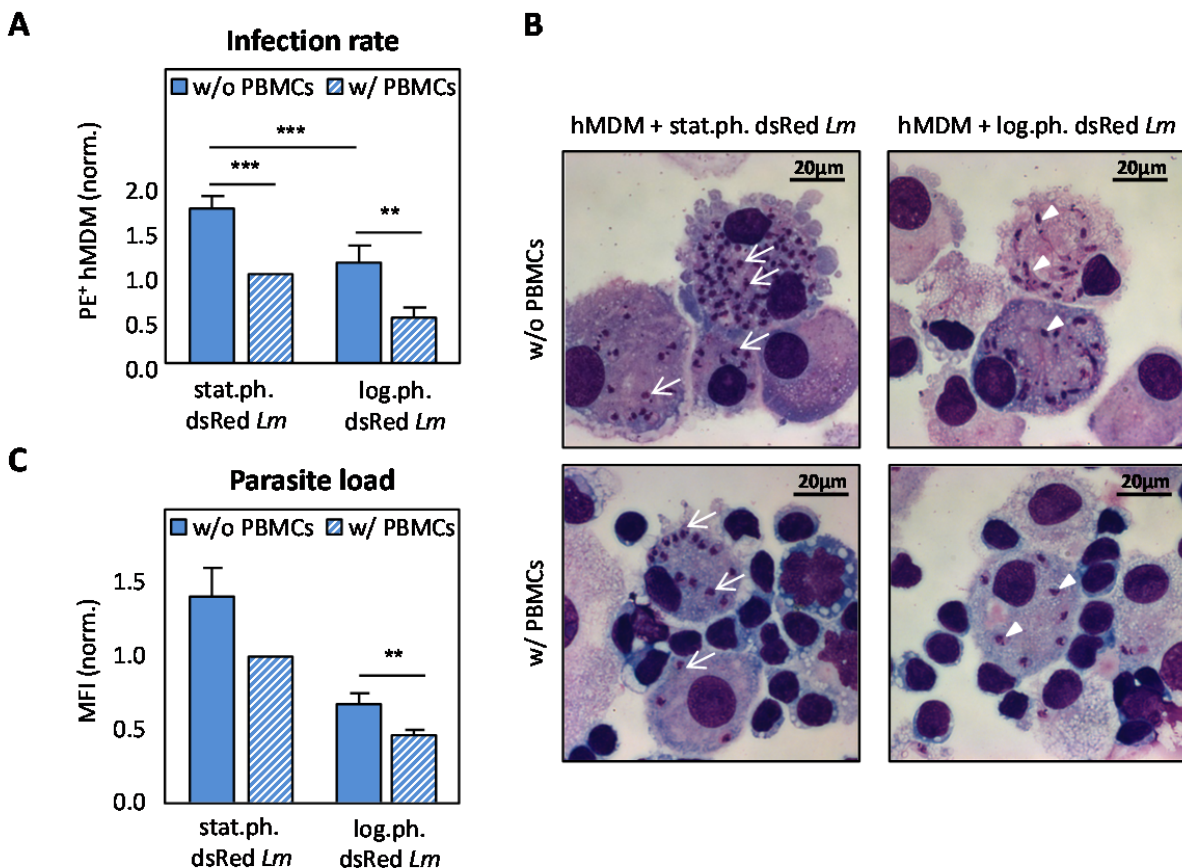
Figure 30: The presence of apoptotic parasites rescues intracellular survival. hMDM2 were infected with log.ph. or stat.ph. transgenic dsRed expressing *Lm* (MOI=10). After 24 h hMDM2 were washed following co-culturing with (w/, stripped bars) or

without (w/o, filled bars) autologous CFSE labeled PBMCS (ratio 1:5). After 6 days, infection rates of hMDM2 were analyzed by flow cytometry, as dsRed (PE$^+$) positive hMDM (**A**). The mean fluorescence intensity (MFI) of Lm dsRed infected (PE$^+$) hMDM2 were analyzed to determine the parasite load (**B**). Data were normalized. (**C**) Representative DiffQuick© pictures of hMDM2 infected with log.ph. *Lm* (arrow heads) or stat.ph. *Lm* (thin arrows) in the presence or absence of autologous PBMCs, are depicted. Data, presented as mean ± SEM, are of six independent experiments (**: p < 0.01; ***: p < 0.001).

5.4 Intracellular fate of *Leishmania* in hMDM

To better understand the immunological consequence of *Leishmania* infection, we investigated the intracellular fate of *Leishmania* parasites. A previous publication of our group could already show uptake of promastigotes to occur actively, involving membrane ruffling (Wenzel et al., 2012). To gain a better understanding on parasite host cell interactions, a live cell imaging platform was acquired and established. This LSM7 Live confocal system enabled us to image this dynamic process at high speed. In agreement with previous findings, preliminary data showed labeled (Deep Mask Red) macrophages to phagocytize the CFSE labeled parasites, in a small timeframe (0-81s) (**Figure 31**).
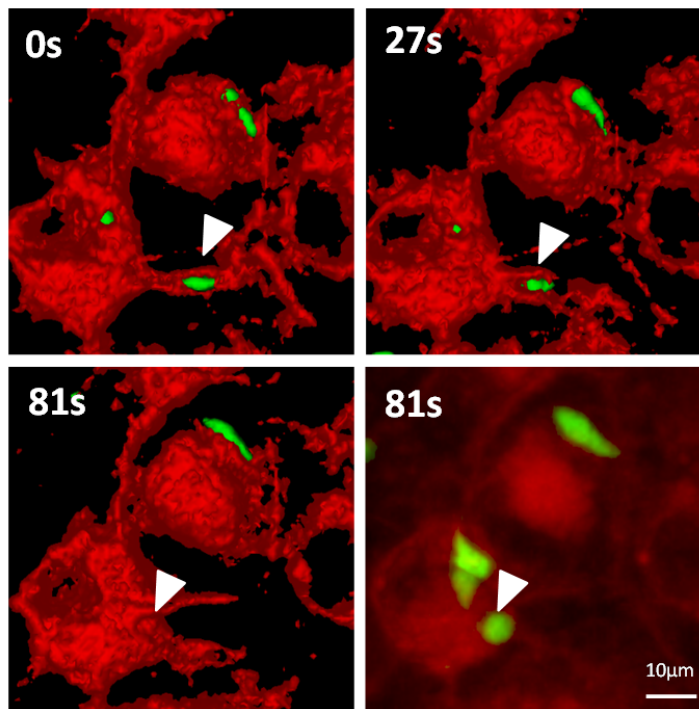
Figure 31: Macrophages actively internalize *Leishmania* promastigotes. hMDM2 were seeded in chamber slides prior to fluorescent labeling using Deep Mask Red Stain. Next, CFSE labeled stat.ph. *Lm* were added to the labeled hMDM2 after which movies were acquired. High speed live imaging, using an LSM7 Live, allowed us to make Z-stacks over time. Surface or transparent projections were generated from a hMDM2 internalizing a parasite (arrow heads), as depicted.

5.4.1 Apoptotic *Lm* induce LC3-associated-phagocytosis in hMDM

Upon infection of hMDM2 with stat.ph. *Lm*, consisting out of viable and apoptotic parasites, we found 67.2% (± 2.1) of the parasites to reside in compartments, being positive for the autophagy marker LC3 (**Figure 32A**). Autophagy is known to be involved in the clearance of apoptotic cells (Bernard and Klionsky, 2013). Therefore we investigated whether the LC3^{+} phagosomes preferentially harbor the apoptotic promastigotes. Based on preliminary data of S. Gottwalt and additional experiments using ANXA5-MACS separated populations, we found upon infection of hMDM2 that apoptotic parasites resided in a LC3^{+} compartment (92% ± 0.7), whereas the majority of the viable parasites did not (7% ± 1.0) (**Figure 32B and C**).
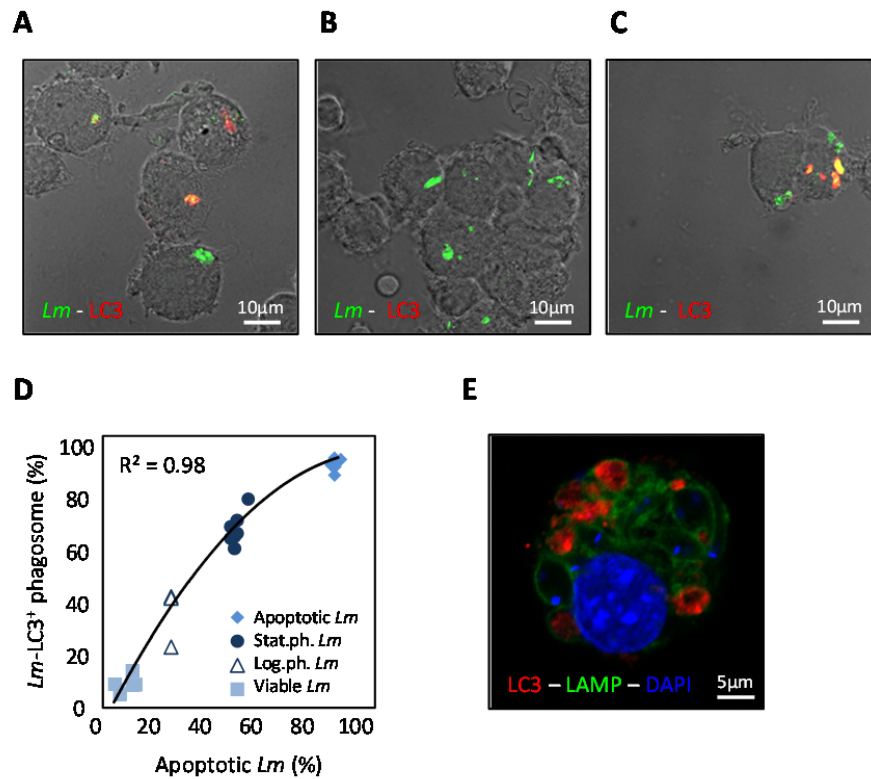
Figure 32: Apoptotic parasites induce autophagy in hMDM. hMDM2 were infected with log.ph., stat.ph. *Lm* (**A**) or MACS purified viable *Lm* (**B**) or co-cultured with purified apoptotic *Lm* (**C**) (MOI=10). After 3 h samples were fixed, stained for *Lm* parasites and LC3 using antibodies, after which *Lm*-LC3 double positive compartments were quantified by immunofluorescence analysis. (**D**) As depicted, the apoptotic rate of the *Lm* population was plotted against the percentage of *Lm*-LC3 double positive compartments, showing a correlation R. (**E**) hMDM2 were infected with stat.ph. *Lm* (MOI=10). After 3 h samples were fixed and stained for LC3 and LAMP using antibodies, counterstained with DAPI hereby visualizing the nuclei of the host cell and of parasites. Data are presented as single data points and immunofluorescence micrographs are representative for at least 3 independent experiments.

Furthermore, we could demonstrate that the rate of apoptotic parasites correlated with the amount of compartments harboring parasites, being LC3 positive (R=0.98) (**Figure 32D**). In line with these data we analyzed by quantification of immunofluorescence stainings, that log.ph. *Lm* parasites induced only low levels of LC3$^+$ compartments (34.7% ± 6.3) in hMDM2, compared to infection with stat.ph. parasites (68.9% ± 3.8) (**Figure 32D**). Compartments harboring apoptotic and viable parasites also matured, becoming positive for the lysosome-associated membrane proteins 2 (LAMP2), indicating lysosomal fusion. Compartments in which apoptotic parasites reside, became double positive for LC3 and LAMP, whereas viable parasites were found to be located in only LAMP positive phagolysosomes (**Figure 32E**).

In addition, we examined the autophagy activity using western blot analysis. Upon infection with log.ph. *Lm* (containing only a small fraction of apoptotic cells), already a significant increased conversion ofLC3-I to LC3-II was detected, which was even higher with increasing amounts of apoptotic *Lm* (stat.ph. *Lm*) (**Figure 33A and B**). To gain a better understanding of the autophagy pathway, we analyzed the expression of the ubiquitin-binding adaptor SQSTM1, a marker of conventional autophagy of which the expression correlates inversely with LC3-I to LC3-II conversion. Interestingly, upon infection with either of both *Leishmania* stages, no difference in SQSTM1 expression was observed (**Figure 33A and B**).
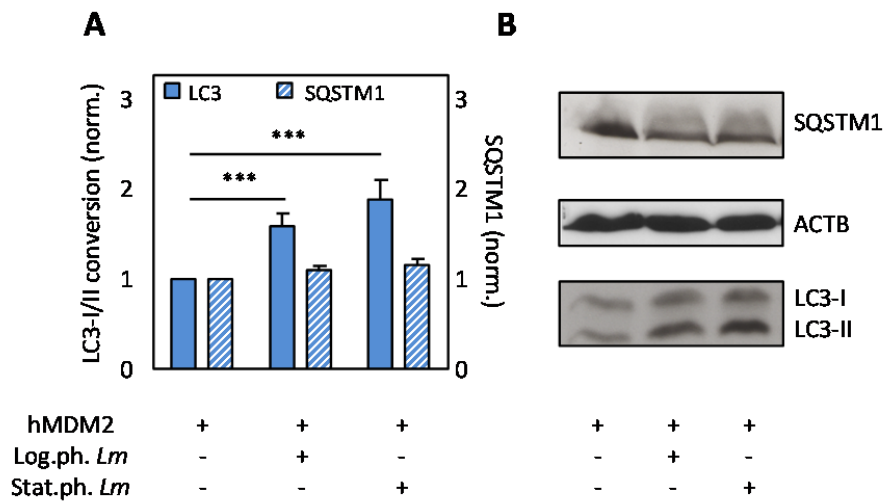
Figure 33: Apoptotic parasites induce LC3 conversion in hMDM. hMDM2 were infected with stat.ph. or log.ph. *Lm* (MOI=10). After 3 h, lysates were made after which LC3 conversion (filled bars) and SQSTM1 levels, normalized to β-actin (ACTB) expression, (stripped bars) were assessed by western blot and densitometry analysis (**A**). Immunoblots (**B**) and data, presented as mean ± SEM, are representative for at least 3 independent experiments (***: $p < 0.001$).

Another hallmark of conventional autophagy is the formation of autophagosomes, consisting out of a multimembrane membrane structures (**Figure 34A**). To examine the ultrastructure of parasite containing compartments, we preserved the samples by high pressure freezing, followed by electron microscopy analysis. Preliminary findings demonstrated that parasites were surrounded by a single lipid bilayer, as depicted (**Figure 34B**). A more detailed analysis was performed in the project of M. Thomas, focusing on compartment development. Taken together,

these data already suggest LC3 associated phagocytosis to play a role in the biogenesis of phagosomes containing apoptotic *Lm* parasites in hMDM.
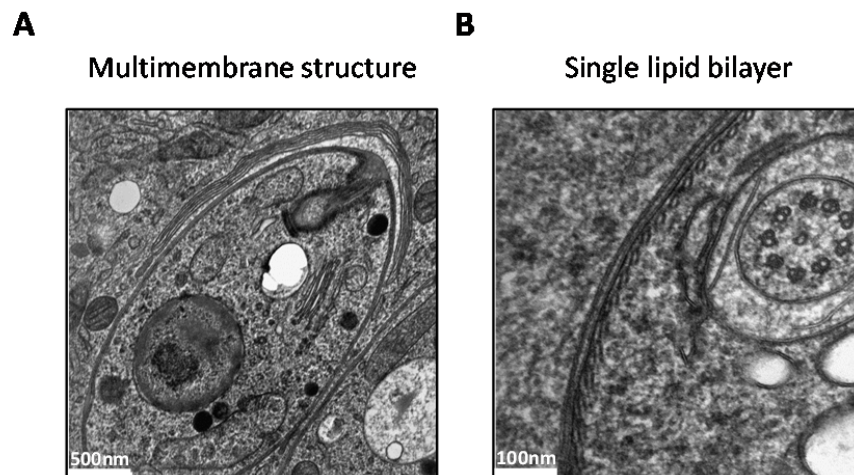
Figure 34: Conventional autophagy versus LAP. By high pressure freezing, samples were prepared for electron microscopy analysis showing a hMDM harboring a *Lm* amastigote in a multimembrane (**A**) and a *Lm* promastigote in a single membrane (**B**) compartment, indicating conventional autophagy and LC3 associated phagocytosis (LAP), respectively.

In a next step we analyzed whether apoptotic parasites were also able to induce autophagy in DCs, compared to hMDMs. In both hMDM1 and hMDM2 a significantly increased conversion of LC3-I to LC3-II could be demonstrated upon infection in the presence of apoptotic parasites, respectively 2.3 fold (± 0.3) and 2.1 fold (± 0.3). Infection with log.ph. *Lm* induced only a significantly enhanced conversion in hMDM2 (1.8 fold ± 0.2). Infection of DCs with log.ph. *Lm* did not induce a significant increase of LC3-I to LC3-II conversion, as expected (**Figure 35A and B**). Surprisingly in the presence of apoptotic parasites, also no significantly elevated autophagy activity was detected (**Figure 35C**). Of note, when comparing untreated samples, it could also be observed autophagy activity to be lower in DCs (0.4 fold ± 0.1) compared to either hMDM1 (1.4 fold ± 0.2) or hMDM2 (1.2 fold ± 0.1) (**Figure 35A-C**).
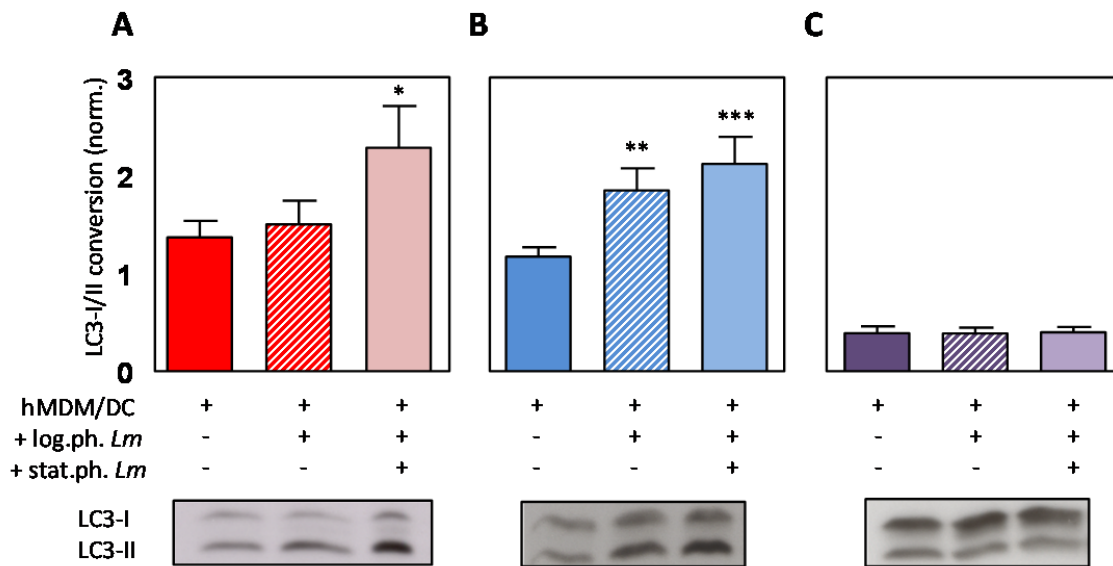
Figure 35: Apoptotic parasites do not induce autophagy in DCs. hMDM1 (**A**), hMDM2 (**B**) and DCs (**C**) were infected with log.ph. or stat.ph. *Lm* for 3 hours. Control and infected cells were lysed and prepared for western blot analysis, after which LC3-I to LC3-II conversion was assessed by densitometry analysis. Data, as mean ± SEM, and immunoblots are representative for at least 3 independent experiments (*: $p < 0.05$; **: $p < 0.01$; ***: $p < 0.001$).

5.5 Establishment of a model to modulate autophagy in human primary APCs

To investigate the role of autophagy, as negative modulator of T cell proliferation, we first established a system to modulate autophagy in human primary macrophages. For setting up the system both phenotypes of macrophages, hMDM1 and hMDM2, were used. As hMDM1 and hMDM2 behaved similarly, only data regarding hMDM2 are depicted below.

5.5.1 Autophagy activity and flux: LC3

The uptake of apoptotic cells by macrophages is known to activate the autophagy machinery, leading to efficient degradation and an anti-inflammatory environment. To mimic the role of the autophagy machinery and apoptotic promastigotes, we chemically modulated autophagy in

hMDM2. As described, PI-103, rapamycin and AZD-8055 are known to interact with the mammalian target of rapamycin, a master regulator of autophagy. Upon autophagy induction (30 min) in hMDM2, autophagy activity, measured as LC3-I to LC3-II conversion, was elevated upon treatment with rapamycin (1.7 fold ± 0.3), AZD-8055 (2.6 fold ± 0.5) and PI-103 (2.9 fold ± 0.6) (**Figure 36A**). Indeed, also by immunofluorescence analysis, an increased LC3 activity could be observed, as depicted (**Figure 36C**).
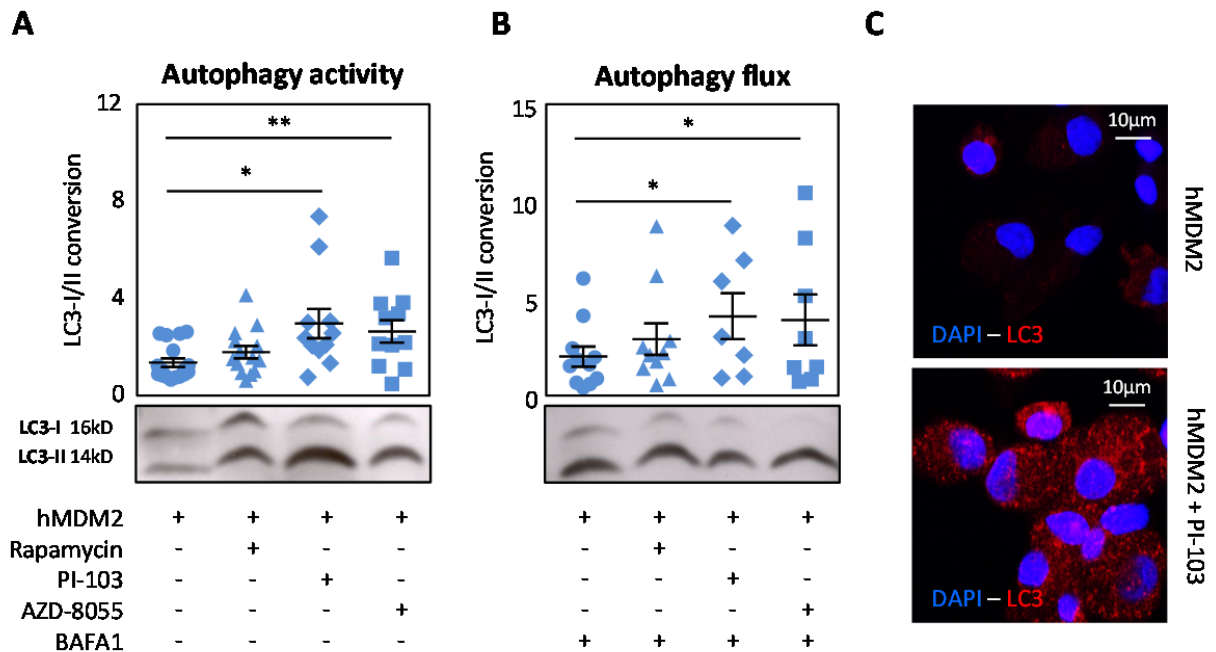
Figure 36: Assessing autophagy activity and flux in human primary macrophages. (**A-C**) hMDM2 were treated with or without bafilomycin A1 (30 nM) for 1 h, following treatment with rapamycin (1 µM), PI-103 (10 µM) and AZD-8055 (10 µM) for 30 min, after which lysates were made. By western blot and densitometry analysis the autophagy activity (**A**) and flux (**B**) were determined as the ratio LC3-II to LC3-I. Alternatively, samples were fixed and an antibody staining was performed to LC3 (red), counterstained with DAPI (blue) (**C**). Immunoblots, fluorescence micrographs and data, presented as mean ± SEM, are representative for at least 3 independent experiments (*: p < 0.01; **: p < 0.01).

The increase in autophagy activity was accompanied with an increased autophagy flux (rapamycin: 3.2 fold ± 0.8; AZD-8055: 4.1 fold ± 1.3; PI-103: 4.3 fold ± 1.2), measured as LC3 accumulation, upon bafilomycin A1 treatment (**Figure 36B**) (Klionsky et al., 2012).

To negatively modulate, hMDM2 were pretreated with several phosphoinositide 3-kinase (PI3K) inhibitors: wortmannin and 3-methyladenine (3-MA), which modulate class III PI3K negatively,

and LY294002, restraining class I PI3K activity. Although the compounds were tested at several concentrations, no optimal concentration / time point was determined by which autophagy could be modulated negatively (data not shown).

5.5.2 Autophagy activity: SQSTM1/p62

In addition to LC3, we assessed protein expression of SQSTM1 by western blot analysis in hMDM2. At early time points after autophagy induction (30 min) using rapamycin, no difference in SQSTM1 levels could be observed compared to untreated hMDM2 (data not shown). However, after 2 h of rapamycin treatment of hMDM2, a strong LC3-I to LC3-II conversion was detected, as also a decreased amount of SQMST1 protein (**Figure 37A and B**).
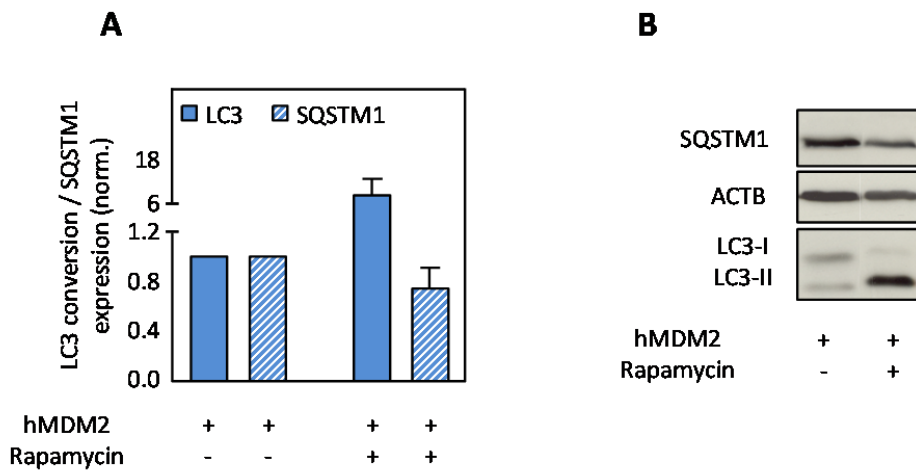
Figure 37: Assessing autophagy in hMDM2 by the marker SQSTM1/p62. (A-B) hMDM2 were treated with 1 µM rapamycin for 2 h after which lysates were made. Both LC3-I to LC3-II conversion as well as the protein expression of SQSTM1 and ß-actin (ACTB) were assessed by western blot and densitometry analysis (**A**). A representative immunoblot is shown (**B**). Data, as mean ± SEM, are representative for at least 3 independent experiments.

5.5.3 Impact of autophagy on phagocytosis

Modulation of PI3 kinases or mTor might also have undesired side effects. Unwanted cytostatic side effects occur or phagocytosis is impaired as reported by Cadwell et al. (Cadwell and Philips, 2013). To exclude that the reduced proliferation is caused by impaired parasite internalization, we analyzed whether autophagy induction influences infection rate and/or parasite load. However, after treatment of hMDM2 with either rapamycin or AZD-8055, no change in infection rate and parasite load was observed 24 h post infection. In contrast, upon treatment with PI-103, parasite uptake was impaired as a significant lower infection rate (**Figure 38A and B**) and parasite load (**Figure 38C and D**) was demonstrated. In addition, also upon modulating autophagy negatively, we found phagocytosis to be impaired at early time points (3 h) after treatment with wortmannin (data not shown).
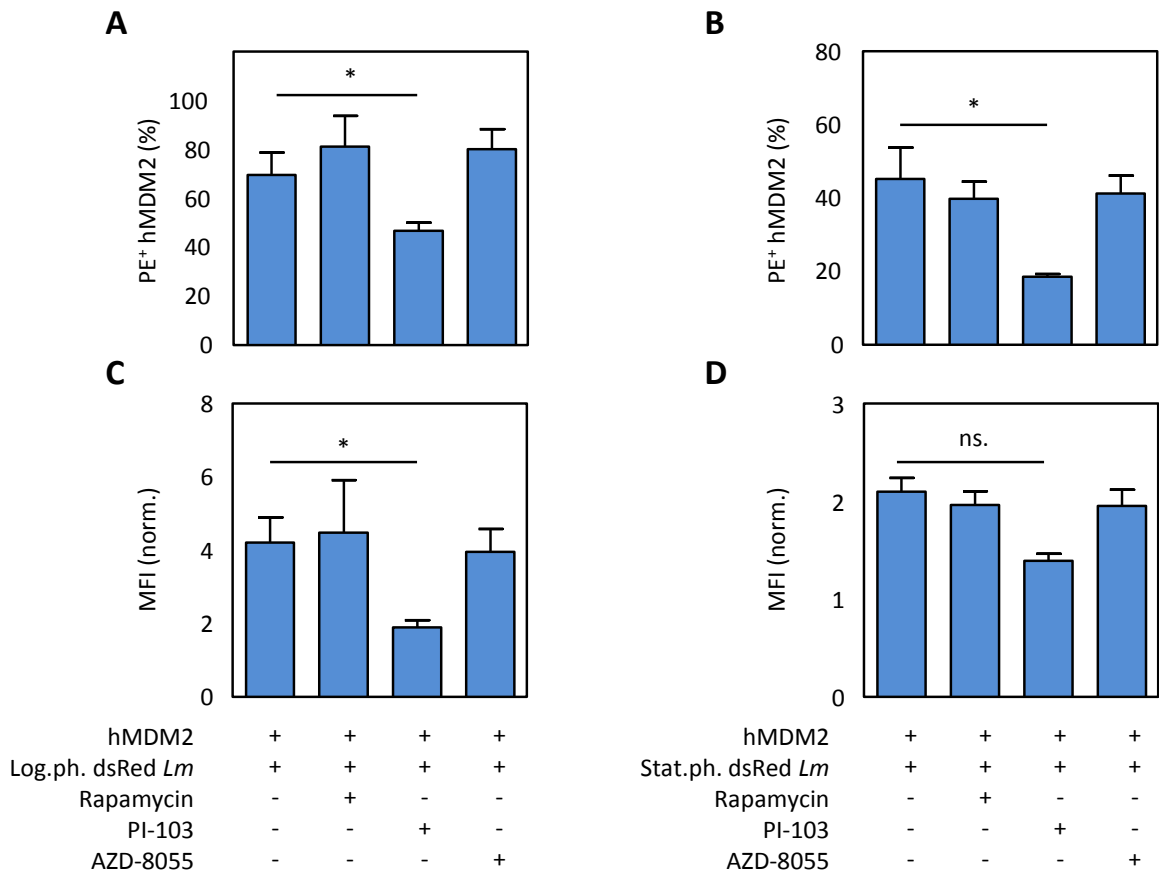
Figure 38: Modulating autophagy using PI-103 influences parasite internalization. (**A-D**) hMDM2 were pretreated with rapamycin (1 μM), PI-103 (10 μM) or AZD-8055 (10 μM) for 30 min after which hMDM2 were infected with transgenic log.ph. or stat.ph. dsRed *Lm* (MOI=10). After 24 h infection rate (PE$^+$ hMDM) (**A and B**) and parasite load (mean fluorescent intensity) (**B and C**) were assessed by flow cytometry. Data, as mean ± SEM, are representative for at least 3 independent experiments (*: p < 0.05; ns.: not significant).

5.5.4 Modulating autophagy using siRNA

Chemical modulation of cell specific process is known to have adverse effects. To target the autophagy pathway more specifically we used a siRNA knockdown approach in human primary macrophages. Therefor the proteins Beclin-1 and ATG7 were chosen, as they both play a crucial role during the process of autophagy and during LC3 associated phagocytosis. For both target proteins, single siRNAs were tested for their efficiency to reduce mRNA levels. Upon treatment of hMDM2, a knockdown efficiency of 94.2% (± 0.5) and 90.5% (± 1.1) was achieved using the most optimal siRNA, for Beclin-1 and ATG7, respectively (**Figure 39A and B**). In the case of ATG7, although the mRNA level was strongly reduced, no reduced protein level could be observed (**Figure 39C**). Of note, a sequential knockdown approach was performed, in which siRNA targeting ATG7 was given twice to the hMDM. Over a time span of 96 h (4 d) a reduced mRNA level was present, nevertheless the protein level remained unaffected.
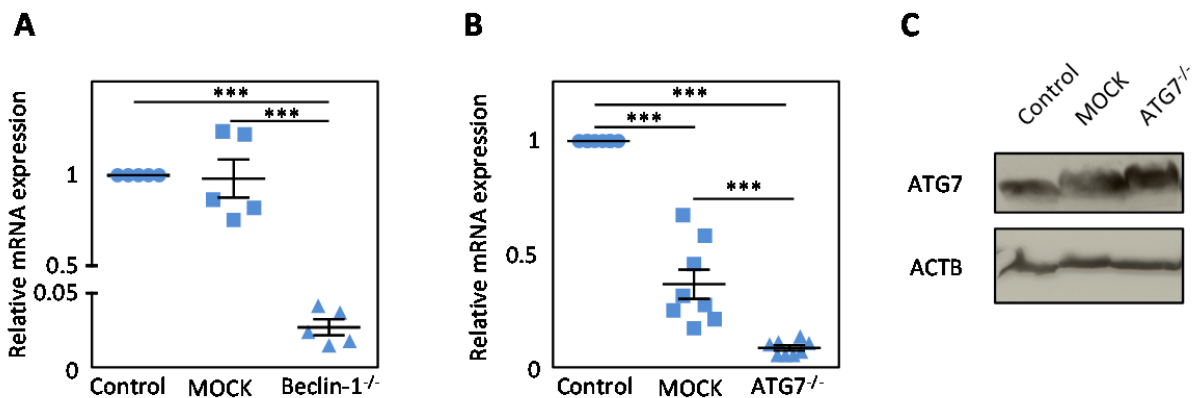
Figure 39: Knockdown efficiency of Beclin-1 and ATG7 in hMDM2. (**A-C**) hMDM2 were targeted with siRNAs against Beclin-1 or ATG7, as described in material and methods. Knockdown efficiency on mRNA level was analyzed using qRT-PCR for Beclin-1 (**A**) and ATG7 (**B**) and on protein level by western blot analysis for ATG7 and ß-actin (ACTB) (**C**). The immunoblots and data, as mean ± SEM, are representative for at least 3 independent experiments (***: p < 0.001).

5.5.5 Impact of autophagy on T cell proliferation during *Lm* infection

Subsequently, we analyzed the effect of autophagy modulation on T cell proliferation. To this end we induced autophagy in hMDM2 and hMDM1, followed by infection with viable parasites only (log.ph. *Lm*). After 6 days of coculturing with autologous PBMCs, a significant lower proliferation was induced by infected hMDM2, treated with rapamycin (5.9% ± 3.8), PI-103 (24.1% ± 5.2) and AZD-8055 (23.7% ± 5.2), as compared to the control (35.4% ± 2.9) (**Figure 40A**). The reduction of proliferation was more pronounced compared to proliferation induced by hMDM2 in which apoptotic parasites reside (23.9% ± 3.4). A similar observation was made upon infection of hMDM1. Infection with viable log.ph. *Lm* resulted in a strong T cell proliferation (38.5% ± 2.6). Proliferation, however was significantly reduced when hMDM1 were pretreated with either PI-103 (15.1% ± 3.7), AZD-8055 (19.3% ± 6.5), rapamycin (4.0% ± 0.5) or in the presence of apoptotic parasites during infection (22.7% ± 2.6) (**Figure 40B**).
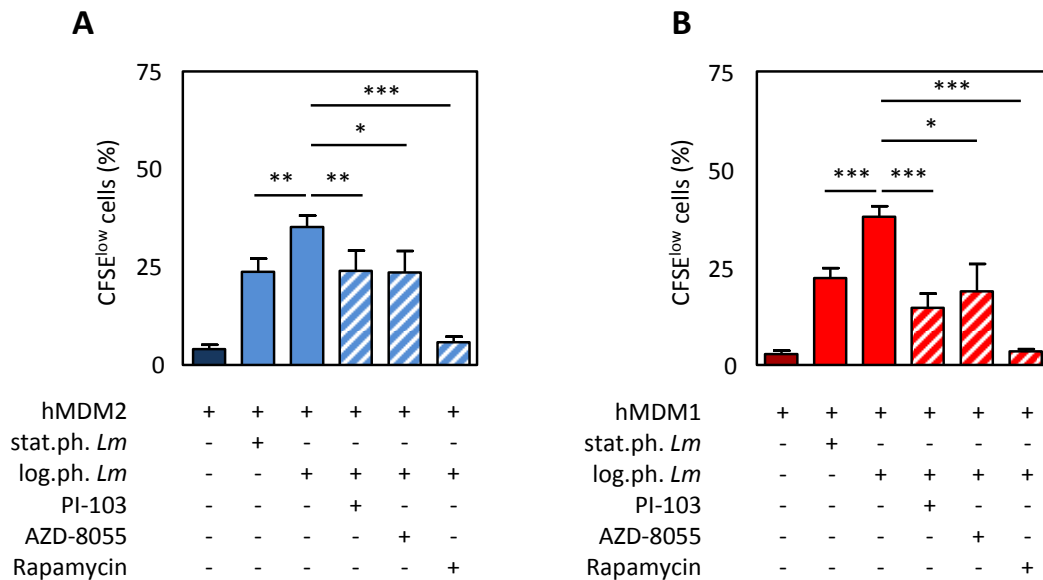
Figure 40: Influence of autophagy on *Lm* induced proliferation. hMDM2 (**A**) or hMDM1 (**B**) were treated (stripped bars) with PI-103 (10 μM), AZD-8055 (10 μM) or rapamycin (1 μM) for 30 min, prior to infection (filled bars) with log.ph. or stat.ph. *Lm* parasites (MOI=10). After 24 h hMDM were washed and cocultured with autologous CFSE labeled PBMCs (ratio 1:5). After 6 days

the CFSE^{low} proliferating cells were quantified by flow cytometry (n=7-24) (*: $p < 0.05$; ***: $p < 0.001$). Data are presented as mean ± SEM and are representative for at least 3 independent experiments.

5.5.6 Impact of autophagy on parasite survival during *Lm* infection

Finally we assessed the effect of autophagy induction on parasite survival during PBMC cocultivation, using transgenic dsRed expressing parasites. In the presence of T cells, the induction of autophagy secured intracellular *Lm* survival. In hMDM2, the *Lm* infection rate (PE$^+$ hMDM) increased up to 3.3 (± 0.2) fold upon treatment with rapamycin, 1.3 (± 0.1) fold using PI-103, 2.1 (± 0.1) fold using AZD-8055, or in the presence of apoptotic parasites upon infection (1.7 fold ± 0.1) (**Figure 41A**). Also in hMDM1 an increased infection rate was observed upon treatment with PI-103 (1.8 fold ± 0.3), AZD-8055 (3.1 fold ± 0.1) or rapamycin (4.3 fold ± 0.2). Also in the presence of apoptotic parasites, survival was enhanced in hMDM1 (1.8 fold ± 0.1) (**Figure 41B**). These data suggest that the activation of the autophagy machinery, induced chemically or by apoptotic parasites, leads to an increased overall parasite survival in hMDM.
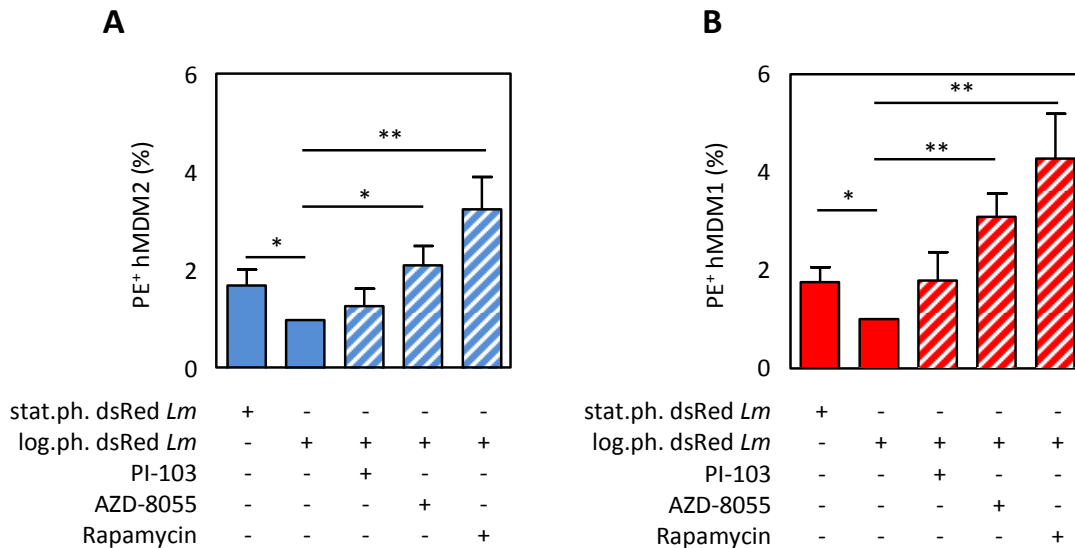
Figure 41: Effect of autophagy induction on parasite survival. hMDM2 (**A**) or hMDM1 (**B**) were treated (stripped bars) with PI-103 (10 µM), AZD-8055 (10 µM) or rapamycin (1 µM) for 30 min, prior to infection (filled bars) with log.ph. or stat.ph. transgenic dsRed *Lm* parasites (MOI=10). After 24 h hMDM were washed and cocultured with autologous CFSE labeled PBMCs (ratio 1:5). After 6 days the *Lm* infection rate (PE$^+$ hMDM) was assessed by flow cytometry (*: $p < 0.05$; ***: $p < 0.001$). Data are presented as mean ± SEM, and are representative for at least 3 independent experiments.

6. Discussion

During lifetime the body is exposed to various threats which may comprise infectious agents like viruses, bacteria or even protozoan parasites. Through evolution, several immune defense mechanisms have evolved, providing the body protection against such agents. By gaining more insight in these pathogen-host interactions, a better understanding arises how infections are established and therefore intervention strategies can be designed. In a joint project, funded by the Carl Zeiss foundation we focused on the interaction of human primary macrophages as host cells with 4 different pathogens being *Listeria monocytogenes*, HIV, HCMV and *Leishmania*. In this thesis, we focused on *Leishmania*-macrophage interactions. We hypothesized that the apoptotic *Leishmania* exploit the host´s autophagy machinery to reduce T cell mediated parasite elimination.

Investigating the virulent *Leishmania* inoculum in detail we could confirm that it consists out of both viable and dying promastigote parasites. These dying parasites were characterized as being apoptotic according to the criteria of the Nomenclature on Cell Death. Upon infection of human myeloid cells – proinflammatory or anti-inflammatory macrophages (hMDM) and dendritic cells (DCs) – we observed all 3 cell types to be permissive for *Leishmania* parasites. Furthermore, upon internalization parasites stage transformation occurred, making hMDMs and DCs suitable as host cells for the parasites. Both hMDMs and DCs are antigen presenting cells, able to degrade internalized parasites. As a consequence antigen presentation occurred which led, unexpectedly, to a *Leishmania* specific T cell response in human adults, previously unexposed to *Leishmania* infection. This strong and effective immune response was dampened in the presence of apoptotic parasites during infection of hMDMs, but not of DCs. As a consequence, proliferation restricted intracellular parasite survival the strongest in DCs. We identified the apoptotic parasites to induce an autophagy like process in hMDMs, as an immune evasion mechanism, to silence adaptive immune responses. As this mechanism was only found in hMDMs, our data demonstrates that hMDM are more suitable as host cells as compared to DCs and define the host cell´s autophagy machinery as a target for therapeutic intervention.

6.1 Parasitology: "Apoptosis among *Leishmania*"

Among metazoans the mechanism of apoptosis has been well described (Elmore, 2007; Kanduc et al., 2002). However the translation of this process to protozoans is a still ongoing process. The fact that increasing evidence arises concerning apoptotic features in single celled organisms, the hypothesis is strengthened that apoptosis is an evolutionary conserved mechanism among eukaryotes. Already two decades ago, features of apoptosis have been described in *Trypanosoma cruzi* (Ameisen et al., 1995). More recently, also among *Plasmodium spp.*, *Toxoplasma gondii*, *Giardia lamblia* and *Leishmania spp.*, characteristics such as PS exposure and DNA fragmentation have been described (Jiménez-Ruiz et al., 2010). In concordance, we were also able to determine these characteristics among dying *Leishmania major* parasites (**Figure 42**). Interestingly, viable parasites, residing in the G_2 phase, also showed DNA to be fragmented, assessed by TUNEL staining, a finding which could be misinterpreted as apoptotic mimicry. Taking a closer look at these viable parasites, which are negative for ANXA5-binding, we observed that only the kinetoplast DNA, comprising maxi- and minicircles, stained TUNEL positive. In line with previous observations this phenomenon is explainable by the fact that prior to *Leishmania* cell divisions, the progeny minicircles replicate and contain nicks or gaps (Kessler et al., 2013; Zangger et al., 2002). While these nicks and gaps are repaired upon division, our data suggest that these nicks are already detectable by TUNEL staining in stages when the parasites are preparing for mitosis (Shapiro and Englund, 1995).

In addition, for the first time, we were able to demonstrate a combination of apoptosis characteristics in parasites. Using a PS specific antibody, combined with a TUNEL assay, apoptotic parasites were defined to be solely PS$^+$, being at an early stage of cell death. In a next stage, parasites expressed PS and contained fragmented DNA. In the late phase of apoptosis, no PS was detectable, but a strong signal of DNA fragmentation was demonstrated. These findings strengthen our hypothesis that also apoptosis in protozoans is a well regulated process. Although we demonstrated features of apoptosis, we can only speculate about the underlying mechanism leading to cell death. In multicellular organisms apoptosis is also a tightly regulated process, in

which however caspase (in)dependent cascades, death receptors, etc. play a role. These cascades remain to be discovered but could be similar in protozoans. Rico et al. could already describe *Leishmania infantum* promastigotes to express a nuclease similar to the endonuclease G (EndoG) of higher eukaryotes. Upon induction of apoptosis, EndoG is released from the kinetoplast and translocates to the nucleus, where it is thought to participate in the process of DNA degradation (Rico et al., 2009). Evidence is also accumulating that a caspase-like pathway is involved in protozoan cell death. Although no homologues of mammalian caspases have been identified, proteins with caspase-like activity were shown to be involved during apoptosis of both *Leishmania spp.* and *Plasmodium spp.* (Al-Olayan et al., 2002; Taylor-Brown and Hurd, 2013). In line with the former pathogen, inhibition of protease activity protected *Leishmania donovani* promastigotes against hydrogen peroxidase induced apoptosis (Das et al., 2001). Distinct pathways may lead to cell death; staurosporine – but not miltefosine – treatment induces a strong reactive oxygen species (ROS) production, indicating a ROS dependent and independent cascade preceding apoptosis (Steinacker/Bank, data not shown). Similarly, also caspase-like independent cascades have been demonstrated to induce protozoan cell death, making it plausible that also an extrinsic and intrinsic pathway, as described for multicellular organisms, induce apoptosis in unicellular organisms (Dolai et al., 2011).

While apoptosis plays a crucial role for survival of the population, it is still matter of debate how apoptosis could be beneficial for a single celled organism. As *Leishmania* parasites are transferred by the sand fly, apoptosis could serve to restrict population growth in the vector, hereby increasing the lifespan of the vector and increasing the transmission rate, as shown for other protozoan parasites (Al-Olayan et al., 2002; Barcinski and DosReis, 1999). The presence of apoptotic parasites might also have an immune silencing effect, as has been shown for apoptotic cell clearance during homeostasis in vertebrates (Poon et al., 2014). A Mexican group described that phosphatidylserine exposure by *Toxoplasma gondii* is fundamental for granting survival of the parasite in murine macrophages (Santos et al., 2011). In concordance, phagocytosis of apoptotic cells by macrophages plays a key role in *Trypanosoma cruzi* persistence, showing the importance of apoptotic parasites for parasite survival (Freire-de-Lima et al., 2000). To gain a

better understanding of how apoptosis could be beneficial for a single celled organism, we further elucidated on the role of apoptotic parasites during host-pathogen interactions.
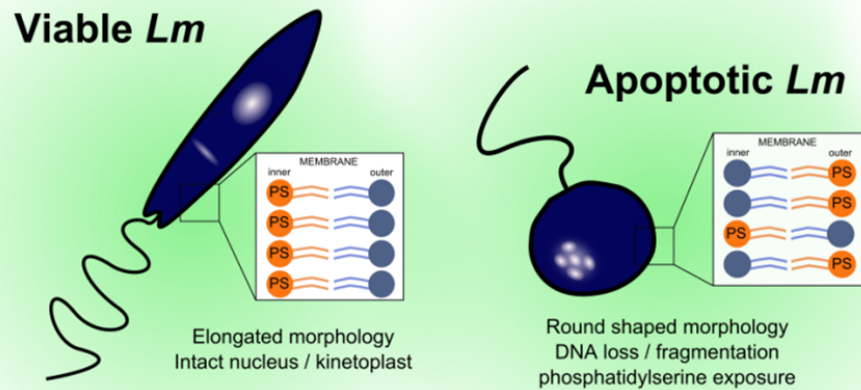

Figure 42: The *Leishmania* virulent inoculum comprises apoptotic parasites. Apoptosis was characterized by a round shaped morphology, DNA fragmentation (TUNEL assay), PS exposure (ANXA5 binding) and loss of DNA (SubG1+, cell cycle analysis).

6.2 Human myeloid cells, being part of the innate immune system, as host cells for *Lm*

Both macrophages and dendritic cells serve as double edged swords in the field of *Leishmania* infection immunology; both playing a role in innate immune defense and as host cell for *Leishmania* parasites. It is well appreciated that macrophages are the final host cell for this protozoan parasite; however dendritic cells are also susceptible, influencing disease development (Ritter et al., 2004). Various receptors have already been described to mediate parasite internalization, such as the scavenger receptor CD163, the mannose receptor, Fcγ-receptors, Toll like receptors (TLRs) and receptors of the complement system. The latter one represents a central player in adhesion of extracellular pathogens to phagocytes. Both complement receptor (CR) 1 and 3 mediate uptake of promastigotes, influencing immune responses (Wenzel et al., 2012). For *francisella tularensis* it could already be demonstrated that uptake by CR3 – not by the inflammatory CR1 – resulted in a silent entry in human macrophages (Dai et al., 2013). In line with this finding the higher ratio of CR3/CR1 positive cells (data not shown) among anti-inflammatory macrophages (hMDM2) as compared to proinflammatory macrophages (hMDM1) suggest the former one to be the better host for *Leishmania* parasites. In addition, also CD163 and MR are highly expressed on hMDM2, explaining the higher uptake and parasite load in hMDM2 compared to hMDM1 and DCs. These findings are reinforced by our own cooperative studies comparing *Listeria monocytogenes,* HCMV and *Leishmania* infection of human primary macrophages, where also hMDM2 internalizes more pathogens then hMDM1 (Bayer et al., 2013; Neu et al., 2013). In addition to the complement system, also TLRs are important during innate immunity. Lipophosphoglycan (LPG) of various *Leishmania spp.* was defined as a TLR2 ligand, leading to the restriction of TLR4 induced signaling cascades by which macrophages were rendered unresponsive to bacterial LPS, dampening immune responses (Faria et al., 2012; de Veer et al., 2003). In contrast, TLR4 and TLR9 also play a role in disease outcome; in the absence – assessed using knockout mice – it could be demonstrated that both receptors play a protective role during *Leishmania* infection, by modulating IL12 production (Kropf et al.,

2004; Liese et al., 2007; Wang et al., 2004). So depending on the receptor usage, immune responses are modulated. Complement receptors and TLRs are found on both macrophages and dendritic cells, making it reasonable that DCs are susceptible for *Leishmania* promastigotes. Indeed, several others, such as the group of David Sacks, demonstrated *Leishmania major* promastigotes to enter DCs. Consequently, IL12 production was induced, known to promote Th1 responses which lead to a healing phenotype (McDowell et al., 2002). In our study, we also observed a small fraction of the DC population to become infected. However, it was surprising to see – independent of the low phagocytic capacity of DCs – that *Leishmania* promastigotes develop more efficiently in the amastigote life stage in DCs, compared to hMDM. Few data are available regarding *Leishmania major* stage transformation in human myeloid cells. Nevertheless, in mice stage transformation of *Leishmania amazonensis* has been proposed in DCs. After 5 days of infection, although no increase in parasite load was observed, the conclusion was drawn that transformation into amastigotes occurred because the parasite load did not decrease (Prina et al., 2004). In order to define whether intracellular amastigote stage transformation occurred in our model, we assessed the parasites´ genetic profile. In line with previous reports, we demonstrated promastigotes to express the gene SHERP more abundantly compared to amastigotes (Leifso et al., 2007). In contrast, a higher amount of GP63 mRNA was detected in amastigotes. The latter finding has been controversially debated as Schneider et al. were only able to detect GP63 in promastigotes (Schneider et al., 1992). Interestingly, in *Leishmania major*, seven distinct genes are encoding the protein GP63. Our data suggest that these genes are differentially expressed during the parasites´ life stage as described for *Leishmania donovani* and *Leishmania mexicana*. Furthermore, by assessing the surface expression of GP63, almost no protein was detected on amastigotes, whereas on promastigotes GP63 was detectable (Bank, data not published). This strengthens the assumption that genes – and also the GP63 protein – are differentially expressed in both *Leishmania* life stages. Both in macrophages and dendritic cells, the promastigote transformation led to the development of amastigotes, which had a similar genetic profile when developing either in macrophages or dendritic cells. However, we found that the parasite load was strongly enhanced in dendritic cells. It is well appreciated that an acidic environment is a prerequisite for an efficient transformation. Both in macrophages and

dendritic cells, this acidic niche is formed due to the fusion of phagosome containing parasites with acidified lysosomes. In line, *Leishmania donovani* developed strategies to delay phagolysosomal maturation, which promotes a better *Leishmania donovani* stage transformation (Winberg et al., 2009). Between dendritic cells and macrophages also a different acidification process occurs. Upon phagocytosis, a strong acidification is observed in macrophages, whereas in dendritic cells alkalization takes place, preceding the acidification process (Russell, 2007). Translating these findings into our model, we can hypothesize that a different acidification process in dendritic cells contributes to a more efficient parasite transformation (**Figure 43**).
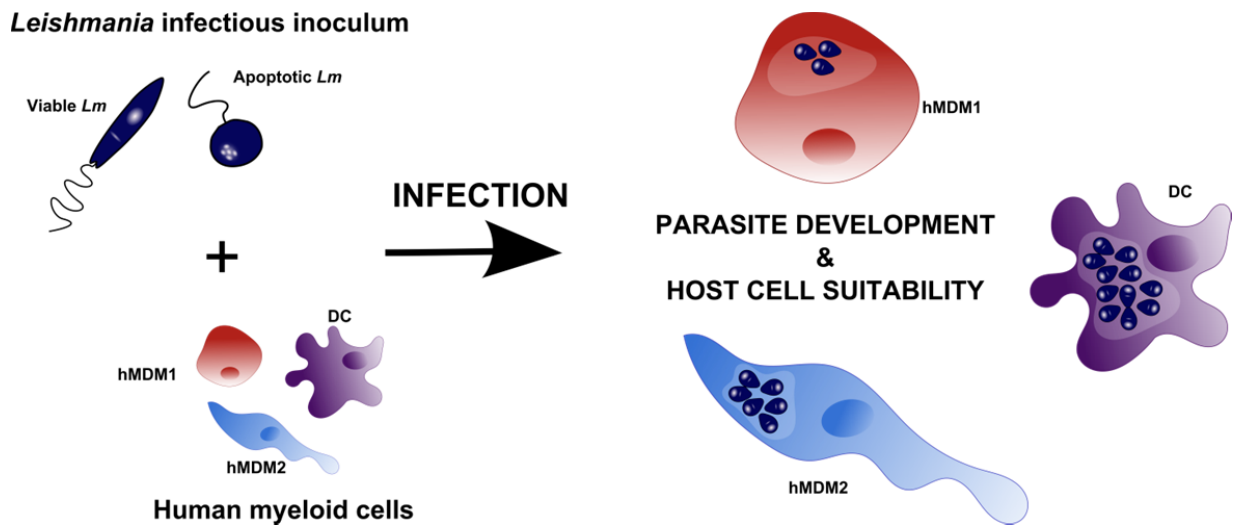
Figure 43: Parasite transformation occurs more efficiently in DCs compared to hMDMs. The *Lm* infectious inoculum, consisting out of viable and apoptotic parasites, is able to infected hMDMs and DCs. During infection, promastigotes transform into the multiplying amastigote life form; a process which occurs most efficiently in DCs, compared to hMDM2, compared to hMDM1.

6.3 Adaptive immunity as a consequence of the "human myeloid cell – *Lm* interaction"

Leishmania parasites have been extensively used as an infection model system to study the murine immune system (Gumy et al., 2004). Using this model, the concept of Th1/Th2 responses, promoting a healing or disease phenotype, was grounded. During *Leishmania* infection, a prominent Th1 response is associated with IL12 production from APCs and IFNG from lymphocytes which leads to pathogen clearance. In contrast, the presence of IL4, IL10 and TGFB profile a Th2 phenotype, which promotes parasite replication. Translating this knowledge to the human immune system – hereby focusing on cutaneous Leishmaniasis – it was demonstrated that the pattern of IL4 and IFNG production is polarized in patients after restimulating PBMCs with crude *Leishmania* extract. Patients who recovered from the disease responded by a strong IFNG production. In contrast, in diseased patients, a mixed Th1/Th2 phenotype was present, which polarized to a predominant Th2 phenotype as the disease worsened (Gaafar et al., 1995; Kemp et al., 1994; Kharazmi et al., 1999). Few studies however are present documenting the immune response early after infection. Rocha et al. assessed the phase of disease preceding skin pathology in American patients and found PBMCs to respond by a predominant TNF and IL10 production, whereas low levels of IFNG were present (Rocha et al., 1999). The conclusion was drawn that T cell responses during early-phase infection are down-regulated by IL10 which may facilitate parasite multiplication (Rocha et al., 1999). In concordance, we could also demonstrate hMDMs to respond to *Leishmania* infection *in vitro* by producing high amounts of IL10 and TNF whereas moderate levels of IFNG were induced. As IL10 dampens immune responses, it is plausible that a successful transformation of promastigotes to amastigotes relies on IL10 production of the host cell. To shed more light on the role of IL10 in our model, further experiments should be performed, in which the role of IL10 could be assessed by using IL10 neutralizing antibodies.

In response to infection, APCs present antigens able to activate the adaptive immune system, more specifically T cells. It is well understood that an optimal T cell response is of key

importance for intracellular pathogen clearance. Crude extracts of *Leishmania major* were already demonstrated to induce both IFNG and IL4 production by PBMCs from unexposed individuals (Turhan et al., 1997). In concordance, Kurtzhals et al. confirmed the presence of circulating *Leishmania* reactive CD4^{+} T cells among PBMCs from healthy individuals, responding by IL4 and IFNG production in response to *Leishmania* (Kurtzhals et al., 1995). Also in our study, we could confirm T cells to respond to *Leishmania major* infection. Surprisingly, the responder population consisted partially out of memory T cells. Although this *Leishmania* specific response was unexpected, other reports stated similar findings. In response to viral antigens, originating from HIV-1, CMV or HSV, Su et al. found an abundance of memory-phenotype CD4^{+} T cells specific to viral antigens in adults who had never been infected before (Su et al., 2013). Also regarding more aggressive pathogens like the Ebola virus; the presence of memory T cells, specific for the envelope glycoprotein of the Ebola virus, was demonstrated. The frequency of Ebola specific T cells was even higher compared to HIV-1 specific T cells, nevertheless 10 fold lower than the frequency of memory T cell specific for the recall antigen tetanus toxoid (Campion et al., 2014). The above data, including ours, shed light on pre-existing memory responses, opening new doors, creating new opportunities, in the field of vaccine development. In the future, not only naïve T cells, but also the antigen specific T cells, which are already present, may be targeted for expansion. The higher the frequency of antigen specific T cells before infection, the faster a T cell response is mounted upon contact with the specific pathogen, preventing disease development. We assessed T cell precursor frequencies after *Leishmania* infection based on CFSE dilutions. The observed precursor frequencies were higher compared to antigen specific T cell frequencies, but are in good agreement with reports of Danke et al. and Novak et al. showing that only a minority of the CFSE^{low} proliferating cells are antigen specific and that a majority (80-96%) of tetramer-negative proliferating cells proliferated as a result of bystander activation (Danke and Kwok, 2003; Novak et al., 2001). Focusing on the parasite *Leishmania*, Gabaglia et al. showed the presence of specific CD4^{+} T cells, partially with a memory phenotype, to *Leishmania* antigens in naïve individuals (Gabaglia et al., 2000). These reports strengthen our finding that adults without a clinical history of Leishmaniasis possess *Leishmania* reactive memory CD4^{+} T cells. We can speculate that this memory may arise during lifetime upon

encountering various infections/diseases. Welsh et al. already proposed a model of cross reactivity, by which memory T cells cross react to antigens the body has not encountered before (Welsh and Selin, 2002). This model is reinforced by the finding that these memory T cells are absent during childhood, and therefor develop during puberty upon infection and pathogenesis, upon contact by heterologous agents (Su and Davis, 2013). Also in this thesis, it is tempting to hypothesize that these *Leishmania* specific T cells are cross-reactive with other pathogenic antigens. By comparing an immune dominant antigen of *Leishmania*, namely LACK (*Leishmania* analogue of the receptors of activated C kinase), with several pathogens for which we are vaccinated, it was observed that the protein sequence of LACK has similarities with protein sequences of *Clostridium tetani* (taxid: 1513, tetanus), *Corynebacterium diphtheriae* (taxid: 1717, diphtheria), *Neisseria meningitidis* (taxid: 487, meningococcal) and even *Streptococcus pneumoniae* (taxid: 1313, pneumococcal), up to almost 30%, 40%, 30% and 40% respectively (data not shown). In contrast, no protein sequence similarities were found with hepatitis B-type viruses (taxid: 10404, heptatitis), Measles virus (taxid: 11234, measles) or Human Influenza A Virus (taxid: 11320, influenza). We further could show the majority of these memory T cells to express the marker L-selectin, indicative for effector memory T cells. Sallusto et al. already proposed a model of central memory and effector memory T cells, based on the role of L-selectin (CD62L) and CC-chemokine receptor 7 (CCR7), which determine the homing properties of T cells (Sallusto et al., 1999). The fact that we observed proliferation of effector T cells is logical as due to L-selectin and CCR7 migration to lymph nodes can still occur, as previously described (Kaech et al., 2002). Furthermore, *Leishmania* infected individuals were demonstrated to possess central (CD62L$^-$) memory CD4$^+$ T cells producing IFNG, whereas the effector (CD62L$^+$) memory CD4$^+$ T cells were for IL10 production (Bourreau et al., 2002). The former study might explain the presence of both IL10 and IFNG in our *in vitro* proliferation system as also both phenotypes of memory T cells could be detected. In ongoing studies, we will try to elucidate on these questions.

As a consequence of proliferation, our data indicate both *Leishmania* infection rate and parasite load to be reduced. From the murine system, it is known that IFNG producing T cells activate *Leishmania* infected macrophages. Upon activation of murine skin macrophages by exogenous IFNG, it was demonstrated intracellular *Leishmania* to be eliminated by a nitric oxide

depending mechanism (von Stebut et al., 2002). The role of L-arginine metabolic pathways is extensively studied, as reviewed by Wanasen et al., however this model is controversially discussed in human *in vitro* studies (Wanasen and Soong, 2008). Nevertheless in skin biopsies from patients with local cutaneous Leishmaniasis a more prominent expression of iNOS was demonstrated in lesions containing small numbers of parasites, compared to lesions where parasite burden was enhanced. Furthermore an anti-leishmanial function of iNOS in human *Leishmania* infections *in vivo* was suggested (Qadoumi et al., 2002). These data are in agreement with other investigations focusing on human primary cells *in vitro* (Panaro et al., 1999; Vouldoukis et al., 1997). To elucidate, in a study of Vouldoukis et al., human primary macrophages were able to eliminate intracellular *Leishmania* by a NO depending mechanism. This process was inducible by IFNG, however inhibited by IL10 (Vouldoukis et al., 1997). In contrast, we were not able to reduce intracellular parasite burden by stimulation of macrophages with IFNG (Bank, unpublished). Nevertheless, in the presence of proliferating T cells and IFNG, we observed parasites to be eliminated. Therefore other pathways, independent of IFNG or in combination with other components are required for anti-leishmanial activity. Indeed, in our group it could be demonstrated that a microbial peptide, cathelicidin (LL37), to be involved in the control of *Leishmania* parasites in inflammatory hMDM1 (Bank, unpublished). Furthermore, a role of serum IgE and its receptor were demonstrated in cutaneous Leishmaniasis, inducing nitric oxide synthase in human macrophages (Vouldoukis et al., 1995). Also the production of NO was induced by T cells, producing IFNG and interacting with macrophages by CD40-CD40L ligation (Stout et al., 1996). Although IFNG has been extensively studied, increasing evidence highlights the role of IFNA/B rather than IFNG being responsible for the early induction of NO production (Diefenbach et al., 1998). Translating these findings into our *in vitro* system, a model can be proposed in which *Leishmania* infected APCs trigger T cell activation and proliferation. As a consequence, antigen specific T cells provide a dual signal (i) secreting soluble factors (type 1 IFN, etc.) and (ii) interacting with receptors on the APC which leads to APC activation. Subsequently, an elevated level of nitric oxide and oxygen radicals, as also increased of activity of microbial products such as cathelicidin restrict *Leishmania* survival.

6.4 Autophagy as an immune evasion mechanism

To circumvent elimination by the immune system and secure survival, intracellular pathogens have evolved strategies to silence their host cells. The bacterium *M. tuberculosis* as also the protozoa *Toxoplasma* try to escape from the phagosome into the cytoplasm, whereas *C. burnetti* delays the autophagolysosomal maturation to benefit its own survival (Gutierrez and Colombo; Sauer et al., 2005; Simeone et al., 2012). Similarly, *Leishmania donovani* delays phagolysosomal maturation to transform into the disease propagating amastigote form (Lodge and Descoteaux, 2006). A recent study in mice using *Leishmania donovani* demonstrated a reduced T cell proliferation caused by the inhibition of processing of *Leishmania* antigens cross-presented on MHC class I molecules (Matheoud et al., 2013). Our group already reported the apoptotic *Leishmania* population to be crucial, as infection of mice with only viable *Leishmania* promastigotes did not result in disease development (van Zandbergen et al., 2006). Indeed, in this PhD project, we found that *Leishmania major* parasites indirectly reduce T cell proliferation and that this inhibitory effect depends on the presence of apoptotic *Leishmania* parasites. To clarify how the apoptotic population secures survival of the viable ones, we analyzed their intracellular fate. Upon phagocytosis, apoptotic parasites were found to reside in a compartment decorated with the autophagy marker LC3 in macrophages – not in DCs. This finding is in agreement with murine data showing that *Leishmania* parasites engage PI3K-AKT signaling, which is an upstream event able to initiate autophagy (Ruhland et al., 2007). In contrast to conventional autophagy, only a single lipid bilayer was found to surround the parasite, indicating that processing of apoptotic parasites occurred in a compartment formed by LC3 associated phagocytosis (Mintern and Villadangos, 2012; Randow and Münz, 2012; Sanjuan et al., 2007). Moreover, we found the protein SQSTM1/p62 not to be involved in the process of LAP induced by apoptotic parasites, as is described for *Listeria* as well (Lam et al., 2013). Up to now we did not discover which ligand is responsible for LC3 recruitment. It might be speculated that phosphatidylserine on the surface of apoptotic parasites triggered LC3 recruitment in macrophages (Kobayashi et al., 2007; Martinez et al., 2011). Also a role for the parasite´s GP63 protein in autophagy activation is possible as GP63 is able to cleave mTOR in the host cell

(Jaramillo et al., 2011). As the process of LC3 associated phagocytosis only occurred in macrophages and not in dendritic cells, further studies could also focus on comparing surface receptors on both phenotypes of cells, able to induce LAP. Our data already revealed CD14 to be exclusively expressed on macrophages, not on dendritic cells (O'Doherty et al., 1994). Furthermore, it is known that CD14 acts as a co-receptor for TLR 2 and 4, of which the latter two have been described to recruit LC3 to the phagosome (Kyrmizi et al., 2013; Sanjuan et al., 2007). As also a role, for both TLR2 and 4, has been described during *Leishmania* infection, it is not unlikely that apoptotic *Leishmania* induce LAP in macrophages by a CD14/TLR dependent mechanism. Not only target molecules on the cell surface may engage LAP signaling. Also the generation of reactive oxygen species, by the phagosomal NADPH oxidase, is demonstrated to recruit LC3 (Lam et al., 2013; Vernon and Tang, 2013). In line with this thought, it is feasible to hypothesize that upon phagocytosis of *Leishmania* by macrophages – in contrast to DCs – the process of acidification occurs, which promotes ROS production (Ma and Underhill, 2013; Riemann et al., 2011).

Overall, autophagy is a key player in maintaining homeostasis, enabling phagocytes to clear apoptotic and necrotic cells efficiently and silently to prevent inflammation and development of autoimmune disorders, like systemic lupus erythematous (Harley et al., 2008). Also in the presence of apoptotic parasites, immune responses were dampened, as infected hMDMs induced a lower T cell proliferation. Clearance of dying cells or even apoptotic *Leishmania* is known to create a more anti-inflammatory environment that is dominated by cytokines such as IL10 and TGFB and suppression of TNF, IL6 and IL1B (Martinez et al., 2011; van Zandbergen et al., 2006). Although uptake of apoptotic parasites led to a reduced IL6 and IL1B production, IL10 was strongly produced in response to viable parasites. This is in agreement with the fact that a strong proinflammatory response may be dampened by anti-inflammatory mediators (Hocès de la Guardia et al., 2013). Tiemessen et al. showed that TGFB has a pronounced inhibitory effect on proliferation of antigen-specific CD4^{+} T cells, a mechanism that could also be functional in our context (Tiemessen et al., 2003). Alternatively, the activation of the autophagy machinery could also lead to an increased presentation of innocuous selfantigens, which contributes to tolerance-inducing mechanisms also dampening adaptive immune

responses (Dengjel et al., 2005; Klein et al., 2010). As a consequence of the reduced T cell response, the parasite´s survival was enhanced, leading to the assumption that activation of the autophagy machinery is beneficial for the parasite. To underscore this statement, we setup a system to modulate autophagy in human primary cells. As chemical modulation might have cytostatic side effects, we aimed to use several modulators to address the same question. Chemical induction of autophagy, hereby simulating the role of apoptotic parasites, strongly reduced proliferation and led to a higher infection rate, which was previously observed upon infection with the related protozoa *T.cruzi* (Romano et al., 2009). In addition, Roberta O. Pinheiro et al. have found that autophagy increases the parasitic replication of *Leishmania amazonensis* inside macrophages (Pinheiro et al., 2009). In contrast, our data did not indicate autophagy to influence replication. However our data suggest that an elevated autophagy activity prevents the elimination of promastigotes. The increased amount of viable promastigotes is then able to transform into the amastigote form, presumably being the source of a higher parasite load that we observed. To explain this phenomenon it can be hypothesized that the autophagy activity alters the phagolysosomal environment or maturation. An enhanced level of autophagy activity was already demonstrated to decrease lysosomal protease activity. The decreased activity of endosomal cysteine proteases (cathepsins) might favor the generation of certain, less immunogenic, MHCII presented peptides due to a less efficient lysosomal protein digestion (Dengjel et al., 2005; Romao et al., 2013). Blocking of cathepsin L was shown to result in less MHCII dependent presentation of leishmanial antigens and the potentiation of Th2-type immune responses (Zhang et al., 2001). Conversely, blocking of cathepsin B resulted in the potentiation of Th1-type immune responses against *Leishmania* (Maekawa et al., 1997). Therefore we propose a model in which LC3 recruitment to phagosomes, containing apoptotic parasites, remodels compartment composition and maturation. Upon lysosomal fusion, the protease activity is altered in a way that a pattern of antigens is generated, elucidating an anti-inflammatory immune response. As lysosomes fuse faster with LC3^{+} compartments and not with compartments, harboring viable parasites, acidification occurs at a slower rate in the later one, providing sufficient time for a successful promastigote-amastigote stage transformation. As a consequence an increased overall parasite survival is guaranteed.
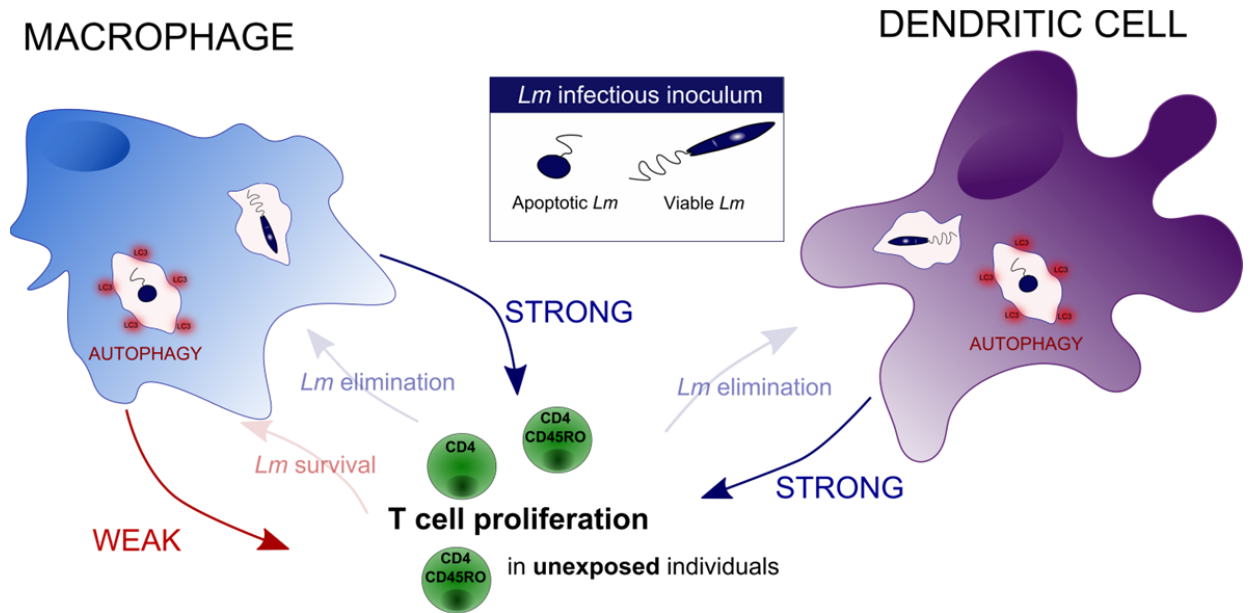
Figure 44: *Leishmania* **specific proliferation is reduced in the presence of apoptotic** *Lm* **in hMDMs, but not in DCs.** Upon infection of either hMDMs or DCs with viable parasites, a strong memory T cell response is observed among PBMCs obtained of previously unexposed individuals. In the presence of apoptotic parasites in hMDMs, proliferation is reduced, by which parasites survival is secured.

7. Concluding remarks

From this PhD work we can conclude that cell death among *Lm* parasites is necessary to guarantee an overall parasite population survival. Furthermore, the general accepted model that macrophages are the final host cell for *Lm* parasites is reinforced by our findings focusing on human myeloid cells. For the first time, we describe a "death-deceiving" immune evasion strategy where apoptotic *Lm* parasites hijack the host cell´s autophagy machinery to dampen T cell mediated immune responses. As a consequence, the overall parasite survival is guaranteed. Nevertheless, several aspects such as the underlying mechanisms, but also the trigger for LC3 recruitment are yet to be defined. To successfully combat infection, one should focus (1) on preventing autophagy activation in the host and (2) on expanding the *Lm* specific precursor cells before initial infection, as highlighted (**Figure 45**). Upcoming research will elucidate on these questions which may define the host autophagy pathway as a potential therapeutic target in treating Leishmaniasis. In all, an increasing knowledge on pathogen – host cell interactions will increase our understanding how to develop strategies to prevent disease development.
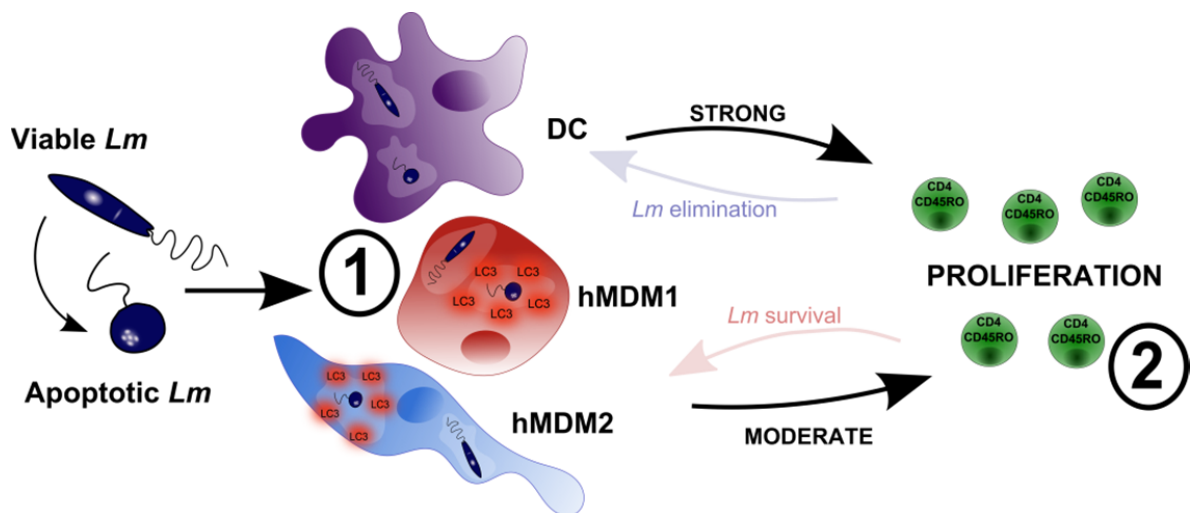
Figure 45: Our model of *Leishmania* infection in the context of human myeloid cells and T cells. Apoptotic parasites induce autophagy in human macrophages, dampening T cells responses hereby securing parasite survival.

8. Figure list

9. References

Al-Olayan, E.M., Williams, G.T., and Hurd, H. (2002). Apoptosis in the malaria protozoan, Plasmodium berghei: a possible mechanism for limiting intensity of infection in the mosquito. International Journal for Parasitology *32*, 1133–1143.

Alexander, J., and Brombacher, F. (2012). T helper1/t helper2 cells and resistance/susceptibility to leishmania infection: is this paradigm still relevant? Frontiers in Immunology *3*, 80.

Ameisen, J.C., Idziorek, T., Billaut-Mulot, O., Loyens, M., Tissier, J.P., Potentier, A., and Ouaissi, A. (1995). Apoptosis in a unicellular eukaryote (Trypanosoma cruzi): implications for the evolutionary origin and role of programmed cell death in the control of cell proliferation, differentiation and survival. Cell Death and Differentiation *2*, 285–300.

Barcinski, M. a, and DosReis, G.A. (1999). Apoptosis in parasites and parasite-induced apoptosis in the host immune system: a new approach to parasitic diseases. Brazilian Journal of Medical and Biological Research = Revista Brasileira De Pesquisas Médicas e Biológicas / Sociedade Brasileira De Biofísica ... [et Al.] *32*, 395–401.

Bayer, C., Varani, S., Wang, L., Walther, P., Zhou, S., Straschewski, S., Bachem, M., Söderberg-Naucler, C., Mertens, T., and Frascaroli, G. (2013). Human cytomegalovirus infection of M1 and M2 macrophages triggers inflammation and autologous T-cell proliferation. Journal of Virology *87*, 67–79.

Bernard, A., and Klionsky, D.J. (2013). Autophagosome formation: tracing the source. Developmental Cell *25*, 116–117.

Berrizbeitia, M., Ndao, M., Bubis, J., Gottschalk, M., Aché, A., Lacouture, S., Medina, M., and Ward, B.J. (2006). Purified excreted-secreted antigens from Trypanosoma cruzi trypomastigotes as tools for diagnosis of Chagas' disease. Journal of Clinical Microbiology *44*, 291–296.

Bhowmick, S., and Ali, N. (2008). Recent developments in leishmaniasis vaccine. Most 789–804.

Bourreau, E., Prévot, G., Gardon, J., Pradinaud, R., Hasagewa, H., Milon, G., and Launois, P. (2002). LACK-specific CD4(+) T cells that induce gamma interferon production in patients with localized cutaneous leishmaniasis during an early stage of infection. Infection and Immunity *70*, 3122–3129.

Brand, S., Beigel, F., Olszak, T., Zitzmann, K., Eichhorst, T., Otte, J., Diepolder, H., Marquardt, A., Jagla, W., Popp, A., et al. (2006). IL-22 is increased in active Crohn's disease and promotes proinflammatory gene expression and intestinal epithelial cell migration. 1–12.

Cadwell, K., and Philips, J. a (2013). Autophagy meets phagocytosis. Immunity *39*, 425–427.

Campion, S.L., Brodie, T.M., Fischer, W., Korber, B.T., Rossetti, A., Goonetilleke, N., McMichael, A.J., and Sallusto, F. (2014). Proteome-wide analysis of HIV-specific naive and memory CD4(+) T cells in unexposed blood donors. The Journal of Experimental Medicine *211*, 1273–1280.

Charmoy, M., Auderset, F., Allenbach, C., and Tacchini-Cottier, F. (2010). The prominent role of neutrophils during the initial phase of infection by Leishmania parasites. Journal of Biomedicine & Biotechnology *2010*, 719361.

Chatelain, R., Varkila, K., and Coffman, R.L. (1992). IL-4 induces a Th2 response in Leishmania major-infected mice. Journal of Immunology (Baltimore, Md. : 1950) *148*, 1182–1187.

Clare, M., and Kharkrang, L. (2010). Mechanisms involved in type II macrophage activation and effector functions By. Cytometry 1–145.

Croft, S.L., Sundar, S., and Fairlamb, A.H. (2006). Drug resistance in leishmaniasis. Clinical Microbiology Reviews *19*, 111–126.

Dai, S., Rajaram, M.V.S., Curry, H.M., Leander, R., and Schlesinger, L.S. (2013). Fine tuning inflammation at the front door: macrophage complement receptor 3-mediates phagocytosis and immune suppression for Francisella tularensis. PLoS Pathogens *9*, e1003114.

Danke, N.A., and Kwok, W.W. (2003). HLA class II-restricted CD4+ T cell responses directed against influenza viral antigens postinfluenza vaccination. Journal of Immunology (Baltimore, Md. : 1950) *171*, 3163–3169.

Das, M., Mukherjee, S.B., and Shaha, C. (2001). Hydrogen peroxide induces apoptosis-like death in Leishmania donovani promastigotes. Journal of Cell Science *114*, 2461–2469.

Davis, M.M., and Bjorkman, P.J. (1988). T-cell antigen receptor genes and T-cell recognition. Nature *334*, 395–402.

Dengjel, J., Schoor, O., Fischer, R., Reich, M., Kraus, M., Müller, M., Kreymborg, K., Altenberend, F., Brandenburg, J., Kalbacher, H., et al. (2005). Autophagy promotes MHC class II presentation of peptides from intracellular source proteins. Proceedings of the National Academy of Sciences of the United States of America *102*, 7922–7927.

Deretic, V. (2006). Autophagy as an immune defense mechanism. Current Opinion in Immunology *18*, 375–382.

Diefenbach, A., Schindler, H., Donhauser, N., Lorenz, E., Laskay, T., MacMicking, J., Röllinghoff, M., Gresser, I., and Bogdan, C. (1998). Type 1 interferon (IFNalpha/beta) and type 2 nitric oxide synthase regulate the innate immune response to a protozoan parasite. Immunity *8*, 77–87.

Dietze, R., Carvalho, S.F., Valli, L.C., Berman, J., Brewer, T., Milhous, W., Sanchez, J., Schuster, B., and Grogl, M. (2001). Phase 2 trial of WR6026, an orally administered 8-aminoquinoline, in the treatment of visceral leishmaniasis caused by Leishmania chagasi. The American Journal of Tropical Medicine and Hygiene *65*, 685–689.

Dolai, S., Pal, S., Yadav, R.K., and Adak, S. (2011). Endoplasmic reticulum stress-induced apoptosis in Leishmania through Ca2+-dependent and caspase-independent mechanism. The Journal of Biological Chemistry *286*, 13638–13646.

Dostálová, A., and Volf, P. (2012). Leishmania development in sand flies: parasite-vector interactions overview. Parasites & Vectors *5*, 276.

El-Hani, C.N., Borges, V.M., Wanderley, J.L.M., and Barcinski, M. a (2012). Apoptosis and apoptotic mimicry in Leishmania: an evolutionary perspective. Frontiers in Cellular and Infection Microbiology *2*, 96.

Elmore, S. (2007). Apoptosis: a review of programmed cell death. Toxicologic Pathology *35*, 495–516.

Faria, M.S., Reis, F.C.G., and Lima, A.P.C.A. (2012). Toll-like receptors in leishmania infections: guardians or promoters? Journal of Parasitology Research *2012*, 930257.

Ferenbach, D., and Hughes, J. (2008). Macrophages and dendritic cells: what is the difference? Kidney International *74*, 5–7.

Florey, O., and Overholtzer, M. (2012). Autophagy proteins in macroendocytic engulfment. Trends in Cell Biology *22*, 374–380.

Freire-de-Lima, C.G., Nascimento, D.O., Soares, M.B., Bozza, P.T., Castro-Faria-Neto, H.C., de Mello, F.G., DosReis, G. a, and Lopes, M.F. (2000). Uptake of apoptotic cells drives the growth of a pathogenic trypanosome in macrophages. Nature *403*, 199–203.

Gaafar, A., Kharazmi, A., Ismail, A., Kemp, M., Hey, A., Christensen, C.B., Dafalla, M., el Kadaro, A.Y., el Hassan, A.M., and Theander, T.G. (1995). Dichotomy of the T cell response to Leishmania antigens in patients suffering from cutaneous leishmaniasis; absence or scarcity of Th1 activity is associated with severe infections. Clinical and Experimental Immunology *100*, 239–245.

Gabaglia, C.R., Valle, M.T., Fenoglio, D., Barcinski, M. a, and Manca, F. (2000). Cd4(+) T cell response to Leishmania spp. in non-infected individuals. Human Immunology *61*, 531–537.

Gomez, M.A., Stuible, M., Shimizu, H., Mcmaster, W.R., Olivier, M., and Tremblay, M.L. (2009). The Leishmania Surface Protease GP63 Cleaves Multiple Intracellular Proteins and Actively Participates in p38 Mitogen-activated Protein Kinase Inactivation * □. Journal of Biological Chemistry *284*, 6893–6908.

Grassi, F., Dezutter-dambuyant, C., Mcilroy, D., Jacquet, C., Yoneda, K., Imamura, S., Boumsell, L., Schmitt, D., Autran, B., Debre, P., et al. (1998). Monocyte-derived dendritic cells have a phenotype comparable to that of dermal dendritic cells and display ultrastructural granules distinct from Birbeck granules to those of CD14-derived DC obtained from cord.

Gumy, A., Louis, J.A., and Launois, P. (2004). The murine model of infection with Leishmania major and its importance for the deciphering of mechanisms underlying differences in Th cell differentiation in mice from different genetic backgrounds. International Journal for Parasitology *34*, 433–444.

Gupta, G., Oghumu, S., and Satoskar, A.R. (2013). Mechanisms of immune evasion in leishmaniasis. Advances in Applied Microbiology *82*, 155–184.

Gutierrez, M.G., and Colombo, M.I. Autophagosomes: a fast-food joint for unexpected guests. Autophagy *1*, 179–181.

Gutierrez, M.G., Master, S.S., Singh, S.B., Taylor, G.A., Colombo, M.I., Deretic, V., and Carolina, N. (2004). Autophagy Is a Defense Mechanism Inhibiting BCG and Mycobacterium tuberculosis Survival in Infected Macrophages. *119*, 753–766.

Hampe, J., Franke, A., Rosenstiel, P., Till, A., Teuber, M., Huse, K., Albrecht, M., Mayr, G., De La Vega, F.M., Briggs, J., et al. (2007). A genome-wide association scan of nonsynonymous SNPs identifies a susceptibility variant for Crohn disease in ATG16L1. Nature Genetics *39*, 207–211.

Harley, J.B., Alarcón-Riquelme, M.E., Criswell, L.A., Jacob, C.O., Kimberly, R.P., Moser, K.L., Tsao, B.P., Vyse, T.J., Langefeld, C.D., Nath, S.K., et al. (2008). Genome-wide association scan in women with systemic lupus erythematosus identifies susceptibility variants in ITGAM, PXK, KIAA1542 and other loci. Nature Genetics *40*, 204–210.

Hocès de la Guardia, A., Staedel, C., Kaafarany, I., Clément, A., Roubaud Baudron, C., Mégraud, F., and Lehours, P. (2013). Inflammatory cytokine and microRNA responses of primary human dendritic cells cultured with Helicobacter pylori strains. Frontiers in Microbiology *4*, 236.

Ivens, A.C., Peacock, C.S., Worthey, E. a, Murphy, L., Aggarwal, G., Berriman, M., Sisk, E., Rajandream, M., Adlem, E., Aert, R., et al. (2005). The genome of the kinetoplastid parasite, Leishmania major. Science (New York, N.Y.) *309*, 436–442.

Jaramillo, M., Gomez, M.A., Larsson, O., Shio, M.T., Topisirovic, I., Contreras, I., Luxenburg, R., Rosenfeld, A., Colina, R., McMaster, R.W., et al. (2011). Leishmania repression of host translation through mTOR cleavage is required for parasite survival and infection. Cell Host & Microbe *9*, 331–341.

Jiménez-Ruiz, A., Alzate, J.F., Macleod, E.T., Lüder, C.G.K., Fasel, N., and Hurd, H. (2010). Apoptotic markers in protozoan parasites. Parasites & Vectors *3*, 104.

Jung, D., and Alt, F.W. (2004). Unraveling V (D) J Recombination : Insights into Gene Regulation V (D) J recombination assembles antigen receptor. *116*, 299–311.

Kaech, S.M., Wherry, E.J., and Ahmed, R. (2002). Effector and memory T-cell differentiation: implications for vaccine development. Nature Reviews. Immunology *2*, 251–262.

Kanduc, D., Mittelman, A., Serpico, R., Sinigaglia, E., Sinha, A.A., Natale, C., Santacroce, R., Di Corcia, M.G., Lucchese, A., Dini, L., et al. (2002). Cell death: apoptosis versus necrosis (review). International Journal of Oncology *21*, 165–170.

Kemp, M., Hey, A.S., Kurtzhals, J.A., Christensen, C.B., Gaafar, A., Mustafa, M.D., Kordofani, A.A., Ismail, A., Kharazmi, A., and Theander, T.G. (1994). Dichotomy of the human T cell response to Leishmania antigens. I. Th1-like response to Leishmania major promastigote antigens in individuals recovered from cutaneous leishmaniasis. Clinical and Experimental Immunology *96*, 410–415.

Kessler, R.L., Soares, M.J., Probst, C.M., and Krieger, M.A. (2013). Trypanosoma cruzi response to sterol biosynthesis inhibitors: morphophysiological alterations leading to cell death. PloS One *8*, e55497.

Kharazmi, A., Kemp, K., Ismail, A., Gasim, S., Gaafar, A., Kurtzhals, J.A., El Hassan, A.M., Theander, T.G., and Kemp, M. (1999). T-cell response in human leishmaniasis. Immunology Letters *65*, 105–108.

Klein, L., Münz, C., and Lünemann, J.D. (2010). Autophagy-mediated antigen processing in CD4(+) T cell tolerance and immunity. FEBS Letters *584*, 1405–1410.

Klionsky, D.J., Abdalla, F.C., Abeliovich, H., Abraham, R.T., Acevedo-Arozena, A., Adeli, K., Agholme, L., Agnello, M., Agostinis, P., Aguirre-Ghiso, J.A., et al. (2012). Guidelines for the use and interpretation of assays for monitoring autophagy. Autophagy *8*, 445–544.

Kobayashi, N., Karisola, P., Peña-Cruz, V., Dorfman, D.M., Jinushi, M., Umetsu, S.E., Butte, M.J., Nagumo, H., Chernova, I., Zhu, B., et al. (2007). TIM-1 and TIM-4 glycoproteins bind phosphatidylserine and mediate uptake of apoptotic cells. Immunity *27*, 927–940.

Kroemer, G., El-Deiry, W.S., Golstein, P., Peter, M.E., Vaux, D., Vandenabeele, P., Zhivotovsky, B., Blagosklonny, M.V., Malorni, W., Knight, R.A., et al. (2005). Classification of cell death: recommendations of the Nomenclature Committee on Cell Death. Cell Death and Differentiation *12 Suppl 2*, 1463–1467.

Kropf, P., Freudenberg, M.A., Modolell, M., Price, H.P., Herath, S., Antoniazi, S., Galanos, C., Smith, D.F., and Müller, I. (2004). Toll-like receptor 4 contributes to efficient control of infection with the protozoan parasite Leishmania major. Infection and Immunity *72*, 1920–1928.

Kropf, P., Fuentes, J.M., Fähnrich, E., Arpa, L., Herath, S., Weber, V., Soler, G., Celada, A., Modolell, M., and Müller, I. (2005). Arginase and polyamine synthesis are key factors in the regulation of experimental leishmaniasis in vivo. FASEB Journal : Official Publication of the Federation of American Societies for Experimental Biology *19*, 1000–1002.

Kurtzhals, J. a, Kemp, M., Poulsen, L.K., Hansen, M.B., Kharazmi, A., and Theander, T.G. (1995). Interleukin-4 and interferon-gamma production by Leishmania stimulated peripheral blood mononuclear cells from nonexposed individuals. Scandinavian Journal of Immunology *41*, 343–349.

Kyrmizi, I., Gresnigt, M.S., Akoumianaki, T., Samonis, G., Sidiropoulos, P., Boumpas, D., Netea, M.G., van de Veerdonk, F.L., Kontoyiannis, D.P., and Chamilos, G. (2013). Corticosteroids block autophagy protein recruitment in Aspergillus fumigatus phagosomes via targeting dectin-1/Syk kinase signaling. Journal of Immunology (Baltimore, Md. : 1950) *191*, 1287–1299.

Lam, G.Y., Cemma, M., Muise, A.M., Higgins, D.E., and Brumell, J.H. (2013). Host and bacterial factors that regulate LC3 recruitment to Listeria monocytogenes during the early stages of macrophage infection. Autophagy *9*, 985–995.

Laskay, T., van Zandbergen, G., and Solbach, W. (2003). Neutrophil granulocytes--Trojan horses for Leishmania major and other intracellular microbes? Trends in Microbiology *11*, 210–214.

Leifso, K., Cohen-Freue, G., Dogra, N., Murray, A., and McMaster, W.R. (2007). Genomic and proteomic expression analysis of Leishmania promastigote and amastigote life stages: the Leishmania genome is constitutively expressed. Molecular and Biochemical Parasitology *152*, 35–46.

Lenschow, D.J., Walunas, T.L., and Jeffrey, A. (1996). CD28 / B7 SYSTEM OF T CELL.

Leprohon, P., Légaré, D., Girard, I., Papadopoulou, B., and Ouellette, M. (2006). Modulation of Leishmania ABC protein gene expression through life stages and among drug-resistant parasites. Eukaryotic Cell *5*, 1713–1725.

Levine, B., and Deretic, V. (2007). Unveiling the roles of autophagy in innate and adaptive immunity. Nature Reviews. Immunology *7*, 767–777.

León, B., López-Bravo, M., and Ardavín, C. (2007). Monocyte-derived dendritic cells formed at the infection site control the induction of protective T helper 1 responses against Leishmania. Immunity *26*, 519–531.

Lieke, T., Nylén, S., Eidsmo, L., McMaster, W.R., Mohammadi, a M., Khamesipour, a, Berg, L., and Akuffo, H. (2008). Leishmania surface protein gp63 binds directly to human natural killer cells and inhibits proliferation. Clinical and Experimental Immunology *153*, 221–230.

Liese, J., Schleicher, U., and Bogdan, C. (2007). TLR9 signaling is essential for the innate NK cell response in murine cutaneous leishmaniasis. European Journal of Immunology *37*, 3424–3434.

Liu, D., and Uzonna, J.E. (2012). The early interaction of Leishmania with macrophages and dendritic cells and its influence on the host immune response. Frontiers in Cellular and Infection Microbiology *2*, 83.

Lodge, R., and Descoteaux, A. (2006). Phagocytosis of Leishmania donovani amastigotes is Rac1 dependent and occurs in the absence of NADPH oxidase activation. European Journal of Immunology *36*, 2735–2744.

Lüder, C.G., Campos-Salinas, J., Gonzalez-Rey, E., and van Zandbergen, G. (2010). Impact of protozoan cell death on parasite-host interactions and pathogenesis. Parasites & Vectors *3*, 116.

Ma, J., and Underhill, D.M. (2013). β-Glucan signaling connects phagocytosis to autophagy. Glycobiology *23*, 1047–1051.

Ma, Y., Galluzzi, L., Zitvogel, L., and Kroemer, G. (2013). Autophagy and cellular immune responses. Immunity *39*, 211–227.

MacLeod, M.K.L., Kappler, J.W., and Marrack, P. (2010). Memory CD4 T cells: generation, reactivation and re-assignment. Immunology *130*, 10–15.

Maekawa, Y., Himeno, K., and Katunuma, N. (1997). Cathepsin B-inhibitor promotes the development of Th1 type protective T cells in mice infected with Leishmania major. The Journal of Medical Investigation : JMI *44*, 33–39.

Mantegazza, A.R., Magalhaes, J.G., Amigorena, S., and Marks, M.S. (2013). Presentation of phagocytosed antigens by MHC class I and II. Traffic (Copenhagen, Denmark) *14*, 135–152.

Martinez, F.O., Gordon, S., Locati, M., and Mantovani, A. (2006). Transcriptional Profiling of the Human Monocyte-to-Macrophage Differentiation and Polarization : New Molecules and Patterns of Gene Expression 1.

Martinez, J., Almendinger, J., Oberst, A., Ness, R., Dillon, C.P., Fitzgerald, P., Hengartner, M.O., and Green, D.R. (2011). Microtubule-associated protein 1 light chain 3 alpha (LC3)-associated phagocytosis is required for the efficient clearance of dead cells. Proceedings of the National Academy of Sciences of the United States of America *108*, 17396–17401.

Matheoud, D., Moradin, N., Bellemare-Pelletier, A., Shio, M.T., Hong, W.J., Olivier, M., Gagnon, E., Desjardins, M., and Descoteaux, A. (2013). Leishmania evades host immunity by inhibiting antigen cross-presentation through direct cleavage of the SNARE VAMP8. Cell Host & Microbe *14*, 15–25.

McDowell, M.A., Marovich, M., Lira, R., Braun, M., and Sacks, D. (2002). Leishmania priming of human dendritic cells for CD40 ligand-induced interleukin-12p70 secretion is strain and species dependent. Infection and Immunity *70*, 3994–4001.

McMahon-Pratt, D., and Alexander, J. (2004). Does the Leishmania major paradigm of pathogenesis and protection hold for New World cutaneous leishmaniases or the visceral disease? Immunological Reviews *201*, 206–224.

Mintern, J.D., and Villadangos, J. a (2012). Autophagy and mechanisms of effective immunity. Frontiers in Immunology *3*, 60.

Moradin, N., and Descoteaux, A. (2012). Leishmania promastigotes: building a safe niche within macrophages. Frontiers in Cellular and Infection Microbiology *2*, 121.

Mosser, D.M. (2003). The many faces of macrophage activation. Journal of Leukocyte Biology *73*, 209–212.

Muleme, H.M., Reguera, R.M., Berard, A., Azinwi, R., Jia, P., Okwor, I.B., Beverley, S., and Uzonna, J.E. (2009). Infection with arginase-deficient Leishmania major reveals a parasite number-dependent and cytokine-independent regulation of host cellular arginase activity and disease pathogenesis. Journal of Immunology (Baltimore, Md. : 1950) *183*, 8068–8076.

Münz, C. (2009). Enhancing immunity through autophagy. Annual Review of Immunology *27*, 423–449.

Neefjes, J., Jongsma, M.L.M., Paul, P., and Bakke, O. (2011). Towards a systems understanding of MHC class I and MHC class II antigen presentation. Nature Reviews. Immunology *11*, 823–836.

Neu, C., Sedlag, A., Bayer, C., Förster, S., Crauwels, P., Niess, J.-H., van Zandbergen, G., Frascaroli, G., and Riedel, C.U. (2013). CD14-dependent monocyte isolation enhances phagocytosis of listeria monocytogenes by proinflammatory, GM-CSF-derived macrophages. PloS One *8*, e66898.

Novak, E.J., Masewicz, S.A., Liu, A.W., Lernmark, A., Kwok, W.W., and Nepom, G.T. (2001). Activated human epitope-specific T cells identified by class II tetramers reside within a CD4high, proliferating subset. International Immunology *13*, 799–806.

O'Doherty, U., Peng, M., Gezelter, S., Swiggard, W.J., Betjes, M., Bhardwaj, N., and Steinman, R.M. (1994). Human blood contains two subsets of dendritic cells, one immunologically mature and the other immature. Immunology *82*, 487–493.

O'Shea, J.J., and Paul, W.E. (2010). Mechanisms underlying lineage commitment and plasticity of helper CD4+ T cells. Science (New York, N.Y.) *327*, 1098–1102.

Panaro, M.A., Acquafredda, A., Lisi, S., Lofrumento, D.D., Trotta, T., Satalino, R., Saccia, M., Mitolo, V., and Brandonisio, O. (1999). Inducible nitric oxide synthase and nitric oxide production in Leishmania infantum-infected human macrophages stimulated with interferon-gamma and bacterial lipopolysaccharide. International Journal of Clinical & Laboratory Research *29*, 122–127.

Parkes, M., Barrett, J.C., Prescott, N.J., Tremelling, M., Anderson, C.A., Fisher, S.A., Roberts, R.G., Nimmo, E.R., Cummings, F.R., Soars, D., et al. (2007). Sequence variants in the autophagy gene IRGM and multiple other replicating loci contribute to Crohn's disease susceptibility. Nature Genetics *39*, 830–832.

Peters, N.C., Egen, J.G., Secundino, N., Debrabant, A., Kimblin, N., Kamhawi, S., Lawyer, P., Fay, M.P., Germain, R.N., and Sacks, D. (2008). In vivo imaging reveals an essential role for neutrophils in leishmaniasis transmitted by sand flies. Science (New York, N.Y.) *321*, 970–974.

Pinheiro, R.O., Nunes, M.P., Pinheiro, C.S., D'Avila, H., Bozza, P.T., Takiya, C.M., Côrte-Real, S., Freire-De-Lima, C.G., and DosReis, G.A. (2009). Induction of autophagy correlates with increased parasite load of Leishmania amazonensis in BALB/c but not C57BL/6 macrophages. Microbes and Infection Institut Pasteur *11*, 181–190.

Poon, I.K.H., Lucas, C.D., Rossi, A.G., and Ravichandran, K.S. (2014). Apoptotic cell clearance: basic biology and therapeutic potential. Nature Reviews. Immunology *14*, 166–180.

Prina, E., Abdi, S.Z., Lebastard, M., Perret, E., Winter, N., and Antoine, J.-C. (2004). Dendritic cells as host cells for the promastigote and amastigote stages of Leishmania amazonensis: the role of opsonins in parasite uptake and dendritic cell maturation. Journal of Cell Science *117*, 315–325.

Privé, C., and Descoteaux, A. (2000). Leishmania donovani promastigotes evade the activation of mitogen-activated protein kinases p38, c-Jun N-terminal kinase, and extracellular signal-regulated kinase-1/2 during infection of naive macrophages. European Journal of Immunology *30*, 2235–2244.

Qadoumi, M., Becker, I., Donhauser, N., Röllinghoff, M., and Bogdan, C. (2002). Expression of inducible nitric oxide synthase in skin lesions of patients with american cutaneous leishmaniasis. Infection and Immunity *70*, 4638–4642.

Randow, F., and Münz, C. (2012). Autophagy in the regulation of pathogen replication and adaptive immunity. Trends in Immunology *33*, 475–487.

Rico, E., Alzate, J.F., Arias, A.A., Moreno, D., Clos, J., Gago, F., Moreno, I., Domínguez, M., and Jiménez-Ruiz, A. (2009). Leishmania infantum expresses a mitochondrial nuclease homologous to EndoG that migrates to the nucleus in response to an apoptotic stimulus. Molecular and Biochemical Parasitology *163*, 28–38.

References

Riemann, A., Schneider, B., Ihling, A., Nowak, M., Sauvant, C., Thews, O., and Gekle, M. (2011). Acidic environment leads to ROS-induced MAPK signaling in cancer cells. PloS One *6*, e22445.

Ritter, U., Wiede, F., Mielenz, D., Kiafard, Z., Zwirner, J., and Körner, H. (2004). Analysis of the CCR7 expression on murine bone marrow-derived and spleen dendritic cells. Journal of Leukocyte Biology *76*, 472–476.

Rocha, P.N., Almeida, R.P., Bacellar, O., de Jesus, A.R., Filho, D.C., Filho, A.C., Barral, A., Coffman, R.L., and Carvalho, E.M. (1999). Down-regulation of Th1 type of response in early human American cutaneous leishmaniasis. The Journal of Infectious Diseases *180*, 1731–1734.

Rogers, M.E., Ilg, T., Nikolaev, A.V., Ferguson, M.A.J., Paul, A., and Bates, P.A. (2004). Transmission of cutaneous leishmaniasis by sand flies is enhanced by regurgitation of fPPG. Nature *430*, 463–467.

Romano, P.S., Arboit, M.A., Vázquez, C.L., and Colombo, M.I. (2009). The autophagic pathway is a key component in the lysosomal dependent entry of Trypanosoma cruzi into the host cell. Autophagy *5*, 6–18.

Romao, S., Gasser, N., Becker, A.C., Guhl, B., Bajagic, M., Vanoaica, D., Ziegler, U., Roesler, J., Dengjel, J., Reichenbach, J., et al. (2013). Autophagy proteins stabilize pathogen-containing phagosomes for prolonged MHC II antigen processing. The Journal of Cell Biology *203*, 757–766.

Rosenzwajg, M., Ekman, M., Biberfeld, P., and Gluckman, J.C. (1997). Differentiation of human dendritic cells from monocytes in vitro. 431–441.

Ruhland, A., Leal, N., and Kima, P.E. (2007). Leishmania promastigotes activate PI3K/Akt signalling to confer host cell resistance to apoptosis. Cellular Microbiology *9*, 84–96.

Russell, D.G. (2007). New ways to arrest phagosome maturation. Nature Cell Biology *9*, 357–359.

Röder, M., Kleiner, K., Sachs, A., Keil, N., and Holzhauser, T. (2013). Detectability of lupine seeds by ELISA and PCR may be strongly influenced by potential differences between cultivars. Journal of Agricultural and Food Chemistry *61*, 5936–5945.

Sacks, D., and Noben-Trauth, N. (2002a). The immunology of susceptibility and resistance to Leishmania major in mice. Nature Reviews. Immunology *2*, 845–858.

Sacks, D., and Noben-Trauth, N. (2002b). The immunology of susceptibility and resistance to Leishmania major in mice. Nature Reviews. Immunology *2*, 845–858.

Sallusto, F., Lenig, D., Förster, R., Lipp, M., and Lanzavecchia, a (1999). Two subsets of memory T lymphocytes with distinct homing potentials and effector functions. Nature *401*, 708–712.

Sanjuan, M. a, Dillon, C.P., Tait, S.W.G., Moshiach, S., Dorsey, F., Connell, S., Komatsu, M., Tanaka, K., Cleveland, J.L., Withoff, S., et al. (2007). Toll-like receptor signalling in macrophages links the autophagy pathway to phagocytosis. Nature *450*, 1253–1257.

Santarém, N., Silvestre, R., Tavares, J., Silva, M., Cabral, S., Maciel, J., and Cordeiro-da-Silva, A. (2007). Immune response regulation by leishmania secreted and nonsecreted antigens. Journal of Biomedicine & Biotechnology *2007*, 85154.

Santos, T.A.T.D., Portes, J.D.A., Damasceno-Sá, J.C., Caldas, L.A., Souza, W.D., Damatta, R.A., and Seabra, S.H. (2011). Phosphatidylserine exposure by Toxoplasma gondii is fundamental to balance the immune response granting survival of the parasite and of the host. PloS One *6*, e27867.

Sauer, J.-D., Shannon, J.G., Howe, D., Hayes, S.F., Swanson, M.S., and Heinzen, R.A. (2005). Specificity of Legionella pneumophila and Coxiella burnetii vacuoles and versatility of Legionella pneumophila revealed by coinfection. Infection and Immunity *73*, 4494–4504.

Schmid, D., Pypaert, M., and Münz, C. (2007). Antigen-loading compartments for major histocompatibility complex class II molecules continuously receive input from autophagosomes. Immunity *26*, 79–92.

Schneider, P., Rosat, J.P., Bouvier, J., Louis, J., and Bordier, C. (1992). Leishmania major: differential regulation of the surface metalloprotease in amastigote and promastigote stages. Experimental Parasitology *75*, 196–206.

Seto, S., Tsujimura, K., Horii, T., and Koide, Y. (2013). Autophagy adaptor protein p62/SQSTM1 and autophagy-related gene Atg5 mediate autophagosome formation in response to Mycobacterium tuberculosis infection in dendritic cells. PloS One *8*, e86017.

Shapiro, T.A., and Englund, P.T. (1995). The structure and replication of kinetoplast DNA. Annual Review of Microbiology *49*, 117–143.

Shio, M.T., Hassani, K., Isnard, A., Ralph, B., Contreras, I., Gomez, M.A., Abu-Dayyeh, I., and Olivier, M. (2012). Host cell signalling and leishmania mechanisms of evasion. Journal of Tropical Medicine *2012*, 819512.

Simeone, R., Bobard, A., Lippmann, J., Bitter, W., Majlessi, L., Brosch, R., and Enninga, J. (2012). Phagosomal rupture by Mycobacterium tuberculosis results in toxicity and host cell death. PLoS Pathogens *8*, e1002507.

Soussi-Gounni, a, Kontolemos, M., and Hamid, Q. (2001). Role of IL-9 in the pathophysiology of allergic diseases. The Journal of Allergy and Clinical Immunology *107*, 575–582.

von Stebut, E., Belkaid, Y., Nguyen, B., Wilson, M., Sacks, D.L., and Udey, M.C. (2002). Skin-derived macrophages from Leishmania major-susceptible mice exhibit interleukin-12- and interferon-gamma-independent nitric oxide production and parasite killing after treatment with immunostimulatory DNA. The Journal of Investigative Dermatology *119*, 621–628.

Stout, R.D., Suttles, J., Xu, J., Grewal, I.S., and Flavell, R.A. (1996). Impaired T cell-mediated macrophage activation in CD40 ligand-deficient mice. Journal of Immunology (Baltimore, Md. : 1950) *156*, 8–11.

Su, L.F., and Davis, M.M. (2013). Antiviral memory phenotype T cells in unexposed adults. Immunological Reviews *255*, 95–109.

Su, L.F., Kidd, B. a, Han, A., Kotzin, J.J., and Davis, M.M. (2013). Virus-Specific CD4(+) Memory-Phenotype T Cells Are Abundant in Unexposed Adults. Immunity *38*, 373–383.

Sypek, J.P., Chung, C.L., Mayor, S.E., Subramanyam, J.M., Goldman, S.J., Sieburth, D.S., Wolf, S.F., and Schaub, R.G. (1993). Resolution of cutaneous leishmaniasis: interleukin 12 initiates a protective T helper type 1 immune response. The Journal of Experimental Medicine *177*, 1797–1802.

Sádlová, J., Price, H.P., Smith, B. a, Votýpka, J., Volf, P., and Smith, D.F. (2010). The stage-regulated HASPB and SHERP proteins are essential for differentiation of the protozoan parasite Leishmania major in its sand fly vector, Phlebotomus papatasi. Cellular Microbiology *12*, 1765–1779.

Tabatabaee, P.-A., Abolhassani, M., Mahdavi, M., Nahrevanian, H., and Azadmanesh, K. (2011). Leishmania major: secreted antigens of Leishmania major promastigotes shift the immune response of the C57BL/6 mice toward Th2 in vitro. Experimental Parasitology *127*, 46–51.

Taylor-Brown, E., and Hurd, H. (2013). The first suicides: a legacy inherited by parasitic protozoans from prokaryote ancestors. Parasites & Vectors *6*, 108.

Tiemessen, M.M., Kunzmann, S., Schmidt-Weber, C.B., Garssen, J., Bruijnzeel-Koomen, C.A.F.M., Knol, E.F., and van Hoffen, E. (2003). Transforming growth factor-beta inhibits human antigen-specific CD4+ T cell proliferation without modulating the cytokine response. International Immunology *15*, 1495–1504.

Turhan, A., Mirshahidi, S., Pişkin, A.K., Citak, B., and Imir, T. (1997). Effects of crude antigenic fractions of Leishmania major on natural killer cell cytotoxicity, interferon-gamma and interleukin-4 secretion from peripheric blood lymphocytes of unexposed individuals. Immunology Letters *55*, 115–118.

de Veer, M.J., Curtis, J.M., Baldwin, T.M., DiDonato, J.A., Sexton, A., McConville, M.J., Handman, E., and Schofield, L. (2003). MyD88 is essential for clearance of Leishmania major: possible role

for lipophosphoglycan and Toll-like receptor 2 signaling. European Journal of Immunology *33*, 2822–2831.

Vernon, P.J., and Tang, D. (2013). Eat-me: autophagy, phagocytosis, and reactive oxygen species signaling. Antioxidants & Redox Signaling *18*, 677–691.

Vouldoukis, I., Riveros-Moreno, V., Dugas, B., Ouaaz, F., Bécherel, P., Debré, P., Moncada, S., and Mossalayi, M.D. (1995). The killing of Leishmania major by human macrophages is mediated by nitric oxide induced after ligation of the Fc epsilon RII/CD23 surface antigen. Proceedings of the National Academy of Sciences of the United States of America *92*, 7804–7808.

Vouldoukis, I., Bécherel, P.A., Riveros-Moreno, V., Arock, M., da Silva, O., Debré, P., Mazier, D., and Mossalayi, M.D. (1997). Interleukin-10 and interleukin-4 inhibit intracellular killing of Leishmania infantum and Leishmania major by human macrophages by decreasing nitric oxide generation. European Journal of Immunology *27*, 860–865.

Vyas, J.M., Van der Veen, A.G., and Ploegh, H.L. (2008). The known unknowns of antigen processing and presentation. Nature Reviews. Immunology *8*, 607–618.

WHO (2014). No Title.

Walsh, K.P., and Mills, K.H.G. (2013). Dendritic cells and other innate determinants of T helper cell polarisation. Trends in Immunology *34*, 521–530.

Wanasen, N., and Soong, L. (2008). L-arginine metabolism and its impact on host immunity against Leishmania infection. Immunologic Research *41*, 15–25.

Wang, N., Satoskar, A., Faubion, W., Howie, D., Okamoto, S., Feske, S., Gullo, C., Clarke, K., Sosa, M.R., Sharpe, A.H., et al. (2004). The cell surface receptor SLAM controls T cell and macrophage functions. The Journal of Experimental Medicine *199*, 1255–1264.

Warburg, A. (2008). The structure of the female sand fly (Phlebotomus papatasi) alimentary canal. Transactions of the Royal Society of Tropical Medicine and Hygiene *102*, 161–166.

Welsh, R.M., and Selin, L.K. (2002). No one is naive: the significance of heterologous T-cell immunity. Nature Reviews. Immunology *2*, 417–426.

Wenzel, U.A., Bank, E., Florian, C., Förster, S., Zimara, N., Steinacker, J., Klinger, M., Reiling, N., Ritter, U., and van Zandbergen, G. (2012). Leishmania major parasite stage-dependent host cell invasion and immune evasion. FASEB Journal : Official Publication of the Federation of American Societies for Experimental Biology *26*, 29–39.

Winberg, M.E., Holm, A., Särndahl, E., Vinet, A.F., Descoteaux, A., Magnusson, K.-E., Rasmusson, B., and Lerm, M. (2009). Leishmania donovani lipophosphoglycan inhibits phagosomal maturation via action on membrane rafts. Microbes and Infection / Institut Pasteur *11*, 215–222.

Xu, W., Zhao, X., Daha, M.R., and van Kooten, C. (2013). Reversible differentiation of pro- and anti-inflammatory macrophages. Molecular Immunology *53*, 179–186.

Yordy, B., and Iwasaki, A. (2011). Autophagy in the control and pathogenesis of viral infection. Current Opinion in Virology *1*, 196–203.

van Zandbergen, G., Bollinger, A., Wenzel, A., Kamhawi, S., Voll, R., Klinger, M., Müller, A., Hölscher, C., Herrmann, M., Sacks, D., et al. (2006). Leishmania disease development depends on the presence of apoptotic promastigotes in the virulent inoculum. Proceedings of the National Academy of Sciences of the United States of America *103*, 13837–13842.

Zangger, H., Mottram, J.C., and Fasel, N. (2002). Cell death in Leishmania induced by stress and differentiation: programmed cell death or necrosis? Cell Death and Differentiation *9*, 1126–1139.

Zangger, H., Ronet, C., Desponds, C., Kuhlmann, F.M., Robinson, J., Hartley, M.-A., Prevel, F., Castiglioni, P., Pratlong, F., Bastien, P., et al. (2013). Detection of Leishmania RNA virus in Leishmania parasites. PLoS Neglected Tropical Diseases *7*, e2006.

Zhang, T., Maekawa, Y., Sakai, T., Nakano, Y., Ishii, K., Hisaeda, H., Dainichi, T., Asao, T., Katunuma, N., and Himeno, K. (2001). Treatment with cathepsin L inhibitor potentiates Th2-type immune response in Leishmania major-infected BALB/c mice. International Immunology *13*, 975–982.

10. Acknowledgments

11. Declaration of Authorship

I hereby declare that I have written the present dissertation with the topic:

"The interaction of *Leishmania major* parasites with human myeloid cells and its consequence for adaptive immunity"

independently, using no other aids then those I have cited. I have clearly mentioned the source of the passages that are taken word for word or paraphrased from other works.

The presented thesis has not been submitted in this or any other form to another Faculty or Examination Institution.

Peter Crauwels

Mainz, 18. December 2014

12. Curriculum Vitae

13. Publications

Only the publications, which are already published or accepted for publication are attached.

Peter Crauwels, Rebecca Bohn, Meike Thomas, Stefan Gottwalt, Florian Jäckel, Susi Krämer, Elena Bank, Stefan Tenzer, Paul Walther, Max Bastian, Ger van Zandbergen. Apoptotic-like *Leishmania* exploit the host´s autophagy machinery to reduce T-cell mediated parasite elimination. **Autophagy 2015, in press**

Neu C, Sedlag A, Bayer C, Förster S, **Crauwels P**, Niess JH, van Zandbergen G, Frascaroli G, Riedel CU. CD14-dependent monocyte isolation enhances phagocytosis of *listeria monocytogenes* by proinflammatory, GM-CSF-derived macrophages. **PLoS ONE 2013, PMID: 23776701**